Universidad de Valladolid

FACULTAD DE MEDICINA

INSTITUTO DE BIOLOGÍA Y GENÉTICA MOLECULAR (IBGM)

Departamento de Bioquímica, Biología Molecular y Fisiología

TESIS DOCTORAL:

BIOENGINEERED CARDIOGENICITY THROUGH NUCLEAR REPROGRAMMING: AN iPS PLATFORM FOR HEART REGENERATION

Presentada por Almudena Martínez Fernández para optar al grado de doctor /ra por la Universidad de Valladolid

Directores:

Dra. Ana Sánchez y Dr. André Terzic

Valladolid, 2010

Parts of this thesis have been published in the following manuscripts:

Nelson TJ, **Martinez-Fernandez A**, Yamada S, Ikeda T, Terzic A. Induced pluripotent stem cells: Advances to applications. *Stem Cells Cloning: Adv and App*. 2010 *In press*

Martinez-Fernandez A, Nelson TJ, Ikeda Y, Terzic A. c-MYC independent nuclear reprogramming favors cardiogenic potential of induced pluripotent stem cells. *J Cardiovas Transl Res*. 2010 *In press*.

Nelson TJ, Behfar A, Yamada S, **Martinez-Fernandez A**, Terzic A. Stem Cell Platforms for Regenerative Medicine*. Clin Transl Sci*. 2009 Jun 1;2(3):222-227.

Martinez-Fernandez A, Nelson TJ, Yamada S, Reyes S, Alekseev AE, Perez-Terzic C, Ikeda Y, Terzic A. iPS programmed without c-MYC yield proficient cardiogenesis for functional heart chimerism. *Circ Res*. 2009 Sep 25;105(7):648-56. (*Issue cover*).

Nelson TJ, **Martinez-Fernandez A**, Yamada S, Perez-Terzic C, Ikeda Y, Terzic A. Repair of acute myocardial infarction by human stemness factors induced pluripotent stem cells. *Circulation*. 2009 Aug 4;120(5):408-16.

Nelson TJ, **Martinez-Fernandez A**, Yamada S, Mael AA, Terzic A, Ikeda Y. Induced Pluripotent Reprogramming from Promiscuous Human Stemness-Related Factors. *Clin Transl Sci.* 2009 April 1; 2(2):118-126. (*Issue cover*).

Nelson TJ, **Martinez-Fernandez A**, Terzic A. KCNJ11 knockout morula re-engineered by stem cell diploid aggregation. *Philos Trans R Soc Lond B Biol Sci*. 2009 Jan 27; 364(1514):269-76.

Martinez-Fernandez A, Nelson TJ, Terzic A. Chimera production through inverted diploide aggregation. *Transgenic Research* 2008 Oct 1; 17(5):1015-16.

or books:

Nelson TJ, **Martinez-Fernandez A**, Yamada S and Terzic A. Chapter 19: Regenerative chimerism bioengineered through stem cell reprogramming. In “Regenerative Medicine – From Protocol to Patient” by Springer Publ, London. *In press.*

Nelson TJ, Yamada S, McDonald R, **Martinez-Fernandez A** and Terzic A. Chapter 21: Induced pluripotent stem cells: Imaging nuclear reprogramming to cardiac regeneration. In: “Cardiac Imaging”, by Springer, editor Kraitchman. *In press.*

Some of the results and techniques included in this work have been presented in the following meetings:

Nelson TJ, **Martinez-Fernandez A**, Yamada S, Perez-Terzic C, Ikeda Y and Terzic A. Myocardial infarction repair with iPS induced by human stemness factors. AHA, Orlando, USA. 14th-18th November 2009, ***Malvin Marcus Young Investigator Competition Winner.***

Nelson TJ, **Martinez-Fernandez A**, Yamada S, Perez-Terzic C, Ikeda Y and Terzic A. Myocardial infarction repair with human stemness factors induced iPS. 6th International symposium on Stem cell therapy and Applied cardiovascular biotechnology. Madrid, Spain. April 23rd-24th, 2009. ***Poster competition winner.***

Martínez-Fernández A, Nelson TJ, Reyes S, Alekseev AE, Yamada S, Pérez-Terzic C, Ikeda Y and Terzic A. Engineered functional cardiogenesis through Myc-independent iPS induction: Technological innovation in cardio-regenerative tools. 6th International symposium on Stem cell therapy and Applied cardiovascular biotechnology. Madrid, Spain. April 23rd-24th, 2009.

Martinez-Fernandez A, Nelson TJ, Terzic A. Chimera production through inverted diploide aggregation. Transgenic Technology. Toronto, Canada. October 27th-28th,2008.

INDEX

ACKNOWLEDGMENTS

ÍNDICE

AGRADECIMIENTOS

ACKNOWLEDGMENTS

Among all the persons that have somehow helped me getting here, there is no doubt that the most important, patient and understanding have been my parents. They have always supported me, helped me decide or listened to me when I needed some out-loud thinking to make my mind up. And even when my decisions took me away from them, they smiled and nodded back as if they knew. I cannot thank them enough for all they have done for me… nor for all I know they'll keep on doing.

I firmly believe when someone expects something from you, it helps you move forward. That is exactly what happened to me with my grandparents: they all expected big things from me and that simple fact made me feel really special. I'm doing my best, and even though I took a different route (and I am not a physician today), I know they would be proud of me. Thanks for believing in me.

And also thanks to Samuel, because it is inspiring to see how doing what you really like can change your life. And because, together with the rest of my family, you stay awake while I talk for hours about how life is going in this side of the world.

Now, on the scientific side of things I want to go back in time to the first day of my 3rd year in Salamanca and thank Dr. García-Marín and Dr. Monte-Río (or José Juan and Mariaje) for giving me the opportunity to join their lab. It was amazing for me to be able to see things from the inside and even get to be part of it. Now I understand how much patience you must have invested to do something like you did. I really appreciate it. To everybody else in the lab at that time, Marta Vallejo, Óscar, Rocío and very, very especially, Marta Rodríguez, you are all part of the reason why I love science.

To Dr. Silva (Tito) and his crowd from the CIB in Madrid I owe my first contact with the 'stem cell world'. It was such a great experience that I changed

many of my plans to get back to it. Thanks for transmitting all your excitement to me.

And after the idea of jumping into stem cells, Dr. Miguel Torres and his wonderful team at the CNB made it real. I wouldn't be here without your help and support. Thank you all. And many thanks to Giovanna, that took the bother to show me so many things in the culture room.

Thanks to La Caixa and Caja Madrid Foundations for believing in me and funding me through this experience. And thanks to the University of Valladolid and Mayo Clinic for hosting me.

Nothing would have been possible without Ana and André. I am truly grateful to them for mentoring not only this work, but the initial steps of my scientific career. It has been quite an interesting trip in which I have learnt a lot from you and I believe I have matured along the way too. Thank you for this great opportunity. And thank you too for the great atmosphere you directly or indirectly have created in your labs. It has been a pleasure to meet all the people I have worked with.

Ana's group in Spain, especially Christine, with whom I worked more closely and interchanged world sides, and Sara were great trip-mates. And everybody in Stabile 5, I have enjoyed so much my time there that you are not getting rid of me so easily! From there, I want to make a very special mention to Tim. Even if before coming here I thought I was motivated, I didn't know the full extent of those words until I got to work with you. In the last two years I have been challenged, squeezed, I have worked as I had never done before… but more than ever before, I've been encouraged and recognized. Above anything else, these months have felt great, and a big part of it has been thanks to you. Thank you SO much.

As unlikely as it sounds and as it still seems to me, coming to Rochester had some other repercussions, like finding the person I want to share my life with. Santi, nobody would have stood by me like you. Your patience goes beyond anything seen before. Thank you for helping me through the difficult times, through the winters (three already!) and through the good moments too. Thank you for learning how to dance with me and make me forget my mood when I am crummy. You are the best.

To the Latin colony in Rochester, Mily and Sofi, Nico and Mimía, Juan and Patri, Caro, Miguel and Megan, Juanca, Ale and Matías, Carlos and Pili… and so many others. Having you there all this time has made me feel at home. I'm really happy I got to meet you all and I hope we'll always be in touch, wherever life takes us.

And last but not least, to my life-long friends. For being there. For reminding me so many times how crazy I am and making me feel proud of it. For understanding me and always try to help. Everybody, Vero, Eva, Sara, Almu, Elo, Manu Suárez, Manu Vázquez, Ángela… you are wonderful. I wouldn't have survived without you!

For all that and for so many reasons…

… thank you

De entre todas las personas que han tenido algo que ver con que yo esté hoy aquí, sin ninguna duda las más importantes (por no hablar de comprensivas y pacientes) son mis padres. Siempre me han transmitido su apoyo, ayudándome a tomar las decisiones difíciles o simplemente escuchándome pensar en voz alta. E incluso cuando mis decisiones me han llevado al otro lado del mundo, alejándome de ellos, no sólo lo han entendido, sino que le han concedido todo el sentido que tenía para mí. No existe la manera de agradecerles todo lo que han hecho por mí… y todo lo que sé que seguirán haciendo.

Estoy convencida de que saber que alguien espera algo de ti te ayuda a avanzar. Y eso es lo que me ha pasado a mí con mis abuelos: esperaban algo grande de mí, y es me ha hecho siempre sentirme muy especial. Hago lo que puedo, y aunque se por un camino diferente que no implique ser médico, sé que estarían muy orgullosos. Gracias por creer en mí.

Gracias también a Samu, porque es increíble ver cómo hacer lo que te gusta puede cambiar tu vida. Es toda una fuente de inspiración. Gracias, junto con él, al resto de mi familia. Sólo ellos son capaces de escucharme hablar durante horas sobre la vida al otro lado del mundo.

En el lado científico, tengo que retroceder en el tiempo hasta el primer día de mi tercer año en Salamanca. Aquel día fue la primera vez que pisé un laboratorio de verdad. Gracias José Juan y Mariaje por darme la oportunidad de unirme a vuestro laboratorio. Para mí fue increíble ver las cosas desde dentro y poder ser parte de ello. Ahora entiendo cuánta paciencia tuvisteis que invertir en mí. A todos los miembros del laboratorio entonces, Marta Vallejo, Óscar, Rocío y muy, muy especialmente, Marta Rodríguez, vosotros sois en gran medida “culpables” de que me encante la ciencia.

A Tito y su grupo en el CIB les debo mi primer contacto con las células madre. Fue una gran experiencia que provocó todo un cambio de planes. Gracias por transmitirme vuestro entusiasmo.

Y tras la idea de entrar en el mundo de las células madre, Miguel Torres y su equipo lo hicieron realidad. No habría llegado hasta aquí sin vuestra ayuda y vuestro apoyo. Gracias a todos, especialmente a Giovanna, que me enseñó tanto en el cuarto de cultivos.

Gracias a las fundaciones de La Caixa y Caja Madrid por creer en mi y brindarme su apoyo a lo largo de estos tres años. Y gracias a la Universidad de Valladolid y a la Clínica Mayo por acogerme en distintos momentos del proceso.

Nada de esto hubiera sido posible sin Ana y André. Les estoy tremendamente agradecida por haber sido mis mentores tanto en la elaboración de esta tesis como en este comienzo de mi carrera científica. Ha sido una experiencia inolvidable en la que he aprendido y madurado mucho. Gracias por darme esta oportunidad. Y gracias también por el fantástico ambiente que habéis sido capaces de crear en vuestros laboratorios. Ha sido un placer trabajar en vuestros grupos.

En el de Ana, en España, especialmente con Christine, con la que comparto no sólo muchas horas de trabajo, sino hasta ahora situaciones opuestas en nuestros continentes respectivos. Y con Sara, aunque fuera en la puerta de al lado. Las dos han sido estupendas compañeras de viaje. En Rochester, he disfrutado tanto en el laboratorio que no va a ser fácil librarse de mí. Y de allí, del Stabile 5 tengo que hablar especialmente de Tim. Puede que en algún momento antes de llegar allí, yo me sintiera motivada, pero no fue comparable con lo que vino después. En los últimos dos años me he sentido desafiada, exprimida, he trabajado como nunca en mi vida… pero por encima de

todo, he sentido muchísimo apoyo y reconocimiento. Ha sido increíble, y en gran medida ha sido gracias a Tim. Muchísimas gracias.

Aunque parezca increíble (y a mí me lo parece) aterrizar en Rochester tuvo otras repercusiones en mi vida, como encontrar a la persona con la que quiero compartirla. Santi, es imposible que nadie lo hubiera hecho tan bien como tú. Está claro que tu paciencia no tiene límites. Gracias por ayudarme a superar los momentos bajos, los inviernos, y por estar conmigo en los momentos buenos. Gracias por bailar conmigo y hacerme olvidar que estoy de mal humor. Eres el mejor.

A la colonia latina de Rochester, Mily y Sofi, Nico y Mimía, Juan y Patri, Caro, Miguel y Megan, Juanca, Ale y Matías, Carlos y Pili… y todos los demás. Estar con vosotros me ha ayudado a sentirme como en casa. Me alegro mucho de haberos conocido y espero que sigamos siempre en contacto, desde donde quiera que estemos.

Y por último, pero para nada menos importante, a mis amigos de siempre. Porque siempre habéis estado ahí, recordándome que estoy un poco loca y haciéndome sentir orgullosa de ello. Siempre comprensivos, siempre tratando de ayudar. Todos, Eva, Sara, Almu, Elo, Manu Suárez, Manu Vázquez, Ángela… sois estupendos. Y no habría sido capaz de llegar hasta aquí sin vosotros.

Por todo eso y por muchas más razones…

… gracias

I. ABBREVIATIONS

ACE	Angiotensin-converting enzyme
AEC	Amniotic epithelial cells
AP	Alkaline phosphatase
ATP	Adenosine-5'-triphosphate
BME	Beta mercapto ethanol
cDNA	Complementary DNA
CHD	Coronary heart disease
CM	Cardiomyocyte
CVD	Cardiovascular disease
Cyp A	Cyclophilin A
DAPI	4',6-diamidino-2-phenylindole
DMEM	Dulbecco's modified Eagle's medium
d.p.c.	Days post coitum
EB	Embryoid bodies
EDTA	Ethylenediaminetetraacetic acid
EF	Ejection fraction
EGTA	Ethylene glycol tetraacetic acid
ESC	Embryonic stem cells
FACS	Fluorescence-activated cell sorting
FBS	Fetal bovine serum
FDG	Fluorescein di[®-D-galactopyranoside]
FESEM	Field-emission scanning electron microscopy
FGF4	Fibroblast growth factor-4
FITC	Fluorescein isothiocyanate
FS	Left ventricular fractional shortening
gDNA	Genomic DNA
GFP	Green fluorescent protein
HBSS	Hank's Buffered Salt Solution
HCG	Human chorionic gonadotrophin
HEPES	4-(2-hydroxyethyl)-1-piperazineethanesulfonic acid
HIV	Human immunodeficiency virus
HLA	Human leukocyte antigen

ip	Intraperitoneal
iPS	Induced pluripotent stem cells
LIF	Leukemia inhibitory factor
LV	Left ventricle
LVDd	Left ventricular end-diastolic dimension
LVDs	Left ventricular end-systolic dimension
LVVd	Left ventricular end-diastolic volume
LVVs	Left ventricular end-systolic volume
MEFs	Mouse embryonic fibroblast
MHC	Major histocompatability complex
MI	Miocardial infarction
MLC-2a	Atrial myosin light chain-2
MLC-2v	Ventricular myosin light chain-2
mRNA	Messenger RNA
NEAA	Non-essential aminoacids
PB	PiggyBac
PBS	Phosphate buffered saline
PCR	Polymerase chain reaction
Pen/Strep	Penicillin/Streptomycin
PMSG	Pregnant mare serum gonadotropin
r.p.m.	Revolutions per minute
RT	Room temperature
RT-PCR	Real time polymerase chain reaction
SCNT	Somatic cell nuclear transfer
SFFV	Spleen focus-forming virus
SMA	Smooth muscle α-actin
SSEA	Stage-Specific Embryonic Antigen
TEM	Transmission electron microscopy
TGF-β	Transforming growth factor-β
UCB	Umbilical cord blood
WT	Wild type

II. RESUMEN EN ESPAÑOL

1. Introducción

Las enfermedades cardiovasculares incluyendo isquemia cardiaca, ictus, hipertensión, insuficiencia cardiaca y defectos congénitos, constituyen la primera causa de muerte en el mundo. Entre ellos, infarto de miocardio y angina, agrupadas como enfermedades isquémicas del corazón, suponen el mayor número de muertes tanto en EEUU como en Europa y España. Al margen de la mortalidad causada por estas enfermedades, el elevado número de casos de isquemia cardiaca refractaria a los tratamientos convencionales supone uno de los mayores retos en este campo, dejando el transplante cardiaco como única solución *curativa*. Sin embargo, la escasez de donantes y la efectividad sub-óptima de esta opción terapéutica a medio y largo plazo ponen de manifiesto la necesidad de desarrollar nuevos tratamientos accesibles y efectivos.

La medicina regenerativa es una disciplina joven cuya finalidad es tratar la causa responsable de la destrucción celular y la pérdida irreversible de función tisular en las enfermedades degenerativas, restableciendo la arquitectura y la capacidad funcional de los órganos afectados (Waldman, 2007). Para ello se utilizan células madre o sus derivados capaces de remplazar, rejuvenecer o regenerar el tejido dañado. Hasta hace unos años, las opciones incluían células madre embrionarias (ESC), perinatales (obtenidas del cordón umbilical o la placenta) o adultas. Sin embargo, el reciente descubrimiento de las células pluripotentes inducidas (iPS) ha ampliado los recursos de la medicina regenerativa aportando un nuevo tipo celular autólogo y pluripotente.

Las iPS se obtienen por reprogramación nuclear a partir de células somáticas. Partiendo del protocolo inicial (Takahashi and Yamanaka, 2006) en el que se utilizaron lentivirus para expresar los factores de transcripción Oct4, Sox2, Klf4 y c-Myc, se han descrito numerosas modificaciones y mejoras relacionadas con la fuente de obtención de las células, los factores inductores de

pluripotencia así como estrategias o factores complementarios para la optimización del proceso. A la hora de validar los diversos protocolos, las células reprogramadas deben cumplir los criterios de pluripotencia descritos para las ESC, incluyendo capacidad de diferenciación *in vitro* e *in vivo* mediante formación de teratomas (para células humanas) y contribución a la formación de los diferentes tejidos embrionarios (pertenecientes al mesodermo, endodermo y ectodermo) mediante agregación diploide o tetraploide en el caso de células murinas.

La tecnología de las iPS sirve de base para nuevas aplicaciones no sólo terapéuticas, sino diagnósticas (células derivadas de pacientes) o como substrato para ensayo de posibles tratamientos farmacológicos. En este trabajo se estudiará la diferenciación *in vitro* de iPS haciendo hincapié en su capacidad cardiogénica y en el potencial terapéutico en un modelo de infarto de miocardio en ratón, con la finalidad última de desarrollar una herramienta terapéutica adecuada para el tratamiento de la enfermedad isquémica cardiaca.

2. Material y métodos

Para el desarrollo de este trabajo se usaron fibroblastos de ratón obtenidos a partir de embriones de 14.5 días *post-coitum* (d.p.c.). Éstos fueron infectados con 3 ó 4 lentivirus que contenían los factores de transcripción humanos SOX2, OCT4 y KLF4 (3F) ó SOX2, OCT4, KLF4 y c-MYC (4F). Se aislaron manualmente colonias individuales con una morfología semejante a la de las ESC de ratón y se expandieron para posteriores experimentos. En algunos casos se realizó un marcaje (también mediante infección con lentivirus) con LacZ, GFP o luciferasa, para facilitar el seguimiento de las células en diferentes sistemas.

La diferenciación cardiaca de iPS se hizo siguiendo un protocolo de diferenciación espontánea en cuerpos embrionarios (EB) seguida de cultivo en placas gelatinizadas (Behfar, 2002; Perez-Terzic, 2003). Los cardiomiocitos generados se aislaron mediante un gradiente de densidad y se caracterizaron utilizando técnicas de inmunofluorescencia, microscopía electrónica y confocal, PCR, imagen de calcio citosólico por micro fluorescencia y estudios electrofisiológicos mediante patch clamp (Karger, 2008).

Se caracterizó la pluripotencia y la capacidad de contribución cardiaca de las iPS generadas mediante agregación diploide de iPS marcadas con embriones en fase de mórula de la especie de ratón control CD1 (Eakin and Hadjantonakis, 2006). Tras 24 horas de incubación *in vitro*, los embriones resultantes fueron transferidos quirúrgicamente en el útero de hembras pseudopreñadas para continuar con el proceso de gestación. Algunos de los embriones fueron recuperados y teñidos entre los días 8.0 y 9.5 d.p.c. y el resto se dejó llegar a término. La contribución de las iPS en el adulto se caracterizó mediante técnicas de imagen *in vivo* de la actividad luciferasa procedente de estas células (originalmente marcadas mediante infección lentiviral) tras inyección intraperitoneal del sustrato luciferina en los ratones quiméricos. También dentro de la caracterización de la pluripotencia de las iPS generadas, se indujo la formación de teratomas mediante inyección subcutánea de 500000 células indiferenciadas en el flanco de ratones inmunodeficientes. Los teratomas obtenidos se fijaron y tiñeron con hematoxilina/eosina para identificar los diferentes tipos de tejido presentes.

Para el estudio de la capacidad regenerativa de las iPS se utilizó un modelo de infarto de miocardio en ratón (Yamada, 2009). Se provocó la isquemia cardiaca mediante el ligamiento quirúrgico de la arteria coronaria izquierda descendente en ratones anestesiados e intubados. Media hora después de la primera operación, se inyectaron 200000 células (fibroblastos

control o iPS) en las inmediaciones de la zona infartada y se siguió la evolución de los animales mediante ecografía transtorácica y electrocardiograma.

3. Resultados y Discusión

3.1. Modificación de células somáticas para la obtención de células pluripotentes

En este trabajo, se utilizaron lentivirus derivados del VIH (virus de la inmunodeficiencia humana) como método altamente eficiente de reprogramación de células somáticas de ratón por transducción con factores humanos relacionados con pluripotencia.

Para conseguir la reprogramación entre diferentes especies (factores humanos en células de ratón) es necesaria la optimización del tropismo de los lentivirus por las células murinas. Para ello se estudió la eficacia de infección de lentivirus con diversas mutaciones en la cápside mediante la transducción de la proteína fluorescente verde (GFP) (Figura 16). Una vez escogida la mutación con efecto más positivo sobre la infectividad del virus en células de ratón, se pasó a expresar individualmente los factores necesarios para la reprogramación (Sox2, Oct4, Klf4 y c-Myc) revelándose su presencia en el interior de la célula mediante inmunofluorescencia y western blot (Figura 17).

Para la realización de este trabajo, se utilizaron dos estrategias de reprogramación, una basada en transducción con los cuatro factores iniciales (4F) y otra similar en ausencia del oncogén c-Myc (3F). En ambos casos se usaron como material de partida fibroblastos embrionarios de ratón. De acuerdo con la literatura existente, dos semanas después de la infección con 4 factores y tres después de la infección con 3 factores (Wernig, 2008), se observaron

cambios morfológicos en los cultivos, incluyendo la aparición de grupos tridimensionales redondeados de células íntimamente agrupadas similares a los presentes en los cultivos de ESC (Figura 18). Estas colonias fueron separadas individualmente y expandidas clonalmente para su posterior análisis. Como se muestra en la figura 3, tanto en las iPS obtenidas tras la infección con 4 factores (4F-iPS) como con 3 factores (3F-iPS) se demostró la integración estable de los factores introducidos en los lentivirus en el ADN genómico, así como la expresión de marcadores de pluripotencia como la fosfatasa alcalina (AP) y el marcador de membrana SSEA1 (Figura 19). La ultraestructura, visualizada mediante microscopía electrónica, coincide con la de las ESC y es claramente diferente de la de los fibroblastos originales (Figura 20).

El perfil de expresión estudiado mediante PCR cuantitativa (Figura 21) muestra un aumento en los niveles de marcadores de pluripotencia tanto incluidos en los transgenes expresados (Sox2 y Oct4) como independiente de éstos (Fgf4), sugiriendo una relación directa entre la transducción y la adquisición de pluripotencia. Así mismo, las células reprogramadas fueron capaces de formar teratomas con tejidos pertenecientes a las tres capas embrionarias tras su inyección en ratones inmunodeprimidos (Figura 22), cumpliendo así uno de los requisitos para ser consideradas pluripotentes.

3.2. Pluripotencia funcional de las células reprogramadas

El modelo murino ofrece la posibilidad de demostrar la pluripotencia de las células reprogramadas más allá de la formación de teratomas. Para ello se recurrió a la técnica de agregación diploide de iPS marcadas (con GFP o Beta galactosidasa mediante infección lentiviral) con embriones receptores sin marcaje alguno.

Tanto en el caso de 4F-iPS como 3F-iPS se demostró que las células reprogramadas tenían la capacidad de integrarse con las mórulas donantes tras 24 h de incubación, formando blastocistos quiméricos (Figura 23). Por el contrario, los fibroblastos originales, no reprogramados, permanecieron al margen del embrión en formación sin llegar a formar parte de éste tras el proceso de agregación (Figura 23). Algunos de los blastocistos quiméricos resultantes se transfirieron en ratonas receptoras pseudopreñadas para su posterior gestación. En embriones recuperados a día 9.5 d.p.c. se observó la contribución de 4F y 3F-iPS a numerosos tejidos en desarrollo (Figura 24), siendo éste un criterio fundamental para considerar una línea celular pluripotente.

3.3. Estudio comparativo del potencial cardiogénico de células reprogramadas en presencia o ausencia de c-Myc

A pesar de todos los esfuerzos dedicados a entender y optimizar el proceso de reprogramación nuclear, se conoce poco sobre los efectos que ésta pueda tener sobre la diferenciación de las células reprogramadas. En este apartado se comparó la diferenciación *in vitro* de 4F-iPS y 3F-iPS centrándose en su capacidad cardiogénica.

Para estos experimentos se utilizó un protocolo de diferenciación espontánea basado en la formación de cuerpos embrionarios en gota colgante durante 48 h, su recuperación y mantenimiento en suspensión durante 48 h más y posteriormente, cultivo en placas gelatinizadas hasta completar 12 días. Se compararon tres clones de 4F-iPS y tres de 3F-iPS. En los estadios iniciales del proceso de diferenciación, no se observaron diferencias en la morfología o cinética de crecimiento de los diferentes clones estudiados (Figura 25), obteniéndose cuerpos embrionarios de forma y tamaño semejante al final del período de crecimiento en suspensión.

Estudios de la expresión génica, sin embargo, revelaron diferencias sustanciales en los niveles de expresión de marcadores de pluripotencia, permaneciendo éstos elevados tras 5 días de diferenciación en 4F-iPS, mientras ya habían disminuido en 3F-iPS (Figura 26). Así mismo, la expresión de genes relacionados con el proceso de gastrulación, habitualmente elevados a día 5, se mantuvo por debajo en los clones de 4F-iPS con relación a los 3F-iPS. Tanto la expresión de marcadores precardiacos como cardiacos fue superior en los clones de 3F-iPS con respecto a los de 4F-iPS entre los días 5 y 12 de diferenciación, haciendo suponer una disminución en la diferenciación cardiaca de 4F-iPS en comparación a 3F-iPS. Este hecho se comprobó tras monitorizar detalladamente la morfología y presencia de áreas de latido en los diferentes clones. A partir del día 8 de diferenciación se observó un crecimiento errático en los clones de 4F-iPS, con aparición de zonas de células desprendidas de la placa (Figura 27), mientras los clones de 3F-iPS mostraron una integridad sostenida de la monocapa celular así como de las zonas con formaciones complejas. Las diferencias se acentuaron hacia el final del protocolo de diferenciación, con los clones de 3F-iPS mostrando áreas de latido en muchas de sus colonias, mientras extensas áreas de 4F-iPS mostraban morfología propia de células muertas y no se encontraron áreas de latido. En un contaje preciso, se determinó la diferencia significativa entre las áreas de latido presentes en los cultivos de 3F-iPS y 4F-iPS en todos los días de diferenciación entre el 7 y el 11 (Figura 28). En conjunto, estos datos apuntan a la mayor capacidad cardiogénica de las células reprogramadas en ausencia de c-Myc.

De manera similar, estudios recientes han descrito que la presencia sostenida de los factores inductores de reprogramación en las iPS es responsable de una disminución en su capacidad de diferenciación hacia endodermo *in vitro* (Sommer, 2009). Esto podría deberse en ambos casos a una expresión residual (propia de los lentivirus utilizados en la transducción) de los factores de transcripción que dificultara la salida del estado indiferenciado

inducido. Sin embargo, al someter a estas células al entorno embrionario propio de las agregaciones diploides o inyecciones en blastocisto, se supera esta limitación, poniendo de manifiesto la idoneidad de estos procedimientos como sistemas de diferenciación.

3.4. Caracterización funcional del potencial cardiogénico de las células reprogramadas en ausencia de c-Myc

Tras determinar que la ausencia del oncogén c-Myc durante el proceso de reprogramación nuclear favorece la cardiogenicidad de las iPS generadas, se procedió al estudio de las características y propiedades de los cardiomiocitos derivados a partir de 3F-iPS.

Para ello, se aislaron cardiomiocitos a partir de los cultivos en gelatina mediante un gradiente de densidad. Imágenes de microscopía electrónica de las células obtenidas mostraron cambios en la morfología celular, así como estructuras contráctiles organizadas en el citoplasma y uniones tipo gap entre células adyacentes (Figura 29). Imágenes adquiridas por microscopía confocal tras inmunoflurescencia revelaron la presencia de diversas proteínas cardiacas, tales como el factor de transcripción Mef2c, α-actinina, conexina 43 y las cadenas ligeras de miosina-2 tanto auricular como ventricular en las células aisladas (Figura 29). Todas estas características coinciden con el fenotipo esperado en cardiomiocitos murinos en desarrollo, así como con los obtenidos a partir de ESC de ratón.

En el plano funcional, se documentó la sincronización de diferentes zonas de latido en cuerpos embrionarios en suspensión (Figura 30), así como la presencia y morfología de potenciales de acción espontáneos, estos últimos estudiados mediante patch clamp (Figura 31). Con esta misma técnica se detectó la presencia de canales de calcio ausentes en los fibroblastos originales

y responsables de la actividad eléctrica espontánea, lo que sugiere un perfil inmaduro de los canales iónicos propios de una célula cardiaca (Boheler, 2002). En experimentos paralelos, se cargaron las células aisladas con el marcador fluorescente de calcio Fluo-4 y se observaron al microscopio confocal. Los cardiomiocitos derivados de 3F-iPS mostraron variaciones rítmicas en el nivel de fluorescencia sincronizadas con contracciones mecánicas (Figura 32), indicando la presencia de la maquinaria propia de cardiomiocitos electro-mecánicamente funcionales.

Posteriormente, se analizó la capacidad de contribución *in vivo* al tejido cardiaco de las 3F-iPS. Para ello, células reprogramadas y marcadas con los casettes de expresión de lacZ y luciferasa se agregaron con 2 embriones en estadio de mórula (agregación diploide). Los blastocistos resultantes se transfirieron quirúrgicamente al útero de hembras receptoras pseudopreñadas, que los gestaron hasta su nacimiento. Algunos de los embriones fueron recuperados entre los días 8.0 y 9.5 d.p.c. En ellos, se observó la presencia de células positivas a la tinción con X-galactosidasa (derivadas por tanto de las iPS agregadas) en el parénquima cardiaco en desarrollo (Figura 33). En los animales que llegaron a término, se observaron manchas oscuras en el pelaje, originalmente blanco procedente de los embriones donantes CD1. Esto se corresponde con la presencia de iPS (procedentes de una línea murina de pelaje negro) en diferentes zonas del organismo. La contribución de las iPS a los diversos tejidos se analizó mediante imagen *in vivo* de la emisión de luz provocada por la luciferasa presente en estas células tras la inyección en los animales quiméricos de luciferina. Los niveles de quimerismo observados fueron variables en los diferentes animales estudiados, como corresponde al proceso de integración aleatoria que sucede en la agregación diploide (Figura 33).

Se estudió, además, el efecto de la integración de las 3F-iPS en las constantes vitales de los animales quiméricos. Al comparar un amplio número de parámetros generales (peso, temperatura corporal, etc, Tabla 7) se observó una

fisiología similar a la de los animales control. Del mismo modo, diversos parámetros de estructura y función cardiaca revelaron el normal funcionamiento del corazón en estos animales (Tabla 7 y Figura 34), sin signos de disrupción de la fisiología cardiaca debidos a la presencia de células ajenas al embrión. En conjunto, estos datos sugieren la capacidad de las 3F-iPS de integrarse en el corazón en desarrollo y adquirir, *in vivo,* todas las características necesarias para mantener una función cardiaca normal a lo largo de la vida del ratón quimérico.

3.5. Capacidad regenerativa de las iPS: modelo de infarto de miocardio en ratón

Entre sus posibles aplicaciones, las iPS suponen un nuevo reactivo aplicable a la medicina regenerativa, ya que pueden ser derivadas a partir de células del propio paciente, induciéndose en ellas la pluripotencia necesaria para que puedan diferenciarse y suplementar cualquier tipo de tejido. En este capítulo se utilizaron iPS indiferenciadas como tratamiento regenerativo en un modelo murino de infarto de miocardio, con el propósito de paliar los efectos de la isquemia cardiaca tanto a nivel morfológico como funcional.

En una primera aproximación *in vitro*, se comprobó que las células propuestas desarrollan un perfil de expresión coherente con la diferenciación cardiaca durante el protocolo aplicado de diferenciación (Figura 35). Se observó un aumento a día 5 de marcadores de gastrulación y mesodermo cardiaco así como una diferencia significativa en los niveles de marcadores cardiacos entre los días 0 y 12 de diferenciación, siendo estos mayores a día 12 (Figura 35). Se comprobó además la capacidad de estas células de participar en el desarrollo cardiaco *in vivo* (tras agregación diploide de iPS marcadas con embriones sin marcar) y su inclusión en el parénquima cardiaco en desarrollo (Figura 36).

Entre los ensayos utilizados para determinar la pluripotencia de las iPS éstas deben cumplir con la capacidad de formar teratomas tras su inyección subcutánea en el flanco de ratones inmunodeficientes. Sin embargo, esta capacidad supone una limitación en cuanto a bioseguridad si no puede ser regulada mediante la dosificación de las células o el efecto guía que pueda ejercer el lugar de inyección o los estímulos derivados del daño tisular. Se comprobó que la capacidad teratogénica de las iPS utilizadas en estos experimentos no desaparecía al ser introducidas mediante inyección intracardiaca en ratones inmunodeficientes previamente sometidos a infarto de miocardio (Figura 37). Por tanto, el entorno biológico creado en el corazón tras un daño isquémico no es suficiente para restringir el crecimiento incontrolado de estas células, siendo estos animales un modelo no válido para comprobar el potencial regenerativo de las iPS.

Se observó a continuación el crecimiento teratogénico tras inyección subcutánea de iPS en el flanco de animales inmunocompetentes. Ninguno de los animales inyectados desarrolló tumores visibles tras 8 semanas de observación (Figura 37), sugiriendo que este modelo podría ser útil a la hora de evaluar el efecto de las iPS en la regeneración post-isquémica.

Tras esta comprobación previa, se pasó a evaluar la permanencia e integración de las iPS en el corazón infartado, tras su inyección intracardiaca y los efectos derivados de ésta. Mediante imagen *in vivo* tras inyección de luciferina en los animales tratados se pudo observar luminiscencia en la parte izquierda del tórax, correspondiente al área de inyección inicial (Figura 38). La señal, procedente de las iPS marcadas, se mantuvo durante al menos 4 semanas, sin que pudiera identificarse crecimiento incontrolado más allá de los límites cardiacos. La lectura electrocardiográfica de los animales tratados mostró que la presencia de las células inyectadas no perturbó la homeostasis eléctrica en comparación con medidas previas (Figura 38).

Mediante estudios comparativos de ecocardiografía entre animales en los que se inyectaron iPS y otros en los que el tratamiento fue con fibroblastos no reprogramados, se determinó la mejora significativa de la función cardiaca tras el tratamiento con células reprogramadas (Figura 39). Los animales tratados con fibroblastos mostraron un descenso marcado en la fracción de eyección y el acortamiento fraccional, así como una disminución en el grosor del miocardio durante la sístole. Todos estos parámetros mejoraron en los animales tratados con iPS (Figura 39). Además, este tratamiento frenó la aparición de cambios estructurales inadecuados secundarios a una respuesta patológica tales como la hipertrofia y el desarrollo de aneurisma, manteniendo unos niveles de contractilidad del miocardio más próximos a los de un animal sano que en aquellos animales tratados con fibroblastos (Figura 40). En resumen, la inyección intracardiaca de iPS en un modelo de infarto de miocardio promueve la recuperación morfológica y de la función cardiaca en mayor medida que el tratamiento con fibroblastos, demostrando así su valor terapéutico.

En el análisis histológico de los corazones tratados al cabo de 4 semanas se observó la recuperación de la masa muscular en ausencia de cicatriz fibrosa tras el tratamiento con iPS (Figura 41). Tinciones con inmunofluorescencia revelaron la presencia de músculo estriado cardiaco, músculo liso y células del endotelio vascular derivados todos ellos de las células reprogramadas inyectadas. La participación de las iPS transplantadas a los diversos tipos celulares cardiacos explicaría, al menos en parte, las mejoras funcionales y morfológicas determinadas en este estudio.

En resumen, las iPS respondieron con una integración controlada y la formación de tejido quimérico al ser inyectadas en los alrededores del tejido cardiaco infartado, dando lugar a una recuperación de la función cardiaca así como a una reconstrucción tisular compuesta predominantemente por cardiomiocitos, pero con una pequeña contribución al músculo liso y endotelio

vascular. Esto pone de manifiesto el potencial de esta tecnología como terapia emergente para el tratamiento de las enfermedades cardiacas.

4. Pies de Figura y Tablas

Figura 1. Mortalidad global por enfermedad cardiovascular (en miles).

Figura 2. Tasas de enfermedad coronaria en los EEUU ajustadas en función de la edad (muertes por cien mil habitantes).

Figura 3. Tasas de mortalidad por enfermedad coronaria en la Unión Europea (muertes por cien mil habitantes).

Figura 4. Porcentaje de la tasas de mortalidad por enfermedad cardiovascular atribuible a diferentes patologías.

Figura 5. Alcance de la medicina regenerativa. El objetivo fundamental de la medicina regenerativa es reparar un tejido dañado. Las estrategias utilizadas para ello son *reemplazo, regeneración* y *rejuvenecimiento.*

Figura 6. Células madre embrionarias. Aisladas de la masa interna celular del blastocisto, poseen la capacidad de multiplicarse indefinidamente en cultivo y dar origen a células derivadas de las tres capas embrionarias.

Figura 7. Células madre perinatales. La sangre de cordón umbilical es fuente de este tipo de células, que contiene tanto progenitores similares a los de la médula ósea como células semejantes a las células madre embrionarias.

Figura 8. Células madre adultas. Pueden proceder de la médula ósea, grasa o de la sangre circulante. En la médula ósea existen tanto células hematopoyéticas, capaces de diferenciarse a cualquier célula sanguínea, como mesenquimales, con un mayor espectro de diferenciación. Estas últimas se utilizan en aplicaciones clínicas para la regeneración de tejido no hematológico.

Figura 9. Manipulación para la obtención de células pluripotentes. Estas células, con características similares a células madre embrionarias, se pueden producir a partir de células somáticas mediante *clonación terapéutica* o *reprogramación nuclear*. En el primer caso, se combina el contenido nuclear de la célula somática con un oocito desprovisto de núcleo, resultando en el desarrollo de un blastocistos del que se extraen células madre pluripotentes a partir de la masa interna celular. La misma célula somática puede sufrir una reprogramación nuclear por expresión ectópica de cuatro genes (Oct4 y Sox2 junto con Klf4 y c-Myc o Lin28 y Nanog). Son las llamadas iPS (células pluripotentes inducidas).

Figura 10. Herramientas para la indicción de pluripotencia. El ingrediente fundamental para la reprogramación son las células originales, de las que se han usado diferentes tipos y procedencias. Las moléculas inductoras de la reprogramación provocan los cambios estructurales y de expresión necesarios para restablecer la pluripotencia. Se han identificado facilitadores dirigidos a eliminar posibles barreras que limitan la eficiencia del proceso. Las interacciones entre estos tres componentes son fundamentales para optimizar la reprogramación nuclear.

Figura 11. Estrategia de selección de candidatos para la reprogramación. Un grupo original de 24 genes fue estudiado hasta reducir a 4 (Oct4, Sox2, Klf4 y c-Myc) los necesarios para inducir pluripotencia en células somáticas. En otra aproximación, se estudiaron 97 genes candidatos que revelaron una segunda combinación posible, confirmando la presencia de Oct4 y Sox2, como en el caso anterior, y añadiendo Lin28 y Nanog como alternativa a los otros dos componentes.

Figura 12. Estrategias de introducción de factores inductores de pluripotencia. Inicialmente se utilizó la infección con lentivirus o retrovirus para la inducción del proceso de reprogramación, sin embargo la inserción genómica propia de esta técnica supone el riesgo de desarrollo de tumores. Por tanto, se estudiaron otras alternativas como la eliminación enzimática de restos de integración de los factores usados o el uso de vectores que no provoquen este tipo de modificaciones genómicas.

Figura 13. Caracterización rigurosa de la pluripotencia. Las células reprogramadas mediante cualquiera de los métodos descritos, deben cumplir ciertos criterios para poder ser consideradas iPS. Estos son, capacidad de diferenciación a tejidos de las tres capas embrionarias *in vitro*, desarrollo de teratomas *in vivo*, tras su inyección en ratones inmunodeprimidos, así como formación de quimerismo *in utero*, incluyendo transmisión a la línea germinal. Por último, la regeneración *in situ* a partir de células reprogramadas determina la

capacidad de respuesta a los estímulos enviados por el tejido dañado y la generación *de novo* de nuevos tipos tisulares necesarios para su reparación.

Figura 14. Regeneracion terapéutica inducida por iPS. La finalidad última de la reprogramación nuclear consiste en producir células autólogas que contribuyan a la recuperación de la homeostasis funcional una vez transplantadas en un receptor enfermo. Las células, obtenidas de una biopsia mínimamente invasiva, se reprogramarían, diferenciarían a los tejidos de interés, y transplantarían de nuevo para ejercer su función terapéutica en el individuo afectado.

Figura 15. Diagrama explicativo del protocolo de agregación diploide. Generación de embriones donantes salvajes (*amarillo)*. En paralelo, cultivo de células pluripotentes inducidas marcadas con GFP o Beta galactosidasa por infección lentiviral (*azul)*. Obtención de ratonas pseudopreñadas (*verde)* que reciben los blastocistos quiméricos vía transferencia intrauterina (*naranja)* y los gestan hasta el término del embarazo.

Figura 16. La sustitución H87Q en la cápside aumenta la infectividad del vector derivado de VIH en células de ratón. A) Sustituciones naturales en la cápside se introdujeron en la región responsable de la unión a ciclofilina A del gen *gag* del VIH-1 en una construcción del vector de la envoltura, p8.9Ex. Se generaron vectores infectivos de VIH que contenían la proteína fluorescente verde y las mutaciones inducidas, y se normalizó la cantidad de vector en función de la actividad transcriptasa inversa. Se infectaron líneas celulares humanas, murinas y de mono, y se analizó la fluorescencia verde mediante citometría de flujo. B) Se infectaron 50000 fibroblastos de ratón con cantidades crecientes de vectores, comparando el número de células fluorescentes al microscopio (3 días después de la infección, izquierda) o por citometría de flujo (5 días después de la infección, derecha).

Figura 17. Expresión de los factores asociados a pluripotencia en células humanas y murinas. A) Porcentaje de homología entre la secuencia de aminoácidos de los factores de pluripotencia en diversas especies. La homología para LIF sirve de guía. La homología se determinó usando el programa LALIGN (EmBNet). NA= secuencia no disponible. B) Representación esquemática de la construcción usada para expresar los factores de pluripotencia. . ψ; señal de empaquetamiento, LTR; secuencias repetitivas, RRE; Elemento de respuesta a Rev, cPPT; zona central de polipurina, SFFV; promotor del virus formador de focos en el bazo, WPRE; elemento regulador post-transcriptional del virus de la hepatitis de Woodchuck. Los cDNA de OCT3/4, SOX2, KLF4 y c-MYC están bajo un promotor interno SFFV. El vector que codifica para Klf4 no tiene WPRE. B) 2 x 10^5 293T células fueron infectadas con 50

µl de vectores de expresión de los factores. Tres días después de la infección, se verificó la expresión completa de los factores de pluripotencia mediante western blot con los correspondientes anticuerpos. C) 5 x 10^4 fibroblastos (MEFs) se infectaron con 100 µl de vectores sin concentrar. Se visualizaron los niveles de expresión de los transgenes mediante inmunotinción con anticuerpos específicos 4 días después de la infección.

Figura 18. Cinética de reprogramación de fibroblastos embrionarios de ratón con y sin c-Myc. Se infectaron fibroblastos de ratón con 4 (SOX2, OCT4, KLF4 y c-MYC) o 3 (SOX2, OCT4 y KLF4) lentivirus derivados de VIH que contenían los factores humanos, tras un día de cultivo. Colonias redondeadas y compactas similares a las de células madre embrionarias se pudieron observar tras dos semanas de cultivo en el caso de células infectadas con 4 factores y tras tres semanas en las infectadas con 3 factores.

Figura 19. Las células reprogramadas en presencia y ausencia de c-Myc son pluripotentes. A) Se detectó integración genómica de las construcciones virales en las células derivadas, estando c-Myc ausente de las reprogramadas con 3 factores. No se encontró ninguna integración en los fibroblastos originales (control negativo). B) Sólo las células manipuladas fueron positivas para tinción con fosfatasa alcalina (AP) y el marcador de células madre SSEA1, ambos ausentes de los fibroblastos originales identificados por la tinción de núcleos en azul con DAPI.

Figura 20. El proceso de reprogramación causa cambios microestructurales. A) Imágenes de microscopía electrónica de barrido (SEM) revelan profundos cambios morfológicos entre los fibroblastos parentales y los reprogramados. B) Las características citoplasmáticas detectadas por microscopía electrónica de transmisión (TEM), tales como mitocondrias inmaduras (im) y elevada relación núcleo:citoplasma diferencian claramente las iPS y células madre embrionarias de los fibroblastos, éstos últimos con mitocondrias maduras (mm).

Figura 21. Reprogramación del perfil de expresión de marcadores de pluripotencia en las células manipuladas. Tras el proceso de reprogramación, las células infectadas con 4 o 3 factores mostraron una elevada expresión de marcadores relacionados con pluripotencia (Sox2, Oct4 y Fgf4) al compararlas con células control (MEFs).

Figura 22. Diferenciación a tejidos de las tres capas embrionarias en teratomas inducidos *in vivo.* A) Se monitorizó la diferenciación espontánea *in vivo* tras la inyección subcutánea en ratones inmunodeficientes, comparando los fibroblastos nativos e infectados. B) Sólo se detectó crecimiento tumoral tras 1-2 semanas en los lugares de inyección de células

manipuladas. C) Se muestreó tejido tras 4-6 semanas, encontrándose una compleja arquitectura tumoral que contenía tejidos como músculo, queratina, epitelio y cartílago.

Figura 23. Pluripotencia *ex utero* de las células reprogramadas. A-B) MEFs originales o marcados con GFP o lacZ tras la reprogramación se usaron para la agregación diploide con embriones tempranos. C) Agregación entre las células reprogramadas marcadas y los embriones salvajes dio lugar a embriones quiméricos, mientras los fibroblastos originales no se integraron en la mórula compactada tras 24 h de incubación. D) Los embriones quiméricos evolucionaron correctamente desarrollando la esperada cavidad interna y una masa interna celular compuesta de células reprogramadas marcadas y otras salvajes sin marcar.

Figura 24. Organogénesis derivada de las células reprogramadas. Los embriones quiméricos fueron transferidos a ratonas pseudopreñadas y recogidos a día 9.5 d.p.c. para análisis de tejidos. Se observó contribución de las células reprogramadas a diversos tejidos del embrión por medio de microscopía confocal (células reprogramadas con 4 factores, 4F-iPS, marcadas con GFP) o tras una tinción para Beta galactosidasa (células reprogramadas con 3 factores, 3F-iPS). Se identificaron iPS en el sistema nervioso central (A, A') romboencéfalo (B, B'), arcos faríngeos (C, C'), corazón (D, D'), esbozo de las extremidades (E, E') y somitas (F, F').

Figura 25. 4F-iPS y 3F-iPS tienen semejante cinética de crecimiento y de formación de cuerpos embrionarios. A) Se cultivaron diversos clones de 4F-iPS y 3F-iPS en condiciones de indiferenciación. Todos los clones estudiados mostraron semejante morfología, con presencia de colonias compactas y redondeadas. B) Se procedió a la formación de cuerpos embrionarios a mediante el método de gota colgante. Los cuerpos embrionarios resultantes de todos los clones estudiados mostraron tamaños y formas similares. Barra=500 μm.

Figura 26. 4F-iPS y 3F-iPS muestran diferentes perfiles de expresión durante su diferenciación *in vitro*. Se llevó a cabo la diferenciación de iPS mediante la formación de cuerpos embrionarios seguida de su cultivo en placas gelatinizadas. Se tomaron muestras de las células indiferenciadas a día 0, de cuerpos embrionarios en suspensión a día 5 y de los cultivos diferenciados a día 12. A) La expresión de genes relacionados con la pluripotencia disminuye con el comienzo de la diferenciación en 3F-iPS, mientras se mantiene elevada en 4F-iPS. B) Los marcadores de gastrulación estudiados tienen su pico de expresión a día 5 en 3F-iPS, mientras que se muestran erráticos en 4F-iPS. C) Los niveles de expresión de genes precardiacos aumentaron de forma consistente a día 5 en todos los clones estudiados, sin embargo, la expresión relativa fue notablemente superior en 3F-iPS. D) La expresión de factores de

transcripción cardiacos aumentó a día 12 en 3F-iPS, con los clones de 4F-iPS manteniendo niveles más bajos.

Figura 27. 3F-iPS se diferencian dando lugar a áreas de latido mientras 4F-iPS desarrollan una morfología y viabilidad inconsistente *in vitro.* Tras un total de 5 días de crecimiento en suspensión, se procedió al cultivo en placas gelatinizadas de los diferentes clones estudiados. A) Las diferencias morfológicas entre 3F-iPS y 4F-iPS se hicieron evidentes a partir del 8º día de diferenciación. 4F-iPS mostraron zonas de células redondeadas y despegadas de la placa (flechas, izquierda). Todos los clones de 3F-iPS crecieron normalmente expandiéndose hacia el exterior de los cuerpos embrionarios y manteniendo en todo momento la integridad de la capa celular. B) Tras 12 días de cultivo se observó la aparición de extensas áreas de muerte celular en 4F-iPS (flechas, izquierda) mientras el crecimiento de 3F-iPS siguió siendo compacto incluyendo la aparición de numerosas áreas de latido espontáneo (línea punteada roja). Barra=500 µm.

Figura 28. La reprogramación independiente de c-MYC favorece el potencial cardiogénico de las iPS. Se monitorizó diariamente la aparición de áreas de latido en los cultivos de 4F-iPS y 3F-iPS. Entre los días 7 y 11 de diferenciación, so se detectó ninguna actividad espontánea en los clones de 4F-iPS (n=8). En contraste, las áreas observadas en 3F-iPS aumentaron en ese periodo de tiempo y demostraron una actividad sostenida (n=4).

Figura 29. Cardiogénesis estructural a partir de 3F-iPS. A) Microscopía electrónica de cardiomiocitos derivados de 3F-iPS reveló cambios morfológicos de colonias compactas originales a células de aspecto alargado similares a cardiomiocitos (panel superior). Se detenctaron proteínas contráctiles de alta densidad organizadas en estructuras sarcoméricas (panel central) y uniones tipo gap entre células adyacentes (panel inferior). B) Inmunotinción reveló la presencia de la proteína contráctil α-actinin junto con el factor de transcripción Mef2c (panel superior izquierdo), proteína conexina 43 de uniones tipo gap (panel inferior izquierdo) e isoformas auricular (panel superior derecho) y ventricular (panel inferior derecho) de la cadena ligera de la miosina, todos ellos en cardiomiocitos aislados.

Figura 30. Cardiogénesis funcional derivada de 3F-iPS. A) Se documentó la presencia de actividad contráctil sincronizada (rectángulos, panel superior) en cuerpos embrionarios en suspensión (panel inferior). B) Se identificaron potenciales de acción en las células aisladas mediante la técnica de patch clamp en modo corriente constante.

Figura 31. Potenciales de acción espontáneos dependientes de calcio en cardiomiocitos derivados de 3F-iPS. A) Se detectó una corriente hacia el interior en los cardiomiocitos aislados (línea negra) ausente de los fibroblastos originales (línea roja). B) La eliminación del calcio extracelular suprimió dicha corriente. C) Los potenciales de acción espontáneos se suprimieron de manera reversible en medio libre de calcio.

Figura 32. Acoplamiento excitación-contracción dependiente de calcio en cardiomiocitos derivados de 3F-iPS. A) Cardiomiocitos marcados con Fluo-4AM mostraron movimientos de calcio intracelular consistentes con ondas transitorias de calcio. B) Las fluctuaciones rítmicas del calcio intracelular coincidieron con las contracciones mecánicas de la célula.

Figura 33. Las iPS contribuyen de manera sostenida al quimerismo durante el desarrollo y la vida adulta. A-C) Tras la agregación diploide, se documentó la presencia y contribución cardiaca de iPS durante el desarrollo embrionario como se muestra para los días 8.0 a 9.5 d.p.c. D) Los ratones quiméricos sólo se diferenciaron de los control por las manchas en el color del pelo. E) Se detectaron los niveles de quimerismo en función de la distribución de la señal emitida por la luciferasa procedente de las iPS marcadas.

Figura 34. El quimerismo cardiaco contribuye al mantenimiento de la función cardiaca normal. A) Las medidas electrocardiográficas fueron equivalentes entre quimeras y controles. B) Imágenes obtenidas mediante ecocardiografía muestran una estructura normal del corazón, válvulas y grandes vasos, con funciones sistólica y diastólica similares para ambos grupos. Ao: aorta, LV: ventrículo izquierdo; LVDd: diámetro diastólico del ventrículo izquierdo, LVDs: diámetro sistólico del ventrículo izquierdo, RV: ventrículo derecho. Barra=2 mm.

Figura 35. Las iPS recapitulan la diferenciación cardiaca *in vitro.* A) Clones de iPS marcados con Beta galactosidasa se mantuvieron en cultivo indiferenciado previo a la formación de cuerpos embrionarios. B) Aumento de la expresión de marcadores de gastrulación y mesodermo cardiaco a día 5 de diferenciación. C) Comparación de los perfiles de expresión génica a día 0 y 12 de diferenciación, mostrando una inducción significativa de los factores de transcripción cardiacos Mef2c (P=0.049; n=3), Gata 4 (P=0.049; n=3) y Miocardina (P=0.049; n=3).

Figura 36. Recapitulación *in utero* del potencial cardiogénico de las iPS. A) Los embriones salvajes usados para las agregaciones diploides aportan el medio adecuado para

determinar la diferenciación específica de tejido (panel superior izquierdo). Células madre embrionarias de ratón sometidas a agregación diploide contribuyen de forma difusa al desarrollo del embrión, como se pone de manifiesto al teñir una línea marcada con lacZ bajo un promotor ubicuo (panel superior derecho). Cuando el marcaje está bajo el promotor específico cardiaco α-MHC las células sólo se detectan en la zona correspondiente al corazón en desarrollo (panel inferior izaquierdo). iPS marcadas con lacZ bajo el promotor ubicuo CMV aparecen repartidas por todo el embrión (panel inferior derecho). B) El quimerismo obtenido con iPS muestra una importante contribución al corazón en desarrollo a día 9.5 d.p.c. Barra=100 μm. C) El parénquima cardiaco de un embrión quimérico de 9.5 d.p.c. contiene células derivadas de iPS integradas, como se puede observar tras una tinción con Beta galactosidasa. Barra=50 μm.

Figura 37. El comportamiento de las iPS está determinado por el estado inmunológico del receptor. A) La inyección subcutánea de medio millón de iPS en un receptor inmunodeprimido, resultó en el desarrollo de teratomas (línea punteada). B) El transplante intramiocárdico de 200000 iPS en un modelo de infarto agudo de miocardio también dio lugar a la formación de tumores que crecieron de forma dramática durante 4 semanas, como se detectó por luminiscencia. C) Ecocardiografía (panel superior izquierdo) también reveló el tamaño del tumor, que fue posteriormente comprobado en la necropsia de los animales inmunodeprimidos. La histología del tumor mostró una expansión más allá de la pared cardiaca (panel inferior izquierdo) e infiltración en el miocardio infartado (panel inferior derecho). D) Receptores inmunocompetentes no desarrollaron tumores tras la inyección subcutánea de medio millón de iPS (rectángulo amarillo). E) La inyección subcutánea de iPS produjo tumores en el 75% de los animales inmunodeprimidos en contraste con el 0% de los inmunocompetentes.

Figura 38. Las iPS se integran en el tejido receptor sin interrumpir la conducción eléctrica. A) Las iPS introducidas mediante inyección intracardiaca en el miocardio infartado de ratones inmunocompetentes se detectaron por imagen *in vivo* durante las 4 semanas de seguimiento. B) Se encontraron algunos, pero escasos, grupos de células positivas para SSEA1 en el miocardio inyectado. Barra=10 μm. C) El ritmo cardiaco previo al Infarto se mantuvo tras el transplante de iPS durante las 4 semanas de seguimiento, con ondas P (triángulos) precediendo cada complejo QRT (asteriscos), sin que se detectara taquicardia ventricular u ondas ectópicas.

Figura 39. Las iPS restablecen la función cardiaca tras un infarto agudo de miocardio. A) Se inyectaron iPS o fibroblastos 30 minutos después del infarto en ratones randomizados a los dos grupos. Se detectó un cambio significativo en la evolución de la fracción de eyección (EF) de los dos grupos desde una semana después del tratamiento hasta el final del

seguimiento. *P=0.002 por cálculo de ANOVA. B) El acortamiento fraccional fue similar un día después del tratamiento, pero mejoró significativamente en los corazones tratados con iPS. Las líneas indican la mediana. *P=0.01. C) El grosor de la pared durante la sístole se mantuvo tras tratamiento con iPS, pero no con fibroblastos. *P=0.006. D) Imágenes de ecocardiografía del eje largo del corazón revelaron adelgazamiento de la pared anterior y formación de aneurisma en el apex (flechas) en los corazones tratados con fibroblastos, como demostró la akinesis (izquierda) comparada con la motilidad normal de la pared durante la sístole en los corazones tratados con iPS (derecha). E) Imágenes del eje corto del corazón confirmó el adelgazamiento de la pared anterior (línea roja) y una disminución global de la función cardiaca tras la intervención con fibroblastos en comparación con iPS. Las líneas de puntos amarillos y blancos indican endocardio y epicardio respectivamente.

Figura 40. Las iPS evitan el remodelado patológico y preservan la estructura cardiaca. A) Parámetros diastólicos demostraron un descenso significativo de la dimensión global del ventrículo izquierdo en sístole (LVDd) en los animales tratados con iPS en comparación con los tratados con fibroblastos, 4 semanas después de la terapia. *P=0.007. B) Ecocardiografía en M-mode mostró una dilatación en la luz ventricular con reducción en el grosor de la pared anterior y septal (SWTs) durante la sístole tras tratamiento con fibroblastos (panel superior), que mejoró tras tratamiento con iPS (panel inferior). C) El tiempo de repolarización-despolarización ventricular, medido por medio del intervalo QT, resultó significativamente mayor en los corazones tratados con fibroblastos. *P=0.004. D) Los corazones tratados con fibroblastos se hipertrofiaron de manera patológica, incluyendo formación de aneurisma (+) y un adelgazamiento severo de la pared muscular (+) visible por transiluminación, al compararlos con la estructura conservada de los corazones tratados con iPS, que conservaron la geometría apical (-) y paredes gruesas y opacas (-) en una vista por debajo del sitio de ligadura quirúrgica (línea punteada amarilla). Barra=5mm. El aneurisma está delineado por un círculo punteado amarillo. RA: aurícula derecha; LA: aurícula izquierda; LV: ventrículo izquierdo; s: sutura; SWTd: Grosor de la pared septal en diástole; ; SWTs: Grosor de la pared septal en sístole; PWTd: Grosor de la pared posterior en diástole; PWTs: Grosor de la pared posterior en sístole.

Figura 41. El tratamiento con iPS reduce la cicatriz y contribuye a la reconstrucción de varios tipos celulares. A) 4 semanas después del tratamiento, la tinción tricrómica de Masson demostró una reducción en el grosor de la pared anterior (AWT) y presencia de fibrosis (tinción azul) en los corazones tratados con fibroblastos (izquierda), en comparación con los tratados con iPS (derecha). RV: ventrículo derecho. B) Autopsia de los ratones tratados con iPS demostró ausencia de tumores en el corazón, hígado, pulmón y bazo. C) 4 semanas después de la inyección, células derivadas de las iPS expresaban marcadores de

músculo cardiaco (α-actinin, derecha) coexpresadas con Beta galactosidasa (puntas de flecha), ausente tras tratamiento con fibroblastos (izquierda) D, E) Actina de músculo liso (α-SMA) y el marcador endotelial CD31 colocalizaron con la expresión de Beta galactosidasa (punta de flecha) en células derivadas de iPS (derecha), pero no de fibroblastos (izquierda). Núcleos teñidos con DAPI. Barra=5 µm.

Figura 42. Marcadores de diferenciación *in vitro* para células madre embrionarias de ratón. Adaptado de Boheler, 2002.

Tabla 1. Clasificación de células madre.

Tabla 2. Origen de las células somáticas de ratón reprogramadas.

Tabla 3. Origen de las células somáticas humanas reprogramadas.

Tabla 4. Células específicas de paciente reprogramadas.

Tabla 5. Anticuerpos primarios

Tabla 6. Anticuerpos secundarios

Tabla 7. Comparación cardiovascular entre grupo control y de quimeras 3F-iPS. La comparación entre los signos vitales y los parámetros de estructura y función cardiovascular no reveló ninguna diferencia entre ambos grupos.

III. INTRODUCTION

1. Cardiovascular disease

Cardiovascular disease (CVD) is the number one cause of death worldwide. This encompasses disorders of the heart and blood vessels, including coronary (ischemic) heart disease, cerebrovascular disease, peripheral arterial disease, hypertension, heart failure and congenital cardiovascular defects (Lloyd-Jones, 2009). About 17.5 million people died from CVD in 2005, representing 30% of all global deaths, most of them occurring in low and middle income countries (WHO, 2007). From them, an estimated 7.6 million deaths were due to coronary heart disease (CHD) (**Figure 1**). CVD is projected by the World Health Organization to remain the single leading cause of death by 2015.

Figure 1. Global mortality due to cardiovascular disease. Deaths from ischemic heart disease worldwide each year (in thousands)

Approximately one in three American adults suffers from at least one type of cardiovascular problem, with close to 17 million cases of CHD and 5.7 million heart failures in the United States. CHD, comprising heart attack and angina pectoris, is the single leading cause of death in the United States both for males and females (**Figure 2**). Every year, over 600 thousand new cases of myocardial infarction (MI) and 325 thousand recurrent ischemic events arise in the United

States. An estimated of 18 percent of men and 23 percent of women at age 40 or older will die within one year following first MI. This mortality increases up to 33 percent in men and 43 percent in women, within five years following first MI. Beyond this, close to one million Americans suffer from CHD refractory to treatment, with 75 thousand new cases every year. This is a highly impairing condition in which angina occurs at rest or during simple activities. In these patients, the treatment of ongoing, debilitating pain becomes the focus of care without a curative therapy to approach the source of the problem (USDH, 1994).

Overall, the cost of CHD to the healthcare system of the United States for 2009 is expected to be around $165.4 billion (Lloyd-Jones, 2009).

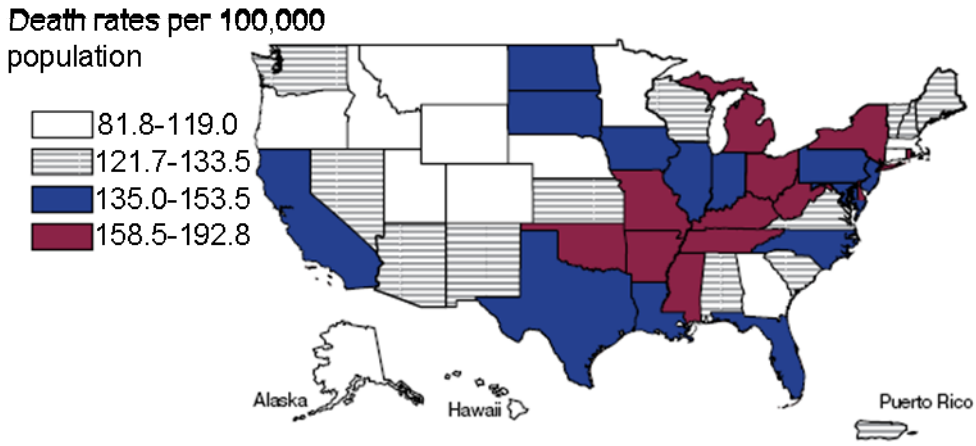

Figure 2. Age-adjusted coronary heart disease rates in the United States

This landscape is not different in Europe (**Figure 3**), where CVD is the largest cause of sickness and morbidity and a major cause of death, premature death and reduced quality of life (Leal, 2006). On the economic side, CVD accounts for about 12 percent of the EU healthcare system costs every year.

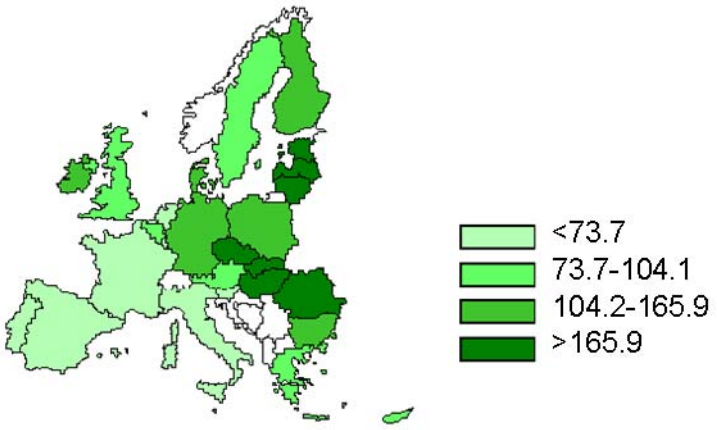

Figure 3. Mortality rates due to coronary heart disease in the European Union countries. Death rates per 100,000 population. Adapted from (2006)

In Spain, CVD causes a third of the total deaths, with cardiac ischemia representing 30 per cent of them, cerebrovascular accidents accounting for 27 per cent and cardiac insufficiency for 16 per cent, as major single contributors (**Figure 4**). Overall, cardiac disease represents above 73 per cent of the total mortality due to cardiovascular disease (2009).

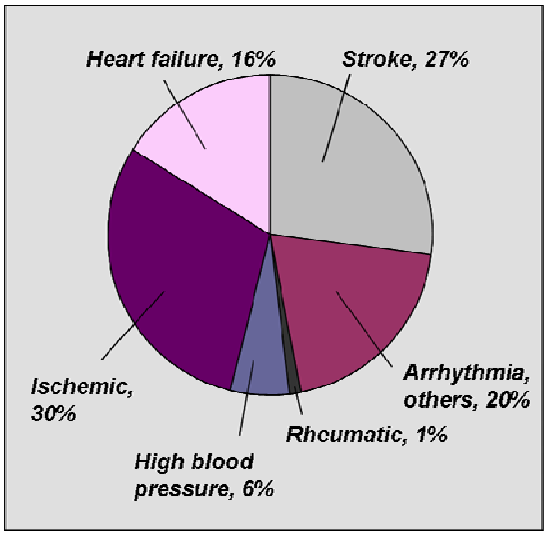

Figure 4. Mortality rates due to cardiovascular disease in Spain.

With the current therapeutic armamentarium, CVD treatment starts with preemptive actions to reduce risk factors, advances through various pharmacological therapies (such as ACE inhibitors, β-blockers, antiplatelet agents, and statin therapy) (Schocken, 2008) in an attempt to prevent heart failure by attenuating structural remodeling and possible symptoms and enters into the surgical approach relatively early in the disease development.

The contribution of CHD to HF is not limited to the initial ischemic insult alone. The progressive nature of CHD also contributes to recurrent cardiovascular events, sudden death, and the progression to HF. An acute MI depletes functional myocyte reserve, with ensuing myocardial fibrosis and development of LV remodeling. The resulting chamber dilation and neurohormonal activation lead to progressive deterioration of the remaining viable myocardium (Sutton and Sharpe, 2000). Long-standing (chronic) ischemia superimposed on damaged myocardium may result in “hibernation,” which produces a further progressive decline of ventricular function. Restoration of blood flow by mechanical or pharmacological revascularization with β-blockers or statins may improve contractility in hibernating areas (Gheorghiade M, 2003).

If these interventions fail, the patient situation usually aggravates substantially, leaving little therapeutic options, with the only curative treatment for a severe cardiac insufficiency being heart transplant. However, this is not an easy approach; at least as many patients as received a heart in the US in 2007 are still on a transplant waiting list (Lloyd-Jones, 2009). Beyond the organ shortage, five-year mortality rates average around 30 percent, highlighting the need for a more accessible and efficient therapeutic option (Lloyd-Jones, 2009).

2. Regenerative Medicine

Regenerative medicine is a young discipline that aims to treat the root cause of a degenerative disease causing cell destruction and irreversible loss of

tissue function, restoring the native cellular architecture and organ performance (Waldman, 2007).Regenerative medicine, propelled by the recent progress made in transplant medicine, stem cell biology, and related biomedical fields, is primed to expand the therapeutic armamentarium available in the clinical setting, and thereby, ameliorate disease outcome by shifting the scope of medical sciences from traditional palliation, which mitigates symptoms, to curative therapy aimed at treating the disease cause (Daley and Scadden, 2008)

2.1. Goals of Regenerative Medicine

Regenerative medicine aims to restore normal structure and function following tissue injury. Stem cells and their natural or engineered products— collectively recognized as *biologics*— provide the functional components of a regenerative therapeutic regimen. Stem cells maintain an autonomous self-renewal potential and respond to guiding signals to differentiate into replacement tissues (Klimanskaya, 2008). By healing an injury, stem cells have the capacity to cure the underlying tissue damage through *de novo* formation of proper structure and function. Restoration of diseased tissues offers a sustained therapeutic advantage in conditions ranging from congenital disease to acquired, age-related pathologies. The outcome depends on the aptitude of the stem cell population to secure maximal, tissue-specific repair and the production of a nurturing niche environment in diseased tissue that enables the execution of repair (Morrison and Spradling, 2008).

Beyond restoration of structure and function, regenerative medicine paves a pathway for prevention and delay in disease progression through prophylactic repair. Due to their plasticity, stem cells provide a unique platform to select, guide, and engineer cellular characteristics required for enhanced tolerance while effectively treating and/or preventing disease manifestation. By anticipating the needs of disease-susceptible tissues, the goal of regenerative medicine becomes the repair of threatened tissues with stress-tolerant cells to prevent irreversible

damage. Preemptive regenerative therapy requires the ability to predict disease susceptibility based on molecular profiling at the earliest stages in order to guide appropriate and timely stem cell-based interventions (Waldman and Terzic, 2008).

2.2. Therapeutic Repair Strategies

Among the used strategies in regenerative medicine we find replacement, regeneration, and rejuvenation (**Figure 5**). These strategies overlap in practice while inherent distinctions conceptualize the scope of regenerative medicine, ranging from transplantation of used parts ("replacement") to development of new parts ("regeneration") to induction of self-renewed parts ("rejuvenation").

2.2.1. Replacement

Replacement refers to transplantation of a cell-based product that re-establishes homeostasis for the recipient through continuation of the tissue function from the donor (Atala, 2008). This includes solid organ transplantation and cell-based replacement, routinely used in the form of red blood cell transfusions to replenish the circulating blood pool. This strategy "recycles" used parts of cells, tissues, or organs to "restore" physiologic function. A significant limitation of the replacement strategy remains the shortage of appropriate donors and the difficulty to match the immunological criteria for a safe and effective transplantation.

2.2.2. Rejuvenation

Rejuvenation refers to self-renewal of tissues from endogenous, resident stem cells to maintain tissue homeostasis and promote tissue healing (Surani and McLaren, 2006). This strategy "renews" tissue structure by "recycling" endogenous stem cells for proactive self-renewal. Rejuvenation ensures continuous production of renewable tissue required for long-term stress tolerance; however, most tissues are able to only partially self-renew. In the

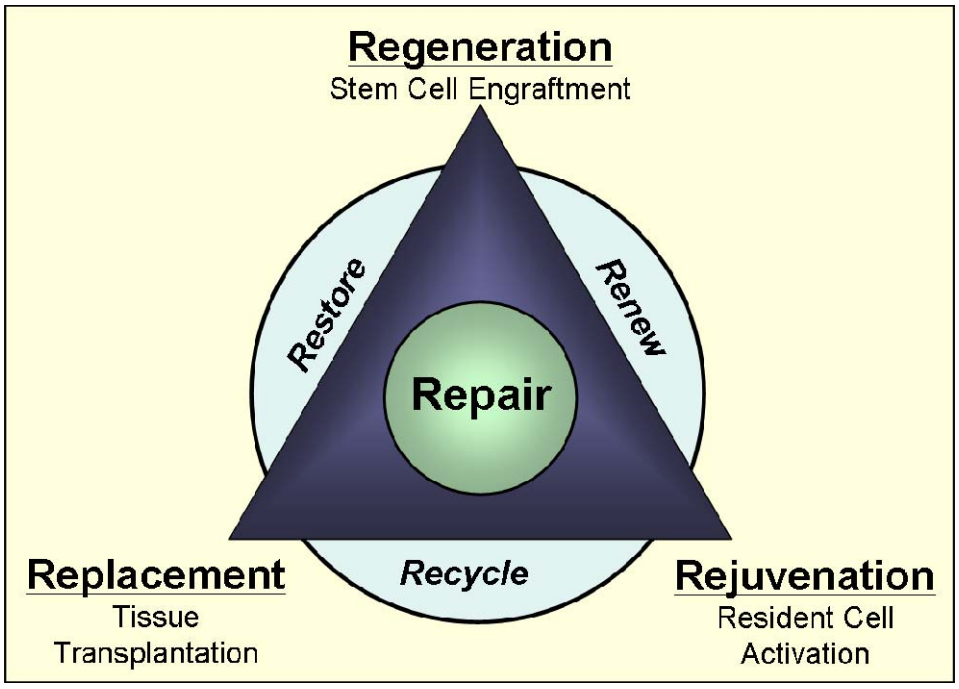

Figure 5. The scope of regenerative medicine
Repair is the central goal of regenerative medicine that encompasses the general strategy triad: replacement, regeneration, and rejuvenation. Replacement is defined as repair of damaged tissue by recycling used parts through tissue/organ transplantation. Regeneration is defined as repair of damaged tissue through differentiation of progenitor cells to replace damaged cells and restore tissue function. Rejuvenation is defined as repair of damaged tissue through activation of endogenous resident stem cells that can stimulate biogenesis and replenish functional tissue. Collectively, therapeutic repair strategies are recognized as the "R3" regenerative medicine paradigm.

context of a massive acute injury, such as myocardial infarction, an inherent repair strategy may be insufficient (Anversa and Nadal-Ginard, 2002). A boost in these natural processes, through biologic or pharmacologic treatment, is likely required to stimulate adaptive response and promote adequate biogenesis of functional tissue in the setting of acute or progressive disease.

2.2.3. Regeneration

Regeneration refers to engraftment of progenitor cells that require in vivo growth and differentiation to establish recipient homeostasis through *de novo*

function of the stem cell-based transplant. Advances in hematology gave rise to the concept of regeneration with the identification of bone marrow-derived stem cells that once harvested could be transplanted in small quantities into the peripheral blood to engraft and reconstitute the functioning bone marrow through continuous production of the entire hematopoietic system (Korbling and Estrov, 2003). This strategy “restores” function by “renewing” the pool of functional progenitor cells to allow differentiation as needed from exogenous stem cells. An intense search is ongoing for tissue-specific, nonhematopoietic stem cells that have the capacity to re-establish lost function when ectopically transplanted into a wide range of diseased tissues, as evident in diabetes, ischemic heart disease, and degenerative neurological diseases.

2.3. Regenerative Medicine Biologics

Regenerative medicine utilizes endogenous as well as exogenous natural or bioengineered stem cells to augment innate healing processes in order to supplement repair deficiencies (Atala, 2008; Chien, 2008). Stem cell platforms offer a continuum of potential lineages ranging from pluripotent to oligopotent cytotypes. Pluripotent stem cells can give rise to all germ layers, and subsequently all adult tissues in the body, providing a universal tool for regeneration (Silva and Smith, 2008). Alternatively, oligopotent progenitors offer a more limited scope of differentiation depending on a particular tissue-specific environment, and thereby provide a focused approach to repair (Orkin and Zon, 2008; Zhao, 2008). Matching the needs of the specific disease condition with the unique abilities of selected progenitor cells has emerged as the critical challenge for effective translation of discovery science into safe clinical applications (Shizuru, 2005). Thus, stem cells are isolated from either natural sources or bioengineered from non-reparative tissues to provide a spectrum of progenitor cells with unique features for diverse regenerative applications (**Table 1**). Examples of naturally derived stem cells include embryonic stem cells (ESC), perinatal stem cells (e.g., umbilical cord-derived stem cells), and adult stem cells

(e.g., bone marrow-derived stem cells). Nuclear engineering processes have enabled the derivation of stem cells by converting somatic donor cells into pluripotent progenitors. The characteristics of each platform determine the potential for safe and effective therapeutic application.

Table 1. Stem cell platforms

PLATFORM	DEFINING CHARACTERISTICS
Embryonic Stem Cell	• Derived from the inner cell mass of blastocyst • Pluripotent and self-renewing • Responsive to environmental cues
Perinatal Stem Cell	• Derived from perinatal sources • Mixture of embryonic-like and adult-like stem cells • Large supply available at time of birth
Adult Stem Cell	• Derived commonly from bone marrow, adipose tissues • Include resident stem cells • Multilineage clinical grade progenitors
Bioengineered Stem Cell	• Derived by reprogramming ordinary tissue sources • Include “therapeutic cloning” and “nuclear reprogramming” • Produce patient-specific embryonic-like stem cells

2.3.1. Natural stem cells

Derived from the inner cell mass of the developing blastocyst, **embryonic stem cells** can be propagated in culture and retain the ability to differentiate into all tissues types, including mesodermal, ectodermal and endodermal derivatives; they are pluripotent cells (**Figure 6**). To date, ESC have been derived from a wide spectrum of species ranging from mouse to human given their suitability to be used in regenerative medicine as a renewable source of transplantable cells. With about a decade of history (Thomson, 1998), human ESC have demonstrated innate ability to give rise to various cell types, including hematopoietic cells (Kyba and Daley, 2003), neuron-like cells (Bain, 1995), glial progenitors Fraichard, 1995 #152}, dendritic cells (Fairchild, 2007), hepatocytes

(Safinia and Minger, 2009), pancreatic islet-like cells (Kahan, 2003), osteocytes (Olivier, 2006), chondrocytes (Kramer, 2003), adipocytes (Olivier, 2006), cardiomyocytes (Hescheler, 1997), as well as muscular (Rohwedel, 1994), endothelial (Risau, 1988), skin (Bagutti, 1996), lung (Coraux, 2005), and retinal tissues (Zhao, 2002). In addition to structural replacement of diseased tissues, ESC have the ability to overcome metabolic deficiencies, deliver trophic support to host cells, and restore disconnected cellular interactions (Fraidenraich and Benezra, 2006). These paracrine effects may prove to be a critical component to the regenerative capacity of ESC in models of human disease, providing future avenues for regenerative medicine.

During their growth and differentiation, ESC sequentially recapitulate embryonic development processes, starting with maintenance of pluripotency. The transcription factor Oct-4 coupled with Sox2 and E1A contribute to the core transcriptional machinery responsible for maintenance of an undifferentiated ground state through fibroblast growth factor-4 (FGF4), Wnt, and transforming growth factor-β (TGF-β) dependent pathways (Silva and Smith, 2008). The pluripotent ground state in mouse embryonic stem cells has been promoted with leukemia inhibitory factor (LIF) through a STAT-3 dependent mechanism. Pluripotency in human embryonic stem cells is dependent on a Src-family of non-receptor tyrosine kinases, and is validated by expression of alkaline phosphatase (AP), POU transcription factor Oct3/4, Nanog, Cripto/TDGF1, proteoglycans TRA-1-60/81, GCTM-2, and stage specific embryonic antigens SSEA-3 and SSEA-4. In this undifferentiated state features such as long telomere length, high nuclear to cytoplasmic ratio and immature cytoplasmic organelles are also characteristic of ESC.

Unrestricted differentiation potential of ESC, together with unlimited self-renewal in culture make of these cells a desirable source for regenerative medicine. However, these characteristics involve an intrinsic risk of teratogenesis or uncontrolled growth which remains one of the hurdles for the clinical

application of ESC, together with ethical considerations and allogeneic origin. With regard to excessive and uncontrollable growth, strategies have been established to guide ESC differentiation into tissue-specific lineages. Ensuring proper regulation of ESC differentiation prior to transplantation or within the microenvironment of transplanted host tissue provides safety required for clinical application (Behfar, 2007; Murry and Keller, 2008). Guidance of targeted differentiation using growth factors, cytokines, hormones, and small molecules provides a pharmacological approach to restrict lineage potential and promote lineage specification. The utilization of specialized biomarkers that identify tissue-specific commitment and remnant undifferentiated progenitors allows physical separation of these population, providing an additional approach to secure lineage specification (Nelson, 2008).

Immunologically, ESC engrafted in an adult are considered allogeneic, since they are derived from non-self embryonic tissue. In spite of the differences in origin, ESC engraftment into non-identical hosts requires minimal immunosuppression. Expression of major histocompatability complex-1 (MHC-1) protein is low in ESC, and is thought to contribute to prolonged survival following allogeneic transplantation by avoiding immunological detection. Other mechanisms such as paracrine production of TGF-β that locally inhibits endogenous T-cell function or presence of ESC-derived dendritic cells are considered to contribute to this immunological tolerance. In this context, production of banks of human leukocyte antigen (HLA) -isotyped ESC lines could provide an “off-the-shelf” resource to be used in regenerative therapies.

Therapeutic application of ESC is still in a pre-clinical stage, with ongoing studies focusing on neurological disorders such as Parkinson’s disease and spinal injury (Goldman, 2005) endocrine disorders such as type-1 diabetes (Kroon, 2008), and cardiovascular disease including ischemic and non-ischemic cardiomyopathy (Fraidenraich and Benezra, 2006; Laflamme and Murry, 2005; Yamada, 2009). At the end of 2009, only one clinical study regarding ESC

treatment in paraplegic patients is approved by the Food and Drug Administration.

Perinatal stem cells, such as umbilical cord blood (UCB) have a differentiation capacity that converts them into a clinically viable source for regenerative medicine. Umbilical cord blood is collected at the time of birth, providing a unique pool of readily available stem cells that are commonly stored in biobanks (van de Ven, 2007). Transplantation of UCB has been clinically successful for hematopoietic stem cell applications resulting in high degree of engraftment, favorable immunotolerance, and limited evidence for graft-versus-host disease compared to adult bone marrow stem cell transplantation.

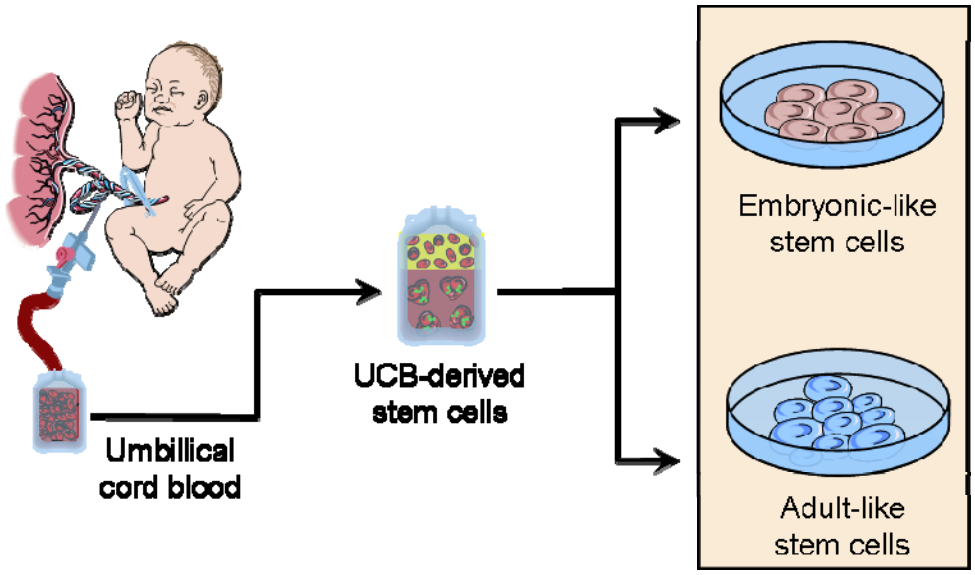

Figure 7. Perinatal stem cells
Umbilical cord blood is one source of perinatal stem cells collected at birth from the umbilical vein containing blood returning from the placenta. These cells have been utilized as hematopoietic stem cells similar to adult bone marrow-derived progenitors. The immaturity of the immune system reduces the risk of detrimental graft-versus-host disease when comparing perinatal to adult sources. Perinatal stem cells also contain populations of cells that behave similar to embryonic stem cells. Pluripotent differentiation potential and unique immunologic status highlight the advantages of perinatal stem cells for regenerative applications, and justify a distinct classification. Perinatal stem cells, that also include amniotic epithelial cells, offer readily available, alternative sources of progenitors.

Reconstitution of the adult hematopoietic system in siblings or in the same individual was the initial rational for UCB-based applications. In addition to providing hematopoietic stem cells, UCB-derived stem cells are capable of *in vitro* expansion, long-term maintenance, and differentiation into representative cells of all three embryonic germinal layers, endodermal (e.g., hepatopancreatic precursor cells, mature hepatocytes, type II alveolar pneumocytes), mesodermal (e.g., adipocytes, chondrocytes, osteoblasts, myocytes, endothelial cells), and ectodermal (e.g., neurons, astrocytes, oligodendrocytes) (van de Ven, 2007). A population of embryonic-like stem cells can be purified form the heterogeneous cell population in the UCB, providing a clinically applicable pluripotent stem cell pool devoid of ethical challenges raised with embryonic sources (De Coppi, 2007) (**Figure 7**). Also in the category of perinatal stem cells, amniotic epithelial cells (AEC) derived from amniotic membranes can be induced to differentiate into diverse and specialized cell types, creating an alternative source of non-embryonic multilineage stem cells.

Adult stem cells comprise a wide range of progenitors derived from non-embryonic, non-fetal tissues such as bone marrow, adipose tissue, and tissue-specific resident stem cell pools (Wagers and Weissman, 2004). (**Figure 8**). These cells are a leading candidate for clinical application in regenerative medicine based on accessibility, autologous status, and favorable proliferative potential (Behfar and Terzic, 2008). Among them, bone marrow derived stem cells are a cornerstone of contemporary applications.

Bone marrow-derived hematopoietic stem cells represent the earliest example of cell-based regenerative medicine, pioneered to address the needs of patients treated with total-body irradiation for leukemia that developed life-threatening infections and irreversible tissue destruction (**Figure 8**). Stem cells defined by expression of the CD34 surface marker can also be obtained *via*

peripheral blood leukapheresis for clinical engraftment. Hematopoietic stem cells have provided the foundation for autologous and allogeneic stem cell transplantation, and offer novel treatments for patients with cancer, autoimmune diseases, and genetic diseases, including severe combined immunodeficiency and thalassemia. Transplant studies have also revealed engraftment of non-hematopoietic cell lineages derived from donor bone marrow, unmasking sub-populations capable of a diverse range of lineage-specific differentiation.

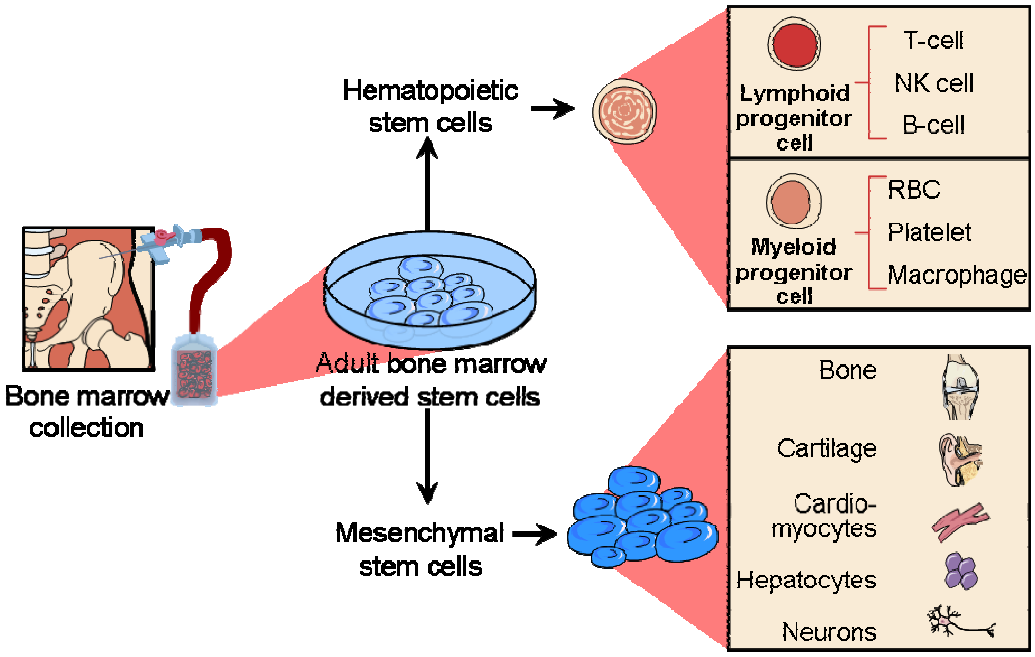

Figure 8. Adult stem cells
Derived from non-embryonic or non-perinatal sources, adult stem cells can be procured from a range of tissues, such as bone marrow, as well as circulating blood or fat. Adult stem cells are generally considered multipotent, as illustrated for bone marrow-derived stem cells that contain both hematopoietic progenitors and mesenchymal stem cells. Hematopoietic stem cells give rise to (i) lymphoid-derived T cells, B cells, and natural killer cells; and (ii) myeloid-derived red blood cells, platelets, and macrophages. Hematopoietic stem cells provide the standard of care for bone marrow reconstitution. Mesenchymal stem cells also have a diverse spectrum of differentiation that includes bone, muscle, cartilage, cardiomyocyte, hepatocyte, and neurons. Mesenchymal stem cells serve as a cell type of choice for clinical applications of non-hematological regeneration based on the availability of autologous stem cell sources, cost-effective isolation, and safety profile.

Mesenchymal stem cells were also discovered in the bone marrow, albeit at low frequency compared to the hematopoietic pool. Mesenchymal stem cells represent ~1 out of 10,000 nucleated cells, and arise from the supporting architecture of the adult marrow (Chamberlain, 2007). They have also been isolated from connective components of adipose and synovial tissue, as well as from peripheral and cord blood. Mesenchymal stem cells exhibit properties of multipotency, with the capacity to contribute to regeneration of bone, cartilage and muscle, tissues of mesodermal origin (Phinney and Prockop, 2007) (**Figure 8**). Evidence also supports the contribution of mesenchymal stem cells to liver and pancreatic islet cell regeneration, and protection in the setting of kidney, heart or lung injury. Mesenchymal stem cells secrete a spectrum of bioactive molecules that provide a regenerative microenvironment to limit the area of damage and to mount a self-regulated regenerative response. The age of the individual, the extent of tissue damage, and the local and whole body titers of mesenchymal stem cells have been all considered to play a role in the ultimate rate and extent of repair. Beyond the supply of differentiated mesenchymal tissues in case of cell loss, mesenchymal stem cell progeny constitutes the stromal environment that is fundamental in the regulation of parenchymal stem cell renewal and differentiation, and immune modulation.

Adult human mesenchymal stem cells are immunoprivileged cells. They are devoid of HLA class II antigens (MHC-II) on the cell surface, and do not express the co-stimulatory molecules CD80, CD86 or CD40 (Chamberlain, 2007). The expressed MHC-I antigens may activate T cells, but, with the absence of co-stimulatory molecules, a secondary signal would not engage, leaving T cells anergic. This particular profile renders mesenchymal stem cells non-immunogenic, optimizing immunosuppression in the event of an allogeneic transplantation (Le Blanc and Ringden, 2007). Moreover, mesenchymal stem cells exhibit immunosuppressive properties, modulating T-cell functions including cell activation, and display immunomodulatory features impairing maturation and

function of dendritic cells and inhibiting human B-cell proliferation, differentiation, and chemotaxis. However, rejection of marrow stromal cells in MHC classes I and class II-mismatched recipients has been reported underscoring the relevance of the immune response in the outcome of stem cell therapy (Le Blanc and Ringden, 2007). At present, the use of allogeneic mesenchymal stem cell therapy in the management of acute disorders, such as myocardial infarction, graft-versus-host disease and exacerbations of inflammatory bowel disorders has been considered. This strategy avoids the need for preparing autologous cells from the recipient. For disorders where mesenchymal stem cells are not needed on an emergency basis, it may be preferable to culture-expand autologous mesenchymal stem cells prior to implantation in an effort to personalize cell-based therapy (Le Blanc and Ringden, 2007). Expansion offers the opportunity to produce a large pool of naïve stem cells, and derive progeny honed for lineage-specification away from multipotency and into tissue-restricted cytopoiesis (Behfar, 2008). Derivation and characterization of specialized mesenchymal stem cell subpopulations, and their selective application to specific disease conditions is an emerging strategy for enhanced therapeutic outcome.

Collectively, natural stem cell platforms have been essential to uncovering fundamental mechanisms of self-maintenance and asymmetrical cell division that are required for continuous production of differentiating progeny. Building on this foundation of knowledge, recent advances have enabled an entirely new platform of stem cells to rapidly emerge with unique characteristics not previously defined in natural stem cells.

2.3.2. Bioengineered Stem Cells

Embryogenesis is a sequential process of differential gene expression dictated by the epigenetic environment. Exploiting epigenetic influence on phenotypic outcome, biotechnology platforms are developed for reversal of differentiation to achieve genetic reprogramming of adult sources back to an

embryonic state (Hochedlinger and Jaenisch, 2006).Such platforms include “therapeutic cloning” and “nuclear reprogramming” that bypass the need for embryo extraction to generate pluripotent stem cell phenotypes from autologous sources (Armstrong, 2006; Jaenisch and Young, 2008).Reprogramming of adult stem cells to generate customized embryonic-like stem cells offers the future for patient-specific regenerative therapies (Park, 2008; Park, 2008; Yamanaka, 2007).

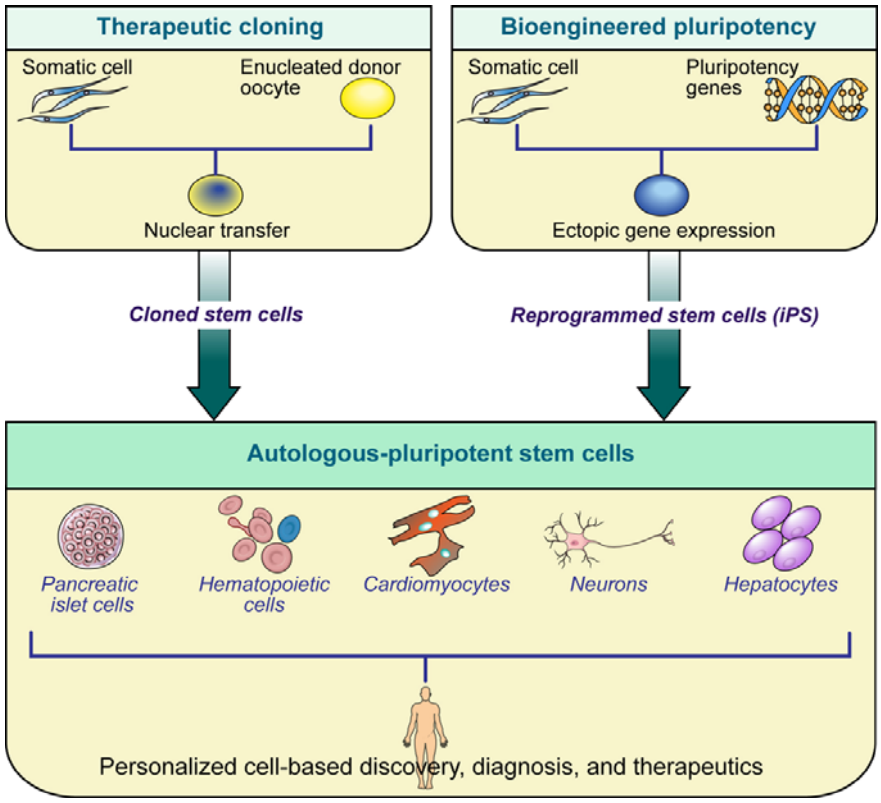

Figure 9. **Bioengineered pluripotent stem cells**. Pluripotent stem cells that function like embryonic stem cells can be produced from ordinary cells through “therapeutic cloning” or “nuclear reprogramming”. Therapeutic cloning combines the nuclear content of a somatic type with the cytoplasm of an enucleated donor oocyte. Transfer of the somatic cell nucleus into the remnant of the fertilized egg is performed by micromanipulation. This process results in the development of a blastocyst to allow harvest of pluripotent stem cells from the inner cell mass (ICM). Alternatively, similar starting somatic cell source can undergo nuclear reprogramming through ectopic expression of four genes (*OCT4* and *SOX2* with either *NANOG* and *LIN28 or KLF4* and *c-Myc*) to produce pluripotent cells independently of embryonic tissues. The bioengineered cells are called induced pluripotent stem (iPS) cells. Importantly, the progeny and tissues derived from engineered pluripotent stem cells are genetically similar to the original somatic cell biopsy, and allow the advent of autologous, embryonic-like stem cells towards individualized cell-based applications.

Therapeutic cloning through somatic cell nuclear transfer- Somatic cell nuclear transfer (SCNT) allows trans-acting factors present in the mammalian oocyte to reprogram somatic cell nuclei to an undifferentiated state (**Figure 9**). Therapeutic cloning refers to SCNT in which the nuclear content of a somatic cell from an individual is transferred into an enucleated donor egg to derive blastocysts that contain pluripotent embryonic-like stem cells. In this way, SCNT has produced cloned embryonic stem cells from multiple mammalian somatic cell biopsies (French, 2008; Yang, 2007). The pluripotency of derived cells has been confirmed through germline transmission, and reproductive cloning. The robustness of this technology was originally highlighted by the successful production of "Dolly the Sheep" in 1996 (Campbell, 1996). This scientific breakthrough was the first demonstration that somatic cell nucleus retained the capacity to undergo reprogramming in the setting of an embryonic environment and execute the proper developmental pathways characteristic of embryonic stem cells. It was thus, in theory, possible to envision a bioengineering strategy to produce patient-specific stem cells for the purpose of therapeutic applications.

Nuclear reprogramming- Bioengineering through nuclear reprogramming of adult cells ("sources") through ectopic introduction of a small number of pluripotency-associated transcription factors ("inductors"), along with complementary strategies to optimize the process ("facilitators"), is an alternative approach to induce an embryonic stem cell-like phenotype (**Figure 9**). This strategy, based on the fundamental discoveries of embryonic stem cells and somatic cell nuclear transfer, demonstrated the ability of a finite number of transgenic factors to recapitulate nuclear reprogramming in the absence of any embryonic tissue (Takahashi and Yamanaka, 2006). This breakthrough enabled a rapid adoption of nuclear reprogramming strategies to a wide-spectrum of scientific questions geared not only to therapeutic applications but also to

fundamental discovery pipelines and individualized diagnostics. In the mouse, such nuclear reprogramming approach has reproducibly yielded induced pluripotent stem cells (iPS) sufficient for *de novo* embryogenesis and complete generation of germline stem cells (Boland, 2009; Meissner, 2007; Okita, 2007; Zhou, 2009). In human cells, the transcription factors sets, Oct4, Sox2, c-Myc and Klf4 or alternatively Oct4, Sox2, Nanog and Lin28, are sufficient to reprogram somatic tissue into pluripotent stem cells that exhibit the essential characteristics of embryonic stem cells, including maintenance of the developmental potential to differentiate into advanced derivatives of all three germ layers (Takahashi, 2007; Yu, 2007). iPS cell lines should largely eliminate the concern of immune rejection given the autologous immunological status of self-derived stem cells. Moreover, iPS-based technology will facilitate the production of cell line panels that closely reflect the genetic diversity of a population enabling the discovery, development and validation of therapies tailored for each individual.

3. Optimization of the bioengineering toolkit

From the first proof of principle study by Yamanaka (Takahashi and Yamanaka, 2006), several strategies have been attempted in order to optimize reprogramming and performance of iPS. With the ultimate goal of rendering this technique applicable in the clinical setting, ongoing efforts focus primarily on improving efficiency and decreasing oncogenic potential of the resulting cells. Among the addressed reprogramming ingredients, source of parental tissue,

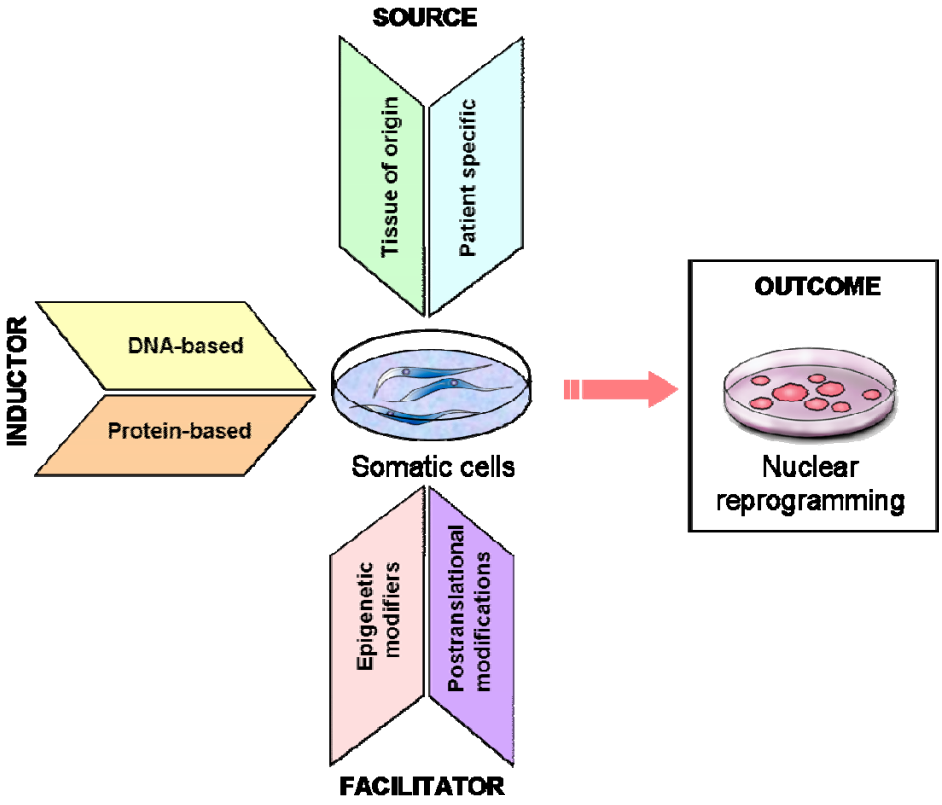

Figure 10. **Toolkit for inducing pluripotency**. Sources of parental cells provide the initial platform for nuclear reprogramming. Various tissues have been used for successful reprogramming in which the original identity of the starting cells may provide constructive influence for the process of reprogramming and subsequent differentiation. Inductors of nuclear reprogramming drive the reversible process of re-establishing a pluripotent ground state through downstream regulation of gene expression, proteome remodeling, conversion of metabolic machinery, and re-structuring of the cyto-architecture. Facilitators provide a complementary axis to target the inherent barriers that limit the efficiency of successful nuclear reprogramming, and may be unique or universal to the parental cell types. Successful interactions between the three principal components of the bioengineering toolkit allow derivation of functional pluripotency in generated progeny to be self-sustained in order to reset the fate of parental cells.

facilitator molecules or conditions, and both identity and delivery strategy of the reprogramming factors have been shown to affect the final product of this bioengineering process (**Figure 10**).

3.1. Tissue origin

The origin of somatic cells used for the reprogramming process is important beyond the issue of nuclear reprogramming efficiency. Depending on tissue source and age of the donor, teratogenic potential of tissue-specific reprogrammed progeny varies when injected into immunodeficient animals (Miura, 2009). The iPS cells derived from adult tail tip fibroblasts and adult hepatocytes demonstrate the highest risk of dysregulated teratoma formation. In contrast, iPS derived from either embryonic fibroblasts or stomach epithelium demonstrate the lowest; yet a propensity similar to embryonic stem cells to form tumors (Miura, 2009). However, stomach epithelium and hepatocytes offer a significant advantage in terms of infectivity and thereby the ability to bioengineer ectopic expression with safer delivery strategies (Aoi, 2008). Other considerations include the efficiency, safety, and availability of donor tissues to initiate the reprogramming process through the most practical source of starting tissue. To date, seven different mouse tissues have demonstrated the ability to reprogram into iPS cells (**Table 2**). Although mouse embryonic fibroblasts were originally used, adult somatic tissue ranging from dermal skin (Hanna, 2007; Nakagawa, 2008), to liver/stomach biopsy (Aoi, 2008), beta-cells from the pancreas (Stadtfeld, 2008), neural stem cells (Kim, 2008; Silva, 2008) and hematopoietic stem cells (Eminli, 2009) have all demonstrated similar efficiencies using standardized methodologies for nuclear reprogramming. The possibility of reprogramming somatic cells derived from different starting tissues at similar efficiency rates fits into the non-elite stochastic model recently proposed by Hanna *et cols.* (Hanna, 2009). According to their findings, almost all mouse donor cells, regardless of their epigenetic state, eventually get reset to the pluripotent state upon continuous overexpression of pluripotent-related genes,

although with different time courses, indicating that differentiation is a reversible process independently of its extent.

Table 2. Murine sources of ordinary tissue for nuclear reprogramming.

Murine Tissue Source	Induction strategy	Pluripotent criteria	Original references
Embryonic fibroblasts	Retrovirus- Oct4, Sox2, Klf4, c-myc	Gene expression, teratoma formation, chimeric embryos	(Takahashi and Yamanaka, 2006)
Tail-tip fibroblasts	Retrovirus- Oct4, Sox2, Klf4, c-myc	Gene expression, teratoma formation, chimeric embryos	(Hanna, 2007; Nakagawa, 2008)
Hepatocytes and gastric epithelial cells	Retrovirus- Oct4, Sox2, Klf4, c-myc	Gene expression, chimeric embryos	(Aoi, 2008)
beta-pancreatic cells	tet-inducible lentiviruses c-*myc*, Klf4, Sox2, and Oct4	Gene expression, teratoma formation, chimeric embryos	(Stadtfeld, 2008)
Neural stem cell	Retrovirus- Oct4, Klf4 +/- Sox2, c-Myc and Retrovirus- Oct4, Sox2, Klf4, c-MycT58	Gene expression, teratoma formation, chimeric embryos	(Kim, 2008; Silva, 2008)
Hematopoietic stem cells	doxycycline-inducible lentiviruse-Oct4, Sox2, Klf4 and c-Myc	Gene expression, chimeric embryos	(Eminli, 2009)
Lymphocytes	doxycycline-inducible lentiviruse-Oct4, Sox2, Klf4 and c-Myc	Gene expression, teratoma formation, chimeric embryos	(Hanna, 2008)

In humans, successful reprogramming has also being possible in an array of starting sources that now include beyond dermal skin (Takahashi, 2007; Yu, 2007) three other tissues, namely keratinocytes (Aasen, 2008), adipose tissue (Sun, 2009), peripheral blood (Loh, 2009) (**Table 3**). Similar criteria for initial functional pluripotency within the collection of these iPS clones have been met according to teratoma formation. However, evidence suggests that iPS clones

retain a memory of their parental source despite full nuclear reprogramming (Marchetto, 2009), and thus may provide the molecular basis for intrinsic differences between iPS clones generated from different parental somatic sources.

Table 3. Human sources of ordinary tissue for nuclear reprogramming.

Human Tissue Source	Induction strategy	Pluripotent criteria	Original references
Dermal skin fibroblasts	Retrovirus- OCT3/4, SOX2, KLF4, and c-MYC and Lentivirus- OCT4, SOX2, NANOG, and LIN28	Gene expression, teratoma formation	(Takahashi, 2007; Yu, 2009)
Keratinocytes	Retrovirus- OCT3/4, SOX2, KLF4, and c-MYC	Gene expression, teratoma formation	(Aasen, 2008)
Adipose tissue	Lentivirus- OCT3/4, SOX2, KLF4, and c-MYC	Gene expression, teratoma formation	(Sun, 2009)
Peripheral blood ($CD34^+$)	Retrovirus- OCT3/4, SOX2, KLF4, and c-MYC	Gene expression, teratoma formation	(Loh, 2009)

Beyond optimization of a new therapy, the bioengineered iPS platform permits the generation of autologous stem cells from individuals independent of disease conditions or genetic mutations. This feature, unique to autologous pluripotent stem cells generated according to induced pluripotent technology, allows patient-specific stem cells to serve as a comparative platform for discovery science that is poised to revolutionize *in vitro* physiological and pharmacological studies. iPS cells have been generated from both genetic and non-inheritable diseases (**Table 4**) including Parkinson disease, Adenosine deaminase-severe combined immunodeficiency, Gaucher disease, Swachman-Bodian-Diamond syndrome, Duchenne muscular dystrophy, Becker muscular dystrophy, Down syndrome, Huntington disease, Lesch-Nyhan syndrome (Park,

2008), myeloproliferative disorders (Ye, 2009), amyotrophic lateral sclerosis (Dimos, 2008), Fanconi anemia (Raya, 2009), type 1 diabetes (Maehr, 2009), spinal muscular atrophy (Ebert, 2009), and familial dysautonomia (Lee, 2009).

Table 4. Patient-specific iPS**.**

Disease or Syndrome	Induction strategy	Tissue source	Original references
Fanconi anemia	Retrovirus- Oct4, Sox2, Klf4, c-myc (mouse)	Dermal fibroblasts	(Raya, 2009)
Amyotrophic lateral sclerosis (ALS)	Retrovirus- *OCT4, SOX2, KLF4, c-MYC*	Dermal fibroblasts	(Dimos, 2008)
Type 1 diabetes	Retrovirus- *OCT4, SOX2, KLF4*	Dermal fibroblasts	(Maehr, 2009)
Adenosine deaminase-severe combined immunodeficiency	Retrovirus- *OCT4, SOX2, KLF4, c-MYC*	Dermal fibroblasts	(Park, 2008)
Gaucher disease type III	Retrovirus- *OCT4, SOX2, KLF4, c-MYC*	Dermal fibroblasts	(Park, 2008)
Duchenne muscular dystrophy	Retrovirus- *OCT4, SOX2, KLF4, c-MYC*	Dermal fibroblasts	(Park, 2008)
Becker muscular dystrophy	Retrovirus- *OCT4, SOX2, KLF4, c-MYC*	Dermal fibroblasts	(Park, 2008)
Down syndrome	Retrovirus- *OCT4, SOX2, KLF4, c-MYC*	Dermal fibroblasts	(Park, 2008)
Parkinson disease	Retrovirus- *OCT4, SOX2, KLF4, c-MYC*	Dermal fibroblasts	(Park, 2008)
Shwachman-Bodian-Diamond syndrome	Retrovirus- *OCT4, SOX2, KLF4, c-MYC*	Bone marrow mesenchymal cells	(Park, 2008)
Huntington disease	Retrovirus- *OCT4, SOX2, KLF4, c-MYC*	Dermal fibroblasts	(Park, 2008)
Lesch-Nyhan syndrome (carrier)	Retrovirus- *OCT4, SOX2, KLF4, c-MYC*	Dermal fibroblasts	(Park, 2008)
myeloproliferative disorders (MPDs)	Retrovirus- *Oct4, Sox2, Klf4, c-myc* (mouse)	Peripheral blood-CD34+ cells	(Ye, 2009)
Spinal muscular atrophy	Lentiviral- *OCT4, SOX2, NANOG* and *LIN28*	Dermal fibroblasts	(Ebert, 2009)
Familial dysautonomia (FD)	Lentiviral- *OCT4, SOX2, KLF4* and *c-MYC*	Dermal fibroblasts	(Lee, 2009)

Therefore, nuclear reprogramming has been successful in health and disease from multiple sources of adult tissues, thus providing a foundation to enable new paradigms of discovery science, novel diagnostics, and potential autologous cell-based therapeutics.

3.2. Inductors of pluripotency

The original ectopic gene set sufficient to reprogram somatic cell types into pluripotent stem cells was revealed following a candidate-based screen strategy that was applied to a short list of 24 genes known to be associated with pluripotency (Takahashi and Yamanaka, 2006). These genes were identified according to their expression profiles within stem cells, thus labeled *stemness-related genes*. All genes were expressed and validated in embryonic fibroblasts through retroviral transduction to screen for cellular characteristics unique to pluripotent stem cells. The search for a combination of genes that were sufficient to reprogram a fibroblast into stem cells was the goal. The results demonstrated a minimum number of necessary genes, i.e., a functional quartet of Oct3/4, Sox2, Klf4, and c-Myc that induced cellular metamorphosis and acquisition of stem cell characteristics (**Figure 11**) (Takahashi and Yamanaka, 2006). The Oct3/4 and Sox2 genes encode for transcription factors essential in the maintenance of pluripotency in early embryos. Complimentary to the pluripotent genes, Klf4 and c-Myc promote self-renewal in order to acquire an essential milestone typical of stem cells. This seminal work was rapidly validated, adapted, and translated into protocols ultimately amenable for disease-specific applications.

Independently, an alternative gene set was identified according to similar candidate-based screening criteria that contained a modification of the quartet gene set. Both strategies prioritized Oct3/4 and Sox2 as core components with Klf4 and c-Myc being replaced with Nanog and Lin28 in the alternative reported gene set sufficient for reprogramming functional pluripotency (Yu, 2007) (**Figure**

11). The collection of pathways that these two sets of ectopic transgenes will activate is likely to be similar in that Lin28 and c-Myc demonstrate overlapping functions. Both gene sets have been utilized in multiple parental cell types across a number of species to establish successful nuclear reprogramming strategies (**Table 2 and Table 3**)**.**

. Recent studies reveal that some of the initial inductor genes can be

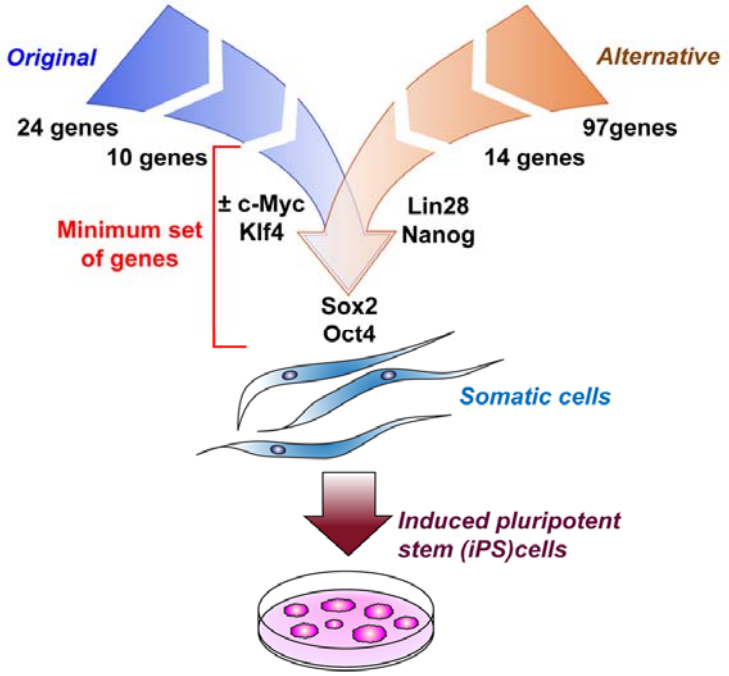

Figure 11. **Candidate-based discovery approach for nuclear reprogramming**. The original set of 24 stemness genes was distilled to 4 genes (Oct4, Sox2, Klf4, and c-Myc) that were sufficient to induce pluripotency from ordinary cell types. Alternatively, an independent screen of 97 candidate genes revealed a second quartet of reprogramming factors that confirmed the robustness of Oct4 and Sox2 in combination with Nanog and Lin28. Both sets of genes have been reproducibly applied, and provide the "gold-standard" for nuclear reprogramming platforms.

replaced by small molecules that have similar downstream effects or might not be necessary when high levels of expression are already present in the original cell type that undergoes reprogramming, in both cases reducing the number of factors to be induced (Kim, 2009; Lyssiotis, 2009). The most extreme example so far is the reprogramming of neural stem cells with only one Sox2 (Kim, 2009).

3.3. Facilitators of reprogramming

The multi-faceted influence of stemness-related gene sets induces a wide range of changes from induction of gene expression, to protein architecture remodeling and metabolic machinery retooling. Applying a complementary strategy to optimize the rate-limiting steps of nuclear reprogramming offers incremental advantages for the overall efficiency of iPS derivation from original parental cell sources. Facilitators are small molecules or conditions designed to improve the efficacy of inductors to drive nuclear reprogramming. Among the class of facilitators, manipulation of the oxygen levels to 5% hypoxia creates a favorable environment that provokes a complex re-arrangement of gene expression profile that favors the induction of reprogramming (Yoshida, 2009). Important to the epigenetic state, histone acetylation and methylation regulates the accessibility of the transcription machinery to the genetic blueprint within the parental cell. In this context, inhibition of histone deacetylase or DNA-methyl transferase using epigenetic modifiers valproic acid or 5-aza-cytidine has benefited the chromatin remodeling and increased the efficiency of standardized reprogramming protocols (Huangfu, 2008; Mikkelsen, 2008). Furthermore, chemical modulation of signaling pathways involved in maintenance of the pluripotent state can significantly improve the overall efficiency of nuclear reprogramming (Lin, 2009). The ubiquitous surveillance activity of p53, which functions as a tumor suppressor gene, has been identified as a critical rate-limiting roadblock during the early stages of nuclear reprogramming. Thus, temporarily p53 knockdown either by gene silencing or protein degradation increases the overall efficiency of successful progression through all stages of nuclear reprogramming (Banito, 2009; Hong, 2009; Kawamura, 2009; Li, 2009; Marion, 2009; Utikal, 2009). Together, these strategies modify the susceptibility of the original somatic cells and boost mechanisms that regulate the checkpoints restricting conversion of cell fate through nuclear reprogramming.

4. Delivery Strategies for nuclear reprogramming

Nuclear reprogramming through triggered cellular de-differentiation offers a revolutionary framework to derive pluripotent stem cells from somatic tissue, independently of an embryo source. The emerging technology demonstrates that ectopic expression of stemness-related genes is sufficient to reset parental cell fate, unlocking the potential of unlimited patient-specific regenerative therapies. Thereby, discovery science has overcome restrictions inherent to embryonic derivation enabling access to a genuine, autologous, pluripotent cell population. Nuclear reprogramming technology must however limit the footprint or residual modifications to the genome in order to establish a safe tool amenable for clinical translation (**Figure 12**).

4.1. Genetic engineering

Retroviral and lentiviral approaches offered the initial methodology that launched the field of gene delivery for nuclear reprogramming, and established the technological basis of iPS with rapid confirmation across multiple vector systems (**Figure 12**). Because the retroviral-based vector systems have built-in sequences that silence the process of transcription upon pluripotent induction, ectopic gene expression was cut-off as cells achieved a stable ground-state. This observation indicated that successful self-maintenance of the pluripotent state was possible independent of persistent transgene expression. Stage-specific silencing is a characteristic property of retroviral constructs in the pluripotent ground state (Hotta and Ellis, 2008). In this way, transient expression of ectopic genes enabled the strategy of nuclear reprogramming to be reconsidered as a temporary exposure to stemness-related factors and allowed the design of traceless approaches that could be utilized for safer applications. Therefore, the random integration and unpredictable genetic alterations of exogenous DNA

inherent to retroviral or lentiviral constructions was not an essential component for next generation technology (Aoi, 2008) as the science moves toward clinical applications. For this reason, new technology aims to identify the most potent stemness-related factors that are able to more efficiently interact with native cellular machinery and successfully re-write the pattern of gene expression without disruption of underlying genetic integrity of the host cell.

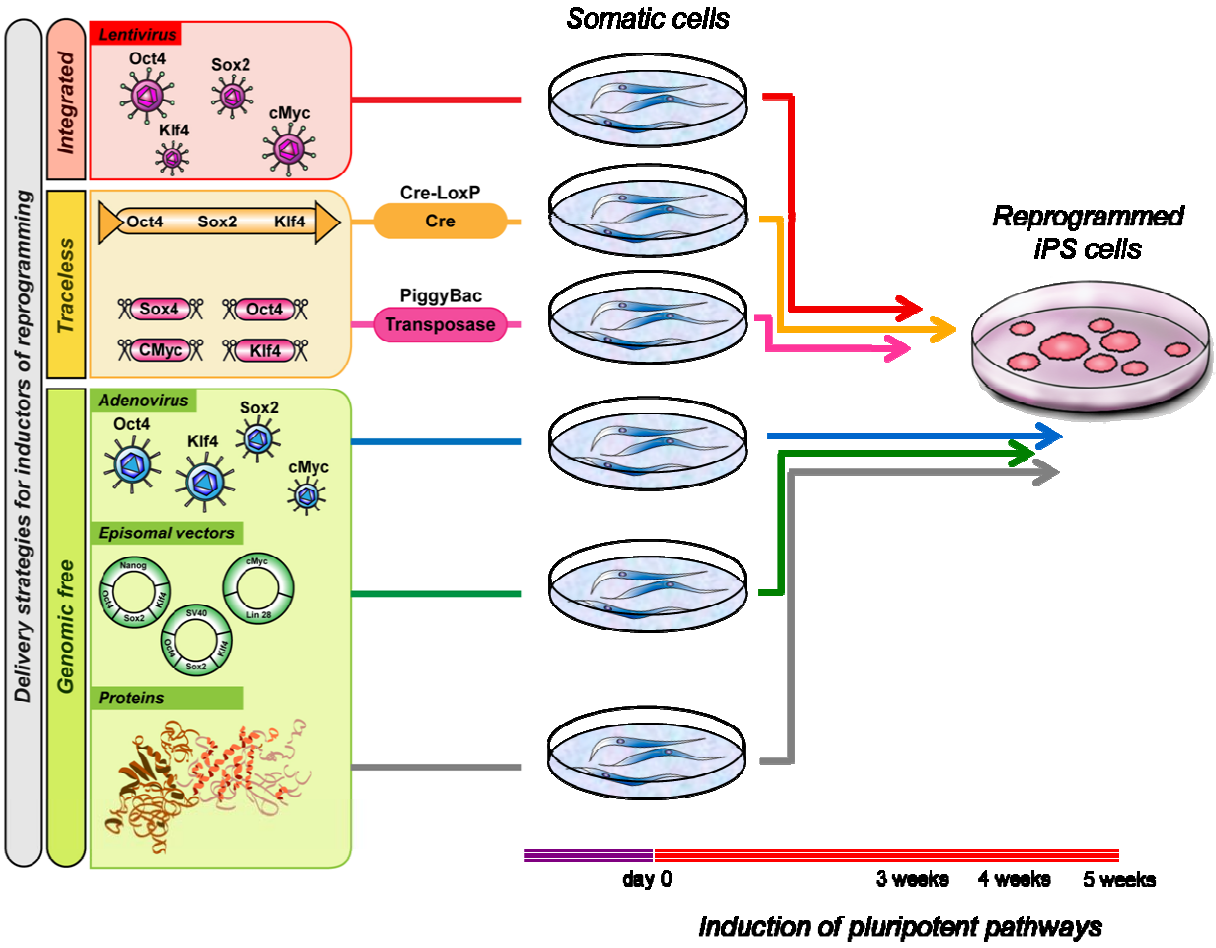

Figure 12. **Strategies to deliver inductors of pluripotency**. Genetic engineering with retrovirus and lentivirus provided the initial strategy to efficiently deliver adequate levels of ectopic transgenes to evaluate the process of nuclear reprogramming. The genomic modifications that are inevitable with use of integrating vectors create however a potential risk of insertional mutagenesis. Traceless engineering was therefore established to remove the risk of genomic modifications by enzymatically cutting the ectopic sequences out of the genome after successful nuclear reprogramming. Alternatively, genomic-modification free technology has established in proof-of-principle studies reprogramming with plasmids, episome vectors, and recombinant proteins.

4.2. Traceless engineering

Following this idea, two traceless approaches have been developed that are able to produce iPS cells independent of permanent genetic modifications. The classical Cre-LoxP method was engineered to delete ectopic sequences from the iPS genome upon successful nuclear reprogramming (Chang, 2009). The “hit and run” system removes residual sequences of the transgene but does leave a small LoxP site at the site of random integration. Moreover, the latest innovation that advances iPS-based technology towards clinical applications has most recently been highlighted in which non-viral approaches are capable of high-efficiency iPS production in truly traceless fashion (Nelson and Terzic, 2009) (**Figure 12**). These newest approaches are dependent on short sequences of mobile genetic elements that can be used to integrate transgenes into host cell genomes and provide a genetic tag to “cut and paste” flanked genomic DNA sequences. The piggyBac (PB) system couples enzymatic cleavage with sequence specific recognition using a transposon/transposase interaction to ensure high efficiency removal of flanked DNA without residual footprint (Woltjen, 2009). Importantly, this technology achieves a traceless transgenic approach in which non-native genomic sequences that are transiently required for nuclear reprogramming can be removed upon induction of pluripotency. Specifically, using the PB transposition system with randomly integrated stemness-related transgenes, the technology has demonstrated that disposal of ectopic genes can be efficiently regulated upon induction of self-maintaining pluripotency according to expression of the transposase enzyme without infringement on genomic stability (Woltjen, 2009). This state-of-the-art system is uniquely qualified to allow safe integration and removal of ectopic transgenes, improving the efficiency of iPS production.

4.3. Genomic-modification free

The risk of oncogenic gene reactivation and insertional mutagenesis inherent to stable genomic integration triggered, in turn, the search for the next generation of iPS production. Thereby, systems were designed for transient production of stemness-related genes without integration into the genome. The first proof-of-principle was achieved by non-integrating viral vector systems, such as adenovirus (Stadtfeld, 2008), and confirmed by repeated exposure to extra-chromosomal plasmid-based transgenes (Okita, 2008). Importantly, these reports demonstrated that expression of stemness-related factors was required for only a limited timeframe until progeny developed autonomous self-renewal, establishing nuclear reprogramming as a bioengineered process that resets a sustainable pluripotent cell fate independent of permanent genomic modifications (**Figure 12**). However, the inherent inefficiency of non-integrated technologies has hindered broader applicability.

Alternatively, the security of unmodified genomic intervention can be achieved with non-integrating episomal vectors (Yu, 2009). Vectors are also being developed based on transient expression and methods to eliminate the risk of permanent insertional mutagenesis (Kaji, 2009). Finally, direct delivery of recombinant proteins engineered to penetrate across the plasma membrane of somatic cells and translocate into the nucleus has succeeded to be sufficient to induce pluripotency in somatic cells, initiating the new concept of DNA-independent reprogramming (Zhou, 2009). Two methodologies have achieved reprogramming with recombinant protein technologies. First, by transiently permeabilizing the cell membrane of the parental fibroblasts, embryonic stem cell extracts have been successful in obtaining a reprogrammed stem cell population (Bru, 2008). Second, bioengineering recombinant proteins with membrane-translocating peptide consisting of multiple arginine amino acids at the N-terminus of the stemness-related factors has enabled an alternative strategy (Kim, 2009; Zhou, 2009).

Collectively, these delivery strategies for nuclear reprogramming accelerate the discovery science of regenerative medicine and bring the technology a step closer to clinical applicability. By producing genetically unmodified progenitor cells that acquire the capacity of pluripotency, advances in the field of nuclear reprogramming make it theoretically possible to generate unlimited, autologous tissues from patients for both diagnostic and therapeutic applications.

5. Stringency tests of pluripotent competency

Originally, somatic cell nuclear transfer established the proof-of-principle concept of genomic intervention to reset cell fate. Transferring the nucleus of an adult cell into the cytoplasmic environment of a host enucleated oocyte revealed the genetic malleability of mammalian somatic cells to re-acquire atavistic developmental competency (Beyhan, 2007; Byrne, 2007; French, 2008; Yang, 2007). Ensuing nuclear-to-cytosol interactions catalyze the epigenetic regulation that reverses the differentiation state of the parental nucleus to achieve genetic reprogramming and recapitulate the embryonic ground state, providing tools to re-engineer the cellular make-up including the mitochondrial machinery of ordinary cells (Tachibana, 2009). The robustness of this process is further evident by successful xenogenic combinations of adult nuclei with primitive cytoplasm components, revealing phylogenic conservation of a permissive gene-environment interface (Beyhan, 2007). Recognition that “terminally differentiated” tissue phenotype is reversible to the pluripotent state paved the way towards embryo-independent engineering.

The discovery that induced pluripotency was achievable in response to ectopic expression of stemness-related transgenes required measurable milestones to establish criteria of embryonic trait re-acquisition, such as germline transmission that was previously only attained by natural embryonic stem cells. Bioengineered iPS clones need to meet multiple levels of pluripotent stringency to collectively validate the presumed primitive characteristics of embryonic stem cells, used as the gold standard. These criteria span from *in vitro* differentiation in

cell culture to *in vivo* functional properties that include *in utero* developmental potential, to ultimately *in situ* regeneration of diseased tissues (**Figure 13**).

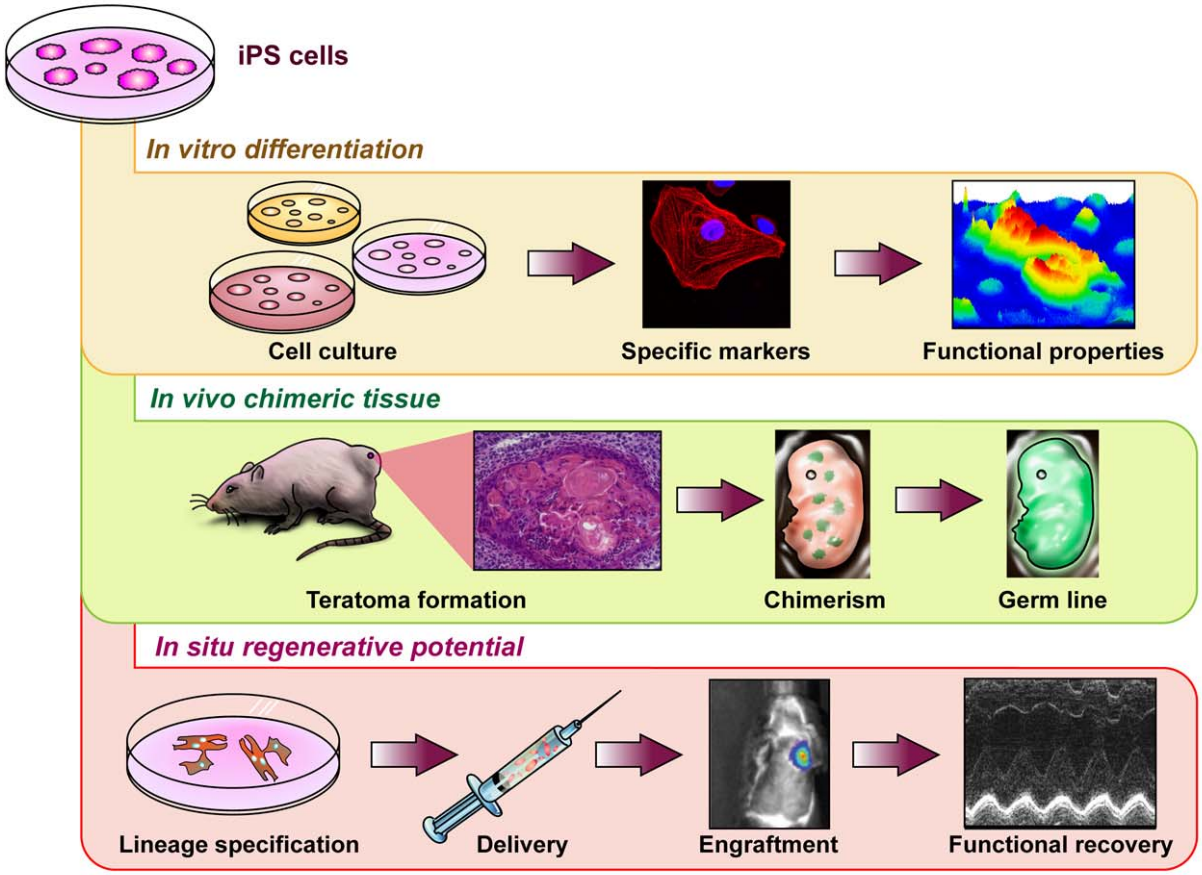

Figure 13. **Stringency tests for pluripotent competency**. Nuclear reprogrammed fibroblasts must meet pluripotent stringency criteria in order to be classified as iPS cells. *In vitro* differentiation provides the initial characterization of bioengineered stem cells to demonstrate the acquisition of specialized cellular differentiation such as cardiomyocytes. *In vivo* chimeric tissue offer an alternative strategy to decipher reprogrammed progeny that have undergone cellular conversion and acquired pluripotent differentiation capacity either in immunodeficient teratoma assay or *in utero* embryonic development leading to germline transmission. *In situ* regeneration potential determines the ability of reprogrammed stem cells to respond to injured tissues or diseased environments, and drive *de novo* cellular repair for restoration of healthy organ function.

5.1. *In vitro* differentiation

As potential pluripotent stem cells, iPS can be cultured *in vitro* and differentiated using existing protocols validated for embryonic stem cells. Differentiation of iPS into functional cell types is a necessary step towards their applicability in regenerative medicine and therapeutic screening (**Figure 13**). So far, embryonic stem cell-designed protocols have been used to differentiate iPS cells, giving rise to adipocytes and osteoblasts (Tashiro, 2009), hematopoietic and differentiated blood cells (Niwa, 2009), cardiovascular cells (Narazaki, 2008; Schenke-Layland, 2008), dendritic cells and macrophages (Senju, 2009), insulin producing cells (Maehr, 2009; Tateishi, 2008; Yu, 2009), hepatocyte-like cells (Song, 2009), retinal cells (Buchholz, 2009; Meyer, 2009; Osakada, 2009), and several types of neurons (Dimos, 2008; Ebert, 2009; Karumbayaram, 2009).

In all cases the identity of differentiated progeny can be confirmed using immuno-fluorescent staining for specific markers coupled with gene expression profiling. Furthermore, mature tissues derived from iPS cells such as neurons, hematopoietic lineages, or other specialized cell types required an additional degree of specificity to characterize the functional properties of individual cell types required to mimic the physiological behavior of natural tissue. In this regard, motor neurons differentiated from reprogrammed cells have been studied, demonstrating that their excitability match characteristics expected from adult cells (Karumbayaram, 2009). Furthermore, endoderm lineages of functional pancreatic beta-cells and liver parenchymal hepatocytes have also been recapitulated *in vitro* to provide the basis for further translation into diagnostic and therapeutic applications (Maehr, 2009). Thus, these data demonstrate the

diversity of lineage specification and functionality that can be produced through *de novo* differentiation from bioengineered pluripotent stem cells.

5.2*. In vivo* chimeric tissue

Pluripotent cells have been defined by their innate ability to give rise to multi-lineage tumors when transplanted subcutaneously in immunodeficient hosts. Beyond artificial modulation of extra-cellular conditions, this *in vivo* model system provides a simple yet sensitive and efficient methodology to test the differentiation potential of bioengineered stem cells (**Figure 13**). Production of three germ layers tumors, known as teratoma, ensures a histological high-throughput readout of the net outcome for multiple cell clones. Importantly, this analysis provides the highest-stringency criteria for human pluripotent or reprogrammed cells given the ethical limitations for alternative tests that can be applied to non-human stem cells.

Since embryonic stem cells are derived from the inner cell mass of a preimplantation blastocyst, non-human pluripotent stem cells should be able to function in an equivalent fashion throughout chimeric embryonic development. As primordial cells, pluripotent stem cells are in theory able to contribute to all the tissues of the developing embryo. Reprogramming of iPS resets their expression profile and characteristics to those of natural embryonic stem cells allowing their integration within pre-implantation embryos (**Figure 13**). To test this capacity, iPS cells of interest are incubated with 8-cell embryos (morula) or injected into a blastocyst and transferred back into the uterus of a staged mother. If nuclear reprogramming has been successfully completed, iPS cells will integrate and populate the developing embryo to generate iPS-derived tissue in the chimeric

offspring generated through diploid aggregation or blastocyst injection. In the event of perfectly healthy and pluripotent cells, they will contribute not only to developing tissue, but also to the specialized germ cells that are capable of germline transmission to naturally breed offspring.

The most stringent test for pluripotency of non-human stem cells requires tetraploid complementation assay. In this assay, two-cell embryos are harvested to allow *ex utero* manipulation. First, the embryos receive a controlled electrical impulse sufficient to fuse the two cells into a single tetraploid cell that now contains two copies (4N) of the genome in a single embryonic cell. The genetic abnormalities created in a 4N tetraploid embryo prevent subsequent development of the embryo proper, yet allow the growth of transient extra-embryonic tissues required to support a developing fetus. If pluripotent stem cells that are functionally equivalent to natural embryonic stem cells are aggregated with the mutant embryo, they will be able to execute developmental processes with 4N extra-embryonic tissues supporting 2N embryonic fetal development (**Figure 13**). The developing embryo and subsequent live born offspring are thus completely derived from the transplanted pluripotent stem cells, and thereby establish the highest-stringency for pluripotency in non-human stem cells (Boland, 2009; Zhao, 2009).

5.3. In situ regeneration potential

iPS technology has overcome inherent restrictions to embryonic stem cells enabling a bioengineered pluripotent stem cell derived from “self” to produce autologous tissues. In this way, the potential for ethical concerns of embryonic tissues and immunological mismatch from non-autologous stem cells is

essentially eliminated. Therefore, a unique advantage of self-repair of multiple tissues allows a new criterion for iPS cells in the context of regenerative medicine (**Figure 13**). Since multiple stem cell populations have demonstrated therapeutic repair following transplantation into diseased tissues, iPS cells have also been put to the task of *in situ* regeneration of disease models. Proof of principle applications for this strategy has been provided to-date in animal models addressing blood (Hanna, 2007; Xu, 2009) or neural disease (Wernig, 2008). The first treated model was a humanized sickle cell anemia mouse, from which iPS were derived, corrected from their genetic defect using homologous recombination and differentiated into healthy hematopoietic cells within a model system of severe disease phenotype (Hanna, 2007). When corrected iPS-derived hematopoietic cells were transplanted into the sickle cell anemia model, they engrafted properly and reversed the disease phenotype (Hanna, 2007). Similarly, deficit in coagulation characteristic of hemophilia A was shown to improve after injection of iPS-derived healthy endothelial cells into the liver of model animals (Xu, 2009). With sufficient expression of Factor VIII from iPS cells, several major organ systems were accordingly repaired. Moreover, in the case of Parkinson's disease, motor neurons obtained from iPS cells were demonstrated to engraft and integrate in the striatum of diseased rats after local injection. Functional engraftment significantly reduced the neurological symptoms in this model system (Wernig, 2008). These examples set the experimental basis for an iPS-based curative approach to manage degenerative diseases that have so far been considered incurable by traditional management.

6. Applications for iPS-based technology

As medical therapy is moving away from a palliative approach towards a curative paradigm for individual patients, regenerative medicine will become a priority to healthcare transformation (Waldman and Terzic, 2007). In this regard, technological advances of induced pluripotent stem cells are driving a new scientific platform that will be increasingly essential for realizing the opportunities of patient-specific, cell-based diagnostics and therapeutics (Nelson TJ, 2010).

6.1. Patient-specific diagnostics

Patient-specific iPS provide a new platform for discovery science to reveal mechanisms of disease. By having an unlimited source of a patient's own cells in the form of a primordial stem cell, detailed mechanistics studies comparing health and disease offer a powerful strategy to dissect the molecular etiology of a disease independent of co-morbidities, drug therapy, age, and the heterogeneity of environmental factors. In the context of monogenetic diseases, multi-generational structured pedigrees have been able to map through linkage analysis disease-causing mutations. However, the mechanism of the disease is often lacking due to the inability to model the disease process. Patient-specific iPS provide a unique opportunity to directly study genotype/phenotype interactions. Well-controlled genetic populations with the benefit of detailed clinical information enable patient-specific iPS cells to contribute to the study of variable penetrance of presumed monogenetic disorders. This novel combination of technologies may produce immediate benefits to the patient and their families through predictive diagnostics based on bioengineered pluripotent stem cells.

In order for iPS to be well established as a model for disease, several technical challenges need to be addressed (Saha and Jaenisch, 2009). Among them, the tissue of origin for the reprogramming has to be carefully chosen in those cases where the genotype might vary among cell types, affecting specifically some organs or tissues. This is the case for myeloid proliferative disorders, with the genotype observed in colony-forming erythroid progenitors, but absent from other somatic cells (Ye, 2009). Knowing this, disease model lines could only be obtained using the mentioned progenitors as cell source. This consideration does not affect other diseases, such as spinal muscular atrophy type I, for which the genetic mutation is present in all the cells (Ebert, 2009), even though the only cell type affected is motor neurons. Another limitation for this iPS application is that diseased phenotypes are often observed only in lineage-committed or differentiated cells, but absent from the pluripotent stages. In this case, *in vitro* differentiation of the reprogrammed lines is necessary to mimic disease effects. So far, **human** iPS have been successfully differentiated to neural progenitors (Chambers, 2009), motor neurons (Dimos, 2008; Ebert, 2009), dopaminergic neurons (Soldner, 2009), retinal cells (Osakada, 2009), hepatocytes (Song, 2009; Sullivan, 2009), blood cells (Choi, 2009; Ye, 2009), adipocytes (Taura, 2009), endothelial cells (Choi, 2009), cardiomyocytes (Zhang, 2009), pancreatic cells (Zhang, 2009) and fibroblasts (Hockemeyer, 2008; Maherali, 2008). However, function of the differentiated cells has only been assayed for a limited number of parameters. Therefore, broader functional characterization, multicellular phenotypes and diseases involving cell types for which *in vitro* differentiation protocols still need to be addressed.

6.2. Therapeutic regeneration

The long-term goal of regenerative medicine that aims to repair and restore normal tissue structure and function in disease has been accelerated by the breakthrough in patient-specific iPS cells (Nelson, 2009) (**Figure 14**). The obvious benefits of "self-derived tissue" eliminate the consideration of immunosuppression for cell-based transplantation. Cytotoxic medications that are required to restrict the ability of innate immune system to destroy transplanted allogeneic tissue have intense side-effects that long-term have been linked to the high occurrence of secondary malignancies and degenerative disease outcomes. Therefore, avoidance of immunosuppression offers a transformation for transplant medicine. Furthermore, creating *bona fide* pluripotent stem cells from patient-derived sources unlocks the restrictions of tissue-specific differentiation that limits non-pluripotent stem cells. Collectively, these two components of induced pluripotent stem cells expand the scope of therapeutic options.

In the 'work in progress' side of the therapeutic use of human iPS, an important step is the generation and maintenance of reprogrammed cells under xeno-free conditions that prevent transmission of non-human pathogens and immune rejection of grafted cells (De Sousa, 2006; Martin, 2005). This has recently being achieved (Rodriguez-Piza, 2009) with media and reagents completely devoid of animal derived ingredients, and using autologous human fibroblasts as supporting feeders.

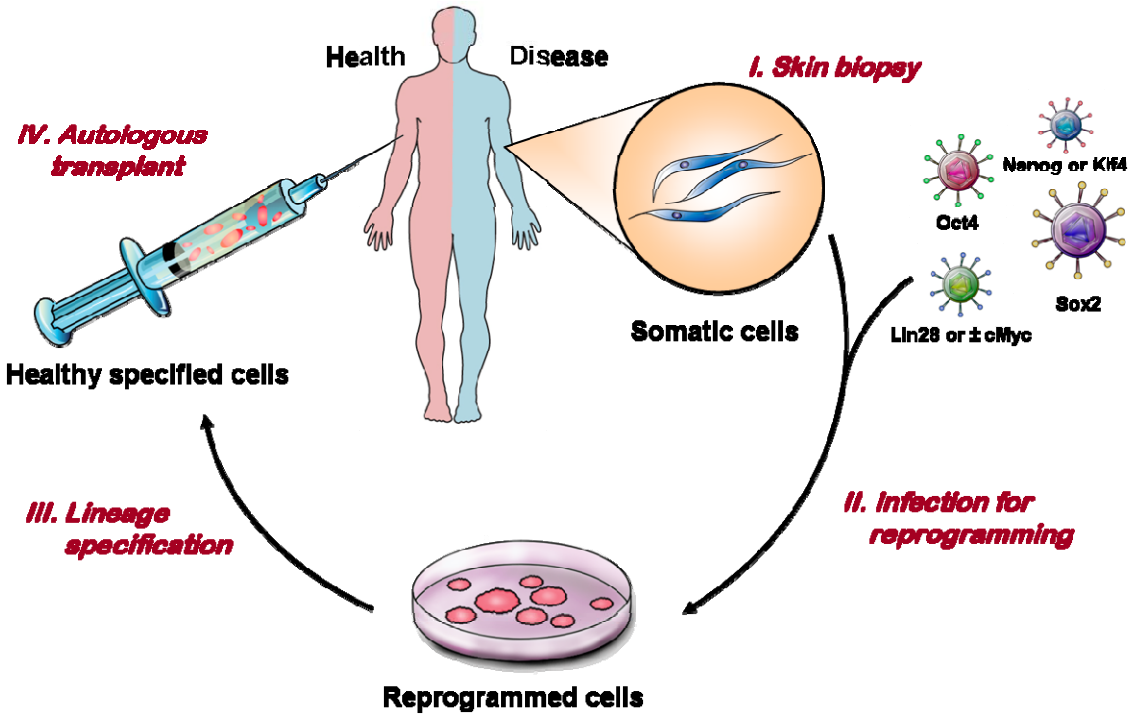

Figure 14. **Therapeutic regeneration using iPS**. The ultimate goal of nuclear reprogramming is to produce autologous cells that contribute to functional homeostasis recovery once they are transplanted into a diseased host. Somatic cells obtained through a minimally invasive biopsy are reset to a pluripotent stage and subsequently differentiated to the tissue of interest before being re-implanted into the patient.

Beyond the elements used for the engineering process, human iPS production will ultimately have to adjust to good manufacturing practices (GMP) and regulations that currently apply for the use of adult stem cells in patients in order to ensure clinical-grade products that can be safely used in the clinical setting.

If applications of iPS cells in regenerative medicine are able to match the right person with the right progenitor cell at the right time, then the future of clinical practice may be able to transition away from the non-curative disease

management models of today, and provide lasting treatments that reverse the degeneration of incurable diseases through personalized patient-specific solutions.

IV. Aims

In the current context of the growing burden imposed by cardiovascular disease worldwide, there is an increasing need for curative approaches to treat the weakened myocardium after an ischemic event. This has been approached by regenerative medicine in the last decade, diversifying the management possibilities. However, the challenge of matching tissue needs with optimized cellular source has impaired the advancement of this promising field.

Nuclear reprogramming of somatic cells into a pluripotent state offers the unique opportunity of a previously unachievable autologous 'biologic' to be used in regenerative medicine. This innovatory platform overcomes restrictive hurdles linked to natural biologics, such as immune rejection in the case of heterologous sources, limited availability, plasticity and comorbidities for adult stem cells or ethical issues involved in the derivation of embryonic stem cells.

While the principles of converting an adult somatic cell into a pluripotent state have been shown feasible, the reparative potential of the progeny derived from bioengineered sources has not been established in the cardiovascular field. In particular, evidence that induced pluripotent stem cells have the capacity to give rise to functional cardiac tissue would set the basis for the development of a new regenerative approach to treat refractory heart disease.

Therefore, the goal of this thesis is ***to determine the functional cardiogenic potential of induced pluripotent stem cells and its applicability as a new therapeutic platform.***

Within this overarching goal, the **Specific Aims** are the following:

1. Derivation of murine induced pluripotent stem cells with human stemness factors and characterization of their pluripotency characteristics.

2. Evaluation of the cardiogenic capacity imposed by the method of nuclear reprogramming.

3. Functional characterization of induced pluripotent stem cell-derived cardiac cells.

4. Determination and characterization of the reparative potential of induced pluripotent stem cells in a murine model of myocardial infarction.

V. METHODS

1. Virus production

1.1. HIV packaging plasmid

The parental packaging plasmid, pCMVR8.91 (Mali, 2008), was used to engineer modifications in the human immunodeficiency virus (HIV)-1 capsid region for increased vector transduction efficiency (Ikeda, 2004; Zufferey, 1997). To generate HIV-1 packaging constructs carrying the capsid mutations, the ApaI, BglII and SpeI sites in the uncoding region of pCMVR8.91 (Mali, 2008) were deleted (p8.9Ex). Naturally occurring capsid amino acid substitutions, which affect the HIV cyclophilin A-dependency, were introduced into the capsid region of the *gag* gene, resulting in pEx-HV, pEX-QI and pEx-QV. Vesicular stomatitis virus glycoprotein G (VSV-G)-expressing plasmid, pMD.G (Mali, 2008), was used for pseudotyping HIV-1 vector particles. Infectious HIV vectors were generated by packaging a green fluorescent protein (GFP)-carrying HIV vector genome with the modified constructs and VSV-G, and the amounts of vectors were normalized by the levels of endogenous reverse transcriptase activity in the vector particles. Human, simian and murine cell lines were infected with various amounts of GFP-expressing vectors, and GFP-positive cell populations were analyzed using fluorescence-activated cell sorting (FACS) and automated quantification (CELL QUEST software; Becton Dickinson, Franklin Lake, NJ). The vector infectivity in each target cell line was determined by infectious units/ng reverse transcriptase activity. For mouse embryonic fibroblast (MEFs) transduction, GFP-carrying HIV vectors were generated with a conventional HIV packaging construct (p8.9Ex) or a packaging construct with the V83L, H87Q and I91V capsid subsitutions (pEx-QV). To determine transduction efficiencies, 5 x 10^4 MEF cells were infected with increasing amounts of unconcentrated vectors overnight. The number of infected MEFs was determined by GFP-positive cells using FACScan.

1.2. HIV-based transfer vectors

pSIN-CSGWdlNotI was generated by deleting one of the two NotI sites in the GFP-expressing HIV vector construct, pSIN-SEW (Kootstra, 2003), which allowed one step cloning of genes of interest by BamHI and NotI. Transfer vectors were generated with full-length human Oct3/4, Sox2, Klf4 and c-Myc cDNAs (Open Biosystems, Huntsville, AL) amplified using the primer pairs:

Oct3/4	5'-ATAGGATCCGCCACCATGGCGGGACACCTGGCTTCGGAT-3'
	5'-ATAGCGGCCGCTCAGTTTGAATGCATGGGAGAGCC-3', BamHI-NotI
Sox2	5'-ATAGGATCCACCATGTACAACATGATGGAGACGGAGC-3'
	5'-ATAGCGGCCGCTCACATGTGTGAGAGGGGCAGTGT-3' BamHI-NotI
Klf4	5'-GACGAATTCGGATCCACCATGAGGCAGCCACCTGGCGAGTCTG-3'
	5'-GACCTCGAGCGGCCGCTTAAAAATGCCTCTTCATGTGTAAG-3',BamHI-XhoI
c-Myc	5'-GCCTGATCAAGGCTCTCCTTGCAGCTGCTTAGACG-3'
	5'-ATAGCGGCCGCTTACGCACAAGAGTTCCGTAGCTG-3', BclI-NotI

cloned into the pSIN-CSGWdlNotI, and resulting in pSIN-Oct3/4, pSIN-Sox2, pSIN-Klf4 and pSIN-cMyc. Human stemness-related factors were driven by a spleen focus-forming virus (SFFV) promoter. HIV vectors were produced by transient transfection of 293T cells using FuGene6 (Roche, Indianapolis, IN) with a weight ratio of 2:1:1 of vector to packaging to VSV-G plasmids (Zufferey, 1997). Transfected cells were washed and grown for 48 h, and supernatants were harvested and passed through a 0.45-μm filter. Vectors were aliquoted and stored at -80°C.

1.3. Western blot

293T/17 cells (CRL-11268; ATCC, Manassas, VA) were maintained in Dulbecco's modified Eagle's medium (DMEM; Invitrogen) supplemented with 10% fetal bovine serum (FBS) and antibiotics. Western blots were run on 12%

SDS PAGE gels and transferred to PVDF membranes using the semi-dry method. Membranes were then blocked overnight. Anti-Oct4 (#2750S), anti-Sox2 (#2748S) and anti-c-Myc (#2276) antibodies (Cell Signalling, Boston, MA) and anti-KLF4 (ab26648-25) antibody (Abcam, Cambridge, MA) were used to verify the expression of human stemness factors in vector-infected cells.

2. Cell culture

Fibroblast medium	**Differentiation medium**
DMEM High glucose (Gibco)	DMEM High glucose (EmbryoMax)
10% FBS	20% FBS
Pen/Strep	Pen/Strep
Glutamax	Glutamax
	Pyruvate
ESC medium	NEAA
DMEM High glucose (EmbryoMax)	BME
15% FBS	
Pen/Strep	
Glutamax	
Pyruvate	
NEAA	
BME	
LIF	

2.1. Mouse embryonic fibroblasts.

Mouse embryonic fibroblasts (MEFs) were obtained from wild type CD1 embryos at 14.5 days post coitum (dpc). Uterus were dissected from the cardiectomized mothers in the general surgical area, put in PBS and carefully transported to a sterile laminar flow hood. All the dissection tools were washed through ethanol 70% from this point on to maintain sterile conditions. Individual embryos were released from their surrounding membranes and washed twice through sterile PBS. Internal organs and head were removed and carcasses finely chopped. Supernatant was collected and maintained on ice prior to digestion of the small tissue pieces at 37°C with 10 ml of 0.25% trypsin-EDTA (Invitrogen, Carlsbad, CA). Digestion was performed three times for 7-10 min each. Obtained suspension was inactivated with equal volume of ice cold

EmbryoMax DMEM (Millipore, Billerica, MA) supplemented with 10% FBS, 1% L-glutamine (Invitrogen) and antibiotics and maintained on ice. After pooling together the suspensions from the three trypsinizations and the first supernatant, total volume was centrifuged for 5 min at 1000 r.p.m. Resulting fibroblasts were plated at a density of two embryos per p100 plate and grown to confluence in the same medium for two passages. Rapidly growing fibroblasts were frozen at this point in nitrogen vials containing 4 million cells. After thawing cells were used or expanded as active fibroblasts or prepared to be inactivated to serve as feeders for pluripotent cells. In this case, fibroblasts were plated, usually onto 2 p150 plates per vial, passaged once more and then inactivated using a final concentration of 10 µg/ml mitomycin C for 2.5 to 3 hours. Cells were then washed twice with PBS, trypsinized for 5 min at 37°C (4 ml 0.25% trypsin-EDTA per p150), 10 ml of fibroblast medium added per plate, centrifuged 5 min at 100 r.p.m. and frozen in vials containing 2-3 million inactive feeders or replated onto gelatinized plates (0.1% gelatin in PBS, for 30 min) at a density of approximately 100,000 cells/cm^2 in fibroblast medium.

2.2. Pluripotent cells.

Culture methods for induced pluripotent stem cells (iPS) were the standard ones for mouse embryonic stem cells (ESC). iPS were usually cultured on mitomycin-inactivated feeders in ESC medium, DMEM (Millipore) supplemented with pyruvate (Lonza, Basel, Switzerland) and L-glutamine (Invitrogen), non-essential amino acids (Mediatech, Herndon, VA), 2-mercaptoethanol (Sigma-Aldrich, St. Louis, MO), 15% FBS (Invitrogen), penicillin/streptomycin (Invitrogen) and LIF (Millipore). Medium was changed every other day. iPS grew as round, compact colonies that were passaged approximately every other day (with occasional one-day delays) when they reached around 50% confluence. At that point, cells were washed three times with PBS followed by a 5 min incubation with 0.25% trypsin-EDTA. After that time, cells were pipetted up and down and checked under the microscope until a

single cell suspension was obtained. Trypsin was inactivated with at least three volumes of ESC medium and cell suspension was centrifuged for 5 min at 1000 r.p.m. Cells were replated at a 1:3 to 1:6 dilution. For some experiments, contamination of inactive feeders was not desirable. In that case, iPS were grown on gelatinized plates for at least 4 passages to allow them to get used to this new condition. *NOTE: Feeder-free iPS stick to the plate and spread out, forming a mono layer of irregular cells instead of compact round clusters. However, staining for pluripotency markers corroborates their pluripotency in spite of the morphological changes*.

2.3. Infection process and clone isolation

Primary fibroblasts were plated at 10^5 cells per 24-well plate for 12 h prior to transduction with a combination of infectious supernatants containing all four human stemness genes. Infectious supernatants were replaced with ESC medium after 12 h. Transduced fibroblasts were replated as cultures became confluent, and individual iPS clones were identified and isolated according to morphology within 2-3 weeks post-transduction. Clonogenic expansion produced reprogrammed cell lines that were maintained in undifferentiation ESC medium. To label iPS with lacZ or luciferase markers, we used HIV vectors carrying lacZ (pLenti6/UbC/V5-GW/LacZ, Invitrogen) or a firefly luciferase-expressing vector, pSIN-Luc (Hasegawa, 2006). LacZ and luciferase vectors were concentrated at 10^5 g using a Beckman L7 ultracentrifuge (SW41 rotor, 25000 r.p.m., 1.5 h, 4°C) and resuspended in 250 µl of serum free medium. Vectors were used to label 10^5 iPS in a 24-well plate for 8-12 h.

2.4. Cell Sorting

LacZ labeled clonal populations were washed and trypsinized into a single cell suspension and small aliquots of 200,000 cells in 100 µl were incubated for 1 min at 37°C with a warm solution of Fluorescein di[®-D-galactopyranoside]

(FDG) (Sigma-Aldrich, F2756) 2 mM for labeling. Loaded cells were immediately mixed with 2 ml of ice cold HBSS (Hank's Buffered Salt Solution) supplemented with 2% Fetal bovine serum, 10 mM Hepes buffer [pH 7.2], 1% penicillin/streptomycin and kept on ice for for 1.5 hours to allow accumulation of fluorescein isothiocyanate (FITC) release from FDG in lacZ positive cells (Guo, 2008). After that time, cells were centrifuged 5 min at 1000 r.p.m. and sorted using a FACS Aria SE flow cytometer (BD Biosciences) where forward and side scatter parameters were used to gate viable cell population, and FITC was excited with a 488 nm argon laser and detected through a 530/30 nm bandpass filter. Recovered lacZ positive cells were centrifuged as previously described and plated on feeders in ESC medium for expansion.

2.5. In vitro differentiation and cardiomyocyte isolation

Transduced cells were differentiated into three-layer embryoid bodies (EB) using the hanging-drop method in differentiation media supplemented with 20% FBS without LIF (Behfar, 2002; Demaison, 2002; Perez-Terzic, 2003). Briefly, 25 μl drops from a 25,000 cell/ml suspension were cultured on the lid of a plate for 48 h. EB were then flushed and kept in suspension for 2 days to allow spontaneous differentiation for a total of 5 days. For further differentiation, EB were either kept in suspension or transferred 30-40 spheroids per p10 into cell culture plates coated with 0.1% gelatin. Cells were maintained in differentiation medium that was changed every 2-3 days. Beating areas were monitored daily starting at day 6. Digital serial images were taken from beating floating EB at days 11-12 and were analyzed with the Metamorph software (Visitron Universal Imaging, Downingtown, PA).

For cardiomyocyte isolation, dual interface Percoll gradient (Invitrogen) was used to enrich high density cardiomyocytes from differentiating embryoid bodies at days 10-12 (Hodgson, 2004). The following solutions were used:

ADS Buffer 10X (500 ml)
34 g NaCl
23.8 g Hepes
0.6 g NaH_2PO_4
2 g KCl
0.5 g $MgSO_4$
Adjust pH to 7.35±0.05
Filter sterile

ADS Buffer 1X (500 ml)
50 ml ADS 10X
450 ml distilled water
0.5 g Glucose
Filter sterile

Digestion mix (50 ml)
30 mg Collagenase IV
5 mg Pancreatin
50 ml ADS buffer
Filter sterile

Percoll stock (50 ml)
45 ml Percoll
5 ml ADS 10X

High density Percoll (10 ml)
7.5 ml Percoll stock
2.5 ml ADS 1X

Low density Percoll (10 ml)
5.5 ml Percoll stock
4.5 ml ADS 1X

Differentiating EB were washed twice with PBS and 3 ml of warm digestion mix were added to each plate and incubated at 37°C for 30 min. With a 5 ml pipette, EB were gently separated from the plate followed by addition of 3 ml of fresh warm digestion mix. Cells were incubated at 37°C for 30 min, being pipetted gently up and down every 10 min. This procedure was repeated until a uniform single cell suspension was obtained. At that point, 5 ml of serum were added to every 45 ml of digestion mix used and total volume was spun down for 5 min at 1000 r.p.m. Digestion mix was aspirated and cells were resuspended in 20 ml of ADS 1X , counted and centrifuged again. Resulting pellet was resuspended at a density of about $15x10^6$ cells/ml ADS 1X.

During this last centrifugation, Percoll gradient was prepared. For that, 3 ml of high density Percoll solution were slowly pipetted into a 15 ml falcon tube without touching the walls of the tube. 1.5 ml of low density Percoll solution were very carefully added on top using a 1 ml pipet set to the slowest speed, followed by 1.5 ml more. A sharp interface should be clear between the two densities. Finally, suspension of cells in ADS 1X is slowly added to the top of the gradient, usually in a 1 to 2 ml. Tubes are centrifuged for 30 min at 3000 r.p.m. without break and with the slowest acceleration and deceleration rates. Cells of interest will stay in the interface between the two Percoll solutions after centrifugation. To recover them, the first layer and part of the second were gently aspirated. Then, with a 1 ml pipet, interface is transferred to a tube containing 10 ml of fresh ADS 1X. Cells are spun down for 5 min at 1000 r.p.m. This step was repeated, counting the cells before centrifugation. 12 and 25 mm round cover glasses were coated for 2 hours at 37°C with 1 μg/cm^2 laminin, followed by 5 rinses with 0.1% gelatin. Resulting cells were plated on coated cover glasses at a density of approximately 10^5/cm^2 for at least 24 h before further experiments.

3. Staining and imaging

3.1. Immunofluorescence

Unless otherwise stated, the protocol used for immunofluorescence in either sections or cell cultures was as follows:

Samples were fixed with 3% paraformaldehyde for 15 min and washed three times with PBS, followed by permeabilization for 30 min with 1% Triton (in PBS) at room temperature (RT). After washing three times with PBS, blocking was performed by directly adding Superblock (Thermo Scientific) and incubating for either 30 min at RT or overnight at 4°C. Solution was removed and without further wash primary antibody solution was added and incubated for 2 hours at RT. *NOTE: If multiple primary antibodies were used in the same sample, a combined solution with equivalent final concentrations was used both in this step and in the secondary antibody incubation*. Antibodies were diluted in antibody dilution buffer (PBS 1X, 1/10 Superblock, 0.1% Tween 20). Primary antibody solution was discarded followed by three washes with post-antibody (PBS 1X, 0.1% Tween 20) and a 1 hour incubation at RT with secondary antibody in antibody dilution buffer. Sample was then washed once with post-antibody was and three times with PBS prior to 4',6-diamidino-2-phenylindole (DAPI) stain for 8 min at RT. DAPI was washed three times with PBS and samples were mounted using Fluoromount-G™ (Southernbiotech) mounting solution. Primary antibodies along with catalog numbers and dilutions are detailed in **Table 5**. Secondary antibodies are listed in **Table 6.**

Table 5. Primary antibodies

Use	Antibody	Dilution	Host	Manufacturer	Cat #
iPS derivation	Oct4	1:200	rabbit	Cell signaling	#2750S
	Sox2	1:200	rabbit	Cell signaling	#2748S
	c-Myc	1:200	mouse	Cell signaling	#2276
	KLF4	1:200	rabbit	Abcam	ab26648
Pluripotency	SSEA1	1:50	mouse	Millipore	MAB4301
Cardiac differentiation	alpha-actinin	1:200	mouse	Sigma	A7811
	connexin43	1:200	rabbit	Zymed	483000
	Mef2c	1:50	rabbit	proteintech	100561-AP
	myosin light chain 2a	1:250	mouse	Synaptic Systems	311011
	myosin light chain 2v	1:250	mouse	Synaptic Systems	311011
	smooth muscle actin	1:200	rabbit	Abcam	ab5694
	CD31	1:200	mouse	Abcam	ab9498
LacZ tracking	β-galactosidase	1:5000	rabbit	Abcam	ab616

Table 6. Secondary antibodies

Fluorochrome	Target	Dilution	Host	Manufacturer	Cat #
FITC	mouse IgG	1:400	donkey	Jackson Immuno Research	715-095-150
FITC	rabbit IgG	1:400	donkey	Jackson Immuno Research	711-095-152
FITC	rabbit IgG	1:250	Goat	Invitrogen	65-6111
Alexa Fluor 568	mouse IgG	1:250	goat	Invitrogen	A11031
Alexa Fluor 488	mouse IgG	1:250	donkey	Invitrogen	A21202

3.2. X-gal staining

1. Phosphate buffer pH 7.3 (500 ml)
115ml 0.1 M sodium phosphate monobasic
385ml 0.1 M sodium phosphate dibasic

2. Fix solution (50 ml)
0.4 ml 25% glutaraldehyde
2.5 ml 100 mM EGTA pH 7.3
0.1 ml 1 M magnesium chloride
47 ml phosphate buffer (1)

3. Wash buffer (200 ml)
0.4 ml 1 M magnesium chloride
2.0 ml 1% deoxycholate
2.0 ml 2% Nonidet-P40
195.6 ml phosphate buffer (1)

4. X-gal stain (52 ml)
2.0 ml X-gal stock (25 mg/ml in di-methyl formamide)
1 ml 0.25 M potassium ferrocyanide
1 ml 0.25 M potassium ferricyanide
48 ml wash buffer (3)

Samples were washed three times in phosphate buffer and fixed with fix solution for 15 min (embryos) or 5 min (cells) at RT, followed by three washes in wash solution. Samples were stained in X-gal solution overnight at 37°C in the dark and kept in wash buffer after three washes.

Transmitted light images were acquired using Zeiss Axiovert 40 CFL microscopes with ProgRes C3 or PogRes C10 plus cameras. Embryos and macroscopic samples were imaged with a Zeiss SteREO Discovery.V20 using a ProgRes C3 camera. In all cases ProgRes Mac Capture Pro 2.5 software was used.

3.3. Hematoxylin/Eosin staining

Cryosections were fixed in 10% buffered formalin for 5 min prior to staining. They were rinsed in distilled water and dipped in hematoxylin solution (Biocare Medical) for 2.5 min prior to a second rinse in running tap water for 40 s

followed by 30 s in 1X Tacha's bluing solution. This was rinsed for 6 min in running water and 30 s in 95% ethanol. Slices were dipped into eosin solution for 45 s and passaged through 95% ethanol, 100% ethanol and xylol prior to mounting with cytoseal/permount.

3.4. Electron microscopy

For ultrastructural evaluation, fibroblasts and iPS were fixed *in situ* with 1% glutaraldehyde and 4% formaldehyde in 0.1 M phosphate buffered saline (PBS; pH 7.2). For field-emission scanning electron microscopy (FESEM), specimens were rinsed in 0.1 M phosphate buffer (pH 7.2) supplemented with 1% osmium, dehydrated with ethanol, dried in a critical point dryer (Ted Pella, Redding, CA) and coated with platinum. Cells were examined on a Hitachi 4700 field emission scanning microscope. For ultrastructural evaluation by transmission electron microscopy (TEM), fixed cells were processed in phosphate-buffered 1% OsO_4, stained en bloc with 2% uranyl acetate, dehydrated in ethanol and propylene oxide, and embedded in low-viscosity epoxy resin. Thin (90-nm) sections were cut with an ultramicrotome (Reichert Ultracut E), placed on 200 µm mesh copper grids, and stained with lead citrate. Micrographs were taken on a JEOL 1200 EXII electron microscope (Perez-Terzic, 2003).

3.5. Confocal imaging

3.5.1. Immunostaining

Immunostained samples were imaged using a Zeiss LSM 510 confocal microscope, and analyzed using Zeiss LSM software.

3.5.2. Calcium

To assess intracellular Ca^{2+} dynamics, cells were washed twice with PBS and loaded with the Ca^{2+}-fluorescent probe Fluo 4-AM (Invitrogen) at a

concentration of 4 µM in medium without serum for 15 min at 37°C. Cells were again washed twice after the incubation and fresh warm differentiation medium was added. Recordings were done in a Zeiss LSM live 5 laser confocal microscope, and analyzed using Zeiss LSM software (Hodgson, 2004).

3.6. In vivo imaging

Two and four weeks after transplantation with luciferase-labeled cells, *in vivo* distribution of fibroblasts and iPS was monitored. Mice were injected i.p. with 150 mg/kg D-luciferin (Xenogen Corp., Alameda, CA) and luciferase-expressing cells were visualized by the IVIS 200 Bioluminescence Imaging System (Xenogen). Bioluminescence signals were analyzed using the Living Image Software (Xenogen).

4. gDNA and RNA extractions, cDNA synthesis and PCR

4.1. Genomic DNA

Genomic DNA (gDNA) was obtained using an Extract-N-Amp™ Tissue PCR kit (Sigma, XNAT2). Cell pellet was incubated with Extraction solution for 10 min at RT followed by 3 min at 95°C. Neutralization solution was added and an aliquot was used for genomic integration polymerase chain reaction (PCR) using solutions included in the kit and the following primers:

SFFVprom-F →CTCACTCGGCGCGCCAGTCCTC
OCT4-R → AGCCGCCTTGGGGCACTAGCCC
KLF4-R →CGCAAGCCGCACCGGCTCCGCC
SOX2-R →AGCCTCGTCGATGAACGGCCGC
c-MYC-R →GGGAGAAGGGTGTGACCGCAAC

Vector integration PCR reaction cycle was as follows: dissociation at 94°C for 5min, thermocycling for 35 cycles of 94°C for 20 s, 57°C for 20 s and 72°C for 30 s and a final step of 5 min at 72°C. PCR products were resolved on 1% agarose gel electrophoresis.

4.2. mRNA extraction

RNeasy plus mini kit from Qiagen was used according to manufacturer instructions on cell precipitates fast-frozen by immersion in liquid nitrogen. Final RNA concentration and quality were measured in a NanoDrop spectrophotometer that used the NanoDrop ND-1000 V3.3.1 software.

4.3. cDNA synthesis

SuperScript® III Reverse Transcriptase kit from Invitrogen was used. 1 µg mRNA was used in a 20 µl total reaction volume. In brief, mRNA volume was supplemented up to 6 µl with RNAse free water and mixed with 1 µl of annealing buffer and 1 µl oligo dT primer and incubated for 5 min at 65°C. 10 µl reaction buffer and 2 1 µl enzyme mix were added after 1 min on ice and reaction was incubated for 50 min at 50°C followed by a final step of 5 min at 85°C. cDNA samples were stored at 4°C until used for real time PCR (RT-PCR).

4.4. Real time PCR

RT-PCR was performed in a Applied Biosystems Prism 7900HT Real Time System using SDS 2.3 software for recording and RQ Manager 1.2 for analysis. All primers used were from Applied Biosystems and included:

Mouse ***Gapdh*** (4352932E as control)	***Sox7*** (Mm00776876_m1)
Sox2 (Mm00488369_s1)	***Nkx2.5*** (Mm00657783_m1)
Oct3/4 (Mm00658129_gH)	***Tbx5*** (Mm00803521_m1)
Fgf4 (Mm00438917_m1)	***Mef2c*** (Mm01340839_m1
Lhx1 (Mm00521776_m1)	***Gata4*** (Mm00484689_m1)
Gsc (Mm00650681_g1)	***Mesp1*** (Mm00801883_g1)
Kdr (Mm00440099_m1)	***Mesp2*** (Mm00655937_m1)
Cxcr4 (Mm01292123_m1)	***Myocardin*** (Mm00455051_m1)
Sox17 (Mm00488363_m1)	

5. Surgical procedures

5.1. Diploid aggregations

5.1.1. Timed pregnancy of superovulating wild type donors

Female CD1 wild type (WT) mice were treated with reproductive hormones to maximize the isolation of stage-specific embryos (Eakin and Hadjantonakis, 2006). In brief, superovulation was achieved in 3-4 week old females at the final stage of prepubescent development. On day 1 at 14:00 h, female donors received a single intraperitoneal (ip) injection (5 units in 0.1 ml) of pregnant mare serum gonadotropin (PMSG) using a 27-gauge needle (**Figure 15**). Two days later at 13:00 h, donors received an ip injection (5 units in 0.1 ml) of human chorionic gonadotrophin (HCG). WT females were immediately paired with CD1 WT studs to achieve timed mating that occurred during the night on day 3 according to circadian rhythm dictated by the light/dark cycle. Superovulated females were removed from studs the following morning, and allowed to proceed through normal pregnancy. WT embryos, at 2.5 d.p.c., were harvested by retrograde flushing from the distal oviduct through the infundibulum using a 32-gauge needle. Superovulated donors produced up to 30 synchronized embryos in a single oviduct.

5.1.2. Collection of zona pelucida-denuded morula

Morula-stage embryos (**Figure 15**) were washed in EmbryoMax M2 medium (Millipore, Billerica, MA) at 37°C to remove cellular debris associated with oviduct flushing (Eakin and Hadjantonakis, 2006). Glycoproteinaceous zona pelucida was removed to produce denuded morula, competent for stem cell integration. A 35-mm culture dish was prepared with a drop of warm M2 and a drop of acid Tyrode solution at room temperature. Embryos, in groups of 20-30, were transferred with as little M2 medium as possible into the acid Tyrode solution, and continuously irrigated to keep neighboring embryos separated until

zona pelucida dissolved within 30-40 s. Once stripped of their zona pelucida, denuded morula were washed in 5 drops of warm M2 followed by 5 drops of warm EmbryoMax KSOM (Millipore, Billerica, MA), preparing them for subsequent in vitro manipulation.

5.1.3. Selection of pluripotent cell clumps

Murine embryonic stem cells (R1-derived line) containing single copy of the constitutively expressed β-galactosidase gene (Nelson, 2008; Nelson, 2006) or either lacZ or GFP labeled iPS were seeded at three different dilutions in ESC medium on inactivated MEF in a 6-well plate on day 1. Cells at the appropriate density were split 1/3, 1/6, and 1/12 on day 3 in order to ensure proper density for diploid aggregation (Nelson, 2004). On day 6, cells at ~60% confluence were digested with 1 ml of warm 0.25% trypsin-EDTA for 4 min at 37°C until they were loosely associated with each other. Gentle mechanical disruption was required to produce small clumps of cells before adding 5 ml of growth medium to inactivate trypsin solution (Eakin and Hadjantonakis, 2006). Care was taken to avoid producing single cell suspensions. The mixture was pre-plated for 40 min on tissue culture plates to allow feeder cells to attach before collection of labeled stem cell clumps. Selected clumps were washed in 5 drops of M2 medium followed by 5 drops of KSOM medium for subsequent diploid aggregation (**Figure 15**).

5.1.4. Synchronized pseudopregnancy of surrogate females

Surrogate mothers are required for proper *in vivo* development of embryos reengineered outside of the natural environment. CD1 WT females, at least 8-12 weeks old, were maintained in a colony of 50-70 animals (Eakin and Hadjantonakis, 2006). On day 4, females in estrus were identified by careful examination of vaginal changes indicated by dry, pink, and swollen external

mucosa. Selected females provided the most reliable source for successful mating when paired with vasectomized studs (**Figure 15**). The estrous cycle in mice is 3-4 days long with ovulation occurring at approximately the midpoint of the dark period (midnight) of a light/dark cycle. Females caged together without a male tend to cycle in unison. Pseudopregnant females were identified the following morning (day 5) upon visualization of a vaginal plug.

5.1.5. Diploid aggregation of wild type embryos with pluripotent cells

Integration of labeled pluripotent cells with competent morula-stage embryos produced mosaic blastocytes *in vitro* that were surgically transferred into the uterus of pseudopregnant females for subsequent embryonic development. Using a KSOM-filled syringe, 12 microdrops (~3 mm in diameter) were placed into a 35-mm tissue culture dish and covered with sterile mineral oil using aseptic procedures. Drops were incubated overnight at 37°C in 5% CO2 to buffer the medium to appropriate pH. The aggregation needle (Type DN-09, BLS Ltd., Hungary) was washed with 70% ethanol, and used to make 5 wells per drop under mineral oil by firmly pressing into the plastic tissue culture plate. Aggregation-competent morula devoid of zona pelucida were micropipetted with a capillary needle. Each well containing two morula also received a single clump of 8-15 labeled pluripotent cells initiating coerced aggregation. The aggregation partners were incubated for 24 hours in KSOM medium in a table top incubator (Thermofisher, Waltham, MA) with continuous flow of a humidified gas mixture (5% CO2/5% O2/90% N2). Cellular integration of labeled cells with endogenous blastomeres of the WT morula developed into a mosaic blastocyte displaying characteristic morphology indicated by progressive cavitation. At this point, some embryos were fixed in 0.25% glutaraldehyde and stained for β-galactosidase to assess pluripotent cell integration into the obtained blastocyst or imaged under a fluorescence microscope to detect GFP labeled cells. The rest of the resulting embryos were collected, washed in M2 medium, and loaded into a glass capillary with a diameter slightly larger than an individual embryo for intrauterine transfer.

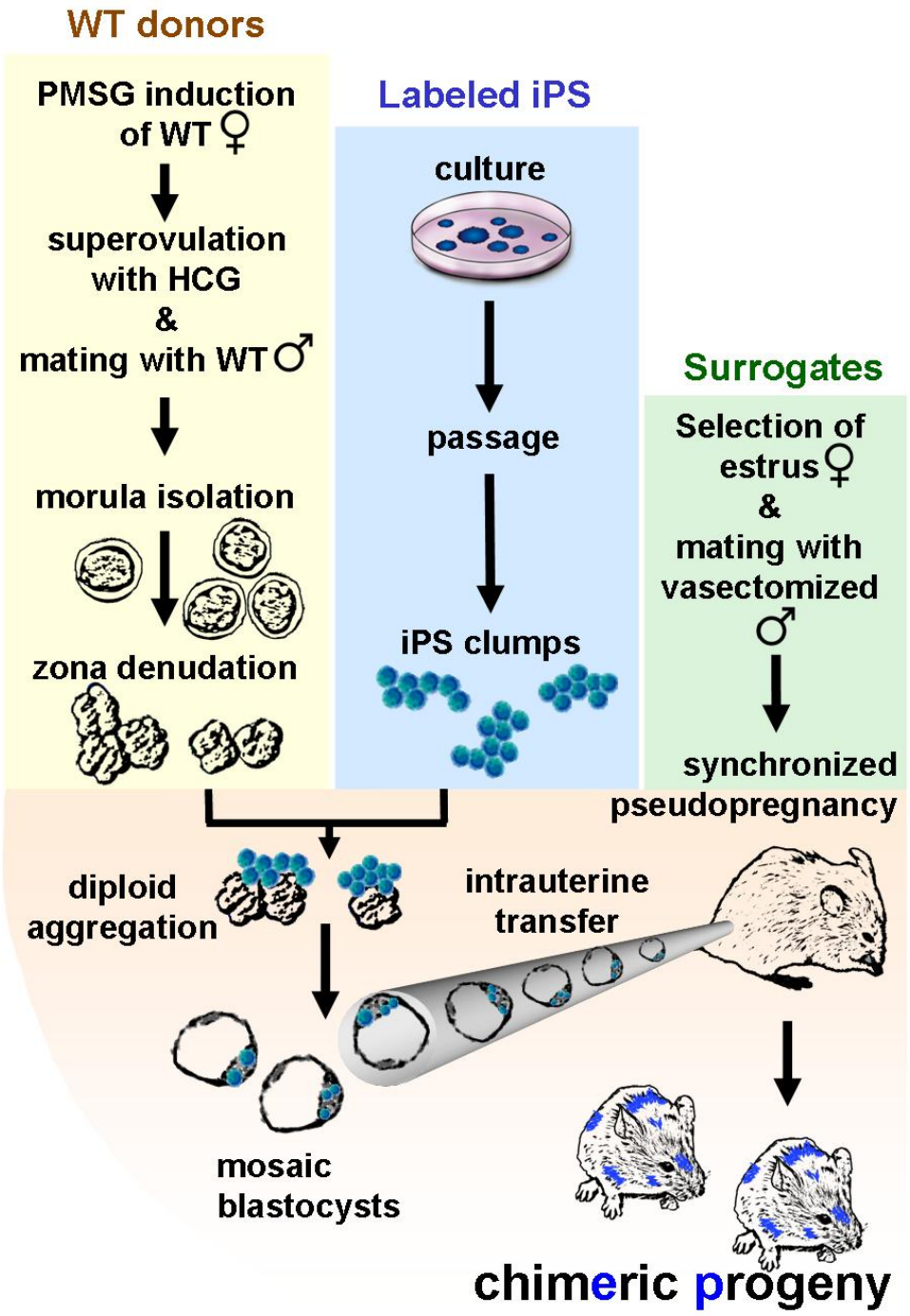

Figure 15. Flowchart of diploid aggregation protocol. *Yellow box*: generation of wild type (WT) donor embryos from timed pregnant females. *Blue box*: simultaneously, labeled cells (induced pluripotent stem cells, iPS) are grown for two passages and digested to obtain small cell clumps. *Green box*: Synchronized pseudopregnant surrogates are produced that receive mosaic blastocyst via intrauterine transfer to be supported through pregnancy (*Orange bottom*)

5.1.6. Intrauterine blastocyte transfer

Pseudopregnant WT surrogates were surgically prepared under general anesthesia (2-3% inhaled isoflurane) for intrauterine blastocyte transfer. The uterus was dissected out through a small incision in the flank of a pseudopregnant surrogate and exposed with the ovary, oviduct, and distal portion of the uterus pulled outside of the peritoneum and secured with a microtissue clamp attached to the ovarian fat pad. Blunt forceps were used to hold the oviduct in order to position and stabilize the transfer site without direct manipulation of the uterus. A 30-gauge needle was used to puncture an entry hole in the distal portion of the uterus using a low-power dissection microscope, followed by immediate insertion of glass capillary and transfer of blastocyte-stage embryos. Pseudopregnant surrogates tolerated the invasive surgical procedure without complications and were capable of full-term pregnancy. Between days 8.0 and 13.0 d.p.c. some embryos were harvested after cardiectomy of the pregnant mothers, fixed in 0.25% glutaraldehyde and stained for β-galactosidase to assess contribution of the labeled pluripotent cells at different stages. The rest of the pregnancies were allowed term. Chimeric offspring were identified by heterogenous coat color derived from a mixture of pluripotent stem cells that produce black coat color and embryonic tissues in the white CD1 WT background (**Figure 15**).

5.2. Myocardial infarction and therapy

Male, 8-12 weeks old C57BL/6 mice underwent myocardial infarction through coronary ligation of the left anterior descending artery (Yamada, 2009). Mice were intubated for mechanical ventilation (Mini Vent 845, Hugo Sacks Electronik, March-Hugstetten, Germany) to allow open thoracotomy and direct visualization of the left coronary artery for permanent ligation with a 9-0 suture. Within 30 min after ligation, myocardial ischemia was confirmed by changes in electrocardiography, echocardiography, and color of the left ventricular wall.

Fibroblasts and iPS, engineered to express the lacZ and luciferase reporter transgenes, were propagated in ESC medium. Simultaneous to surgery, cultured cells were prepared as a single-cell suspension at a density of 200,000 cells in 10 µl of differentiation medium. Cells were maintained on ice until transplanted into ischemic myocardium with four separate injections of 2.5 µl in the peri-infarcted area under microscopic visualization 30 min after coronary ligation.

Post-mortem tissue was processed by rapid freezing and cut by cryosections at 7 µm thickness to be stained with hematoxylin/eosin procedures or immunofluorescence techniques (Behfar, 2007; Yamada, 2008).

5.3. Teratoma formation

Native and transduced fibroblasts were injected subcutaneously into the flank skin of anesthetized athymic nude mice at a dose of 500,000/50 µL differentiation medium. Tumor growth was monitored daily until tissue was harvested. Tumors were processed by rapid freezing and cut by cryosections at 7 µm thickness to be stained with standard hematoxylin/eosin (Behfar, 2007).

6. Cardiac function and structure

Ventricular function and structure were quantified *in vivo* by trans-thoracic echocardiography (RMV-707B scan head, Vevo770, Visual Sonics, Toronto, Canada) prior to and after myocardial infarction - at 30 min (before cell injection), and sequentially after cell injection at 1 day, 1 week, 2 weeks, 3 weeks, and 4 weeks. Animals were kept under light anesthesia. Ejection fraction (%) was calculated as [(LVVd - LVVs)/LVVd] × 100, where LVVd is left ventricular end-diastolic volume (μL) and LVVs, left ventricular end-systolic volume (μL). Left ventricular fractional shortening (% FS) was calculated as [(LVDd - LVDs)/LVDd] × 100, where LVDd is left ventricular end-diastolic dimension (mm) and LVDs, left ventricular end-systolic dimension (mm) (Yamada, 2008). Electrical abnormalities were evaluated using 4-limb-lead electrocardiography (MP150, Biopac, Goleta, CA).

7. Electrophysiology

Dual interface Percoll gradient (Invitrogen) was used to enrich sarcomere-rich high density cardiomyocytes from differentiating embryoid bodies at days 11-12 (Hodgson, 2004). Resulting cells were plated onto laminin (Invitrogen) coated coverglasses for at least 24h before further experiments. Membrane electrical activity of iPS-derived cardiomyocytes or parental fibroblasts was determined by patch-clamp recording in the whole cell configuration using the current- or voltage-clamp mode (Axopatch 1C, Axon Instruments). Action potential profiles and voltage-current relation were acquired and analyzed with the Bioquest software. Cells were superfused with Tyrode solution containing (in mM) 137 NaCl, 5.4 KCl, 2 $CaCl_2$, 1 $MgCl_2$, 10 HEPES, and 10 glucose (with pH adjusted to 7.3 with NaOH) or calcium-free Tyrode in which $CaCl_2$ was replaced by EGTA 5 mM. Patch pipettes (5–10 M•) containing (in mM) 140 KCl, 1 $MgCl_2$, 10 HEPES, 5 EGTA, and supplemented with 5 mM ATP (with pH adjusted to 7.3 with KOH) were used for electrophysiological measurements performed at 34±1°C regulated by a temperature controller (model HCC-100A, Dagan) equipped with a Peltier thermocouple (Karger, 2008).

8. Statistical analysis

Statistics Data are presented as mean ± SEM. Student *t* test was used to evaluate significance of PCR data. Wilcoxon test was used to evaluate physiological parameters between chimeric and non-chimeric cohorts. A probability value <0.05 was predetermined.

VI. Results

1. Converting somatic cells to a pluripotent state

Induced pluripotent stem cell (iPS) platform offers unique opportunities for derivation of autologous pluripotent cells that could be used as biologics in regenerative medicine. Here, we use HIV-derived lentiviruses as a high efficiency delivery method to reprogram the pluripotent ground state of mouse somatic cells by transduction with human stemness-related factors. Isolation of individual engineered clones will allow us to further investigate both pluripotency and differentiation properties of the reprogrammed cells.

1.1. Engineered HIV vector packaging constructs for improved transduction efficiency across species

In order to enable this inter-species reprogramming, an efficient delivery method was required to transduce across species and cytotypes. Seminal iPS derivation protocols employed retroviral or lentiviral vectors to deliver defined pluripotency-related factors (Takahashi and Yamanaka, 2006; Yu, 2007). Unlike conventional retroviral vectors, which transduce only dividing cells, lentiviral vectors can deliver genes into both dividing and non-dividing cells (Mali, 2008). Lentiviral vectors also reach higher titers than retroviral vectors, making them particularly attractive vehicles to deliver multiple pluripotency-associated factors (Demaison, 2002). Lentiviral vectors, however, have an unfortunate drawback of host range restriction and limited tropism (Ikeda, 2002). For instance, human immunodeficiency virus type 1 (HIV)-based lentiviral vectors can transduce most human cell types efficiently, while their infectivity in monkey and mouse cells is relatively poor (Hofmann, 1999; Ikeda, 2002). This is thought to be partly due to species-specific host restriction factors in non-human cells and lack of specific receptors that mediate HIV-1 cell entry (Noser, 2006; Stremlau, 2004; Zhang, 2008). For applications such as iPS generation, multiple genes need to be

delivered simultaneously into a single cell. Thus, the development of specialized lentiviral vectors with broader tropism offers distinct advantages for iPS generation and provides a unique tool to further examine inter-species activity of stemness-related factors.

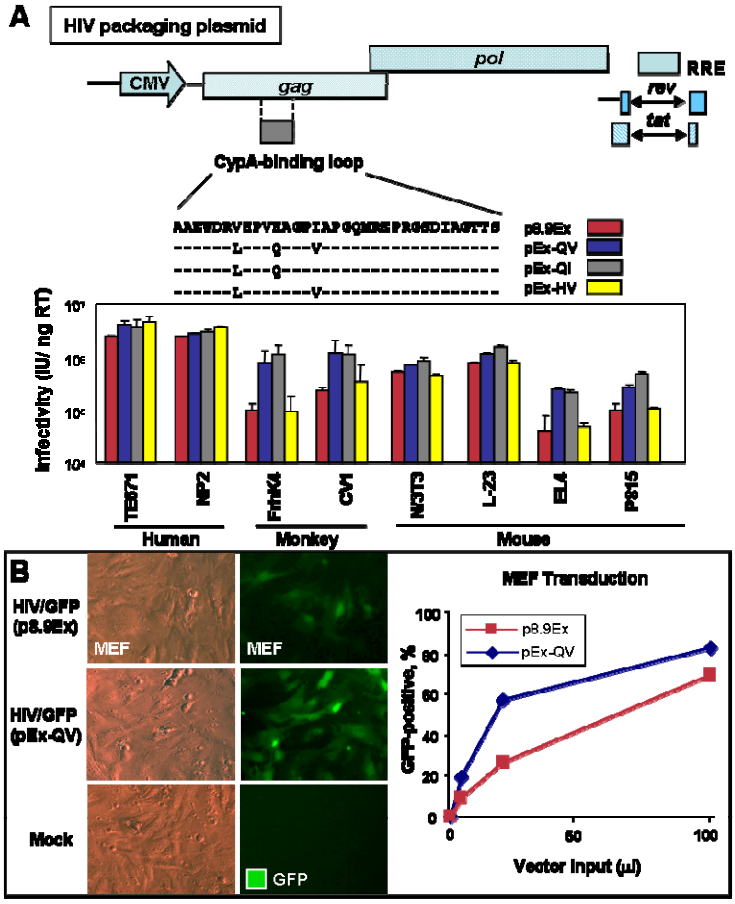

Figure 16. The H87Q capsid substitution in vector packaging constructs increases HIV vector infectivity in murine cells. A) Naturally occurring capsid substitutions were introduced into the cyclophilin A-binding region of HIV-1 *gag* gene of a vector packaging construct, p8.9Ex. Infectious HIV vectors were generated by packaging a GFP-carrying HIV vector genome with the modified constructs, and the amounts of vectors were normalized by the levels of endogenous reverse transcriptase activity. Human, simian and murine cell lines were infected with various amounts of GFP-expressing vectors, and the GFP-positive cell populations were analyzed by flow cytometry. The vector infectivity in each target cell line was determined by infectious units/ng reverse transcriptase activity. B) GFP-carrying HIV vectors were generated with a conventional HIV packaging construct (p8.9Ex) or a packaging construct with the H87Q capsid substitution (pEx-QV). 5 x 10^4 MEF cells were infected with increasing amounts of unconcentrated vectors. The percentage of transfected cells was observed by comparing total cells to GFP-positive cells under UV microscope 3 days after infection (left panels, with 20 µl of vector input) and analyzed by flow cytometry 5 days after vector infection (right panel).

Efficient HIV infection requires cyclophilin A (Cyp A) in target human cells (Thali, 1994), with sequence variations in the Cyp A-binding loop of the capsid protein affecting viral infectivity (Chatterji, 2005; Ikeda, 2004; Kootstra, 2003). Capsid mutations were here used to improve infectivity of HIV-based vectors across species in order to test human stemness related factors in non-human cell types (Figure 1A). By generating GFP-expressing HIV vectors containing specific mutations in the cyclophilin A-binding loop region, efficiency of infectivity was quantified within multiple cell lines. When the vector particle numbers were adjusted to the virion reverse transcriptase activities, the engineered packaging constructs pEx-QV and pEx-QI showed improved infectivity when screened in simian FrhK4 or CV1 cells as well as in murine P815 or EL4 cells compared to the parental p8.9-Ex vector without affecting vector infectivity in human cells (Figure 1A). The absolute infectious vector yields were 2 to 3-fold higher with pEx-QV over p8.9-Ex or modified pEx-QI (**Figure 16A**). Furthermore, the pEx-QV-packaged HIV vector transduced mouse embryonic fibroblasts (MEFs) more efficiently than the parental p8.9-Ex (**Figure 16B**). The validated packaging construct pEx-QV was therefore selected to deliver stemness related factors.

1.2. Efficient expression of human stem cell-related factors in non-human recipients

Human sequences were used to generate reprogramming vector sets to be tested in evolutionary distant somatic cell types. Gene sequences demonstrated a high degree of conservation with the lowest percentage of homologies noted between Oct3/4 orthologs at 84%. This degree of homology is similar to the LIF gene (**Figure 17A**). Human cDNAs for stemness-related factors were amplified by PCR and cloned into the selected pEx-QV HIV vector plasmid to produce expression vectors encoding human OCT-3/4, SOX2, KLF4, AND C-MYC (Figure 17B). Proper expression was verified in human 293T cells with predicted molecular weight transgene products detected by immunoblotting with

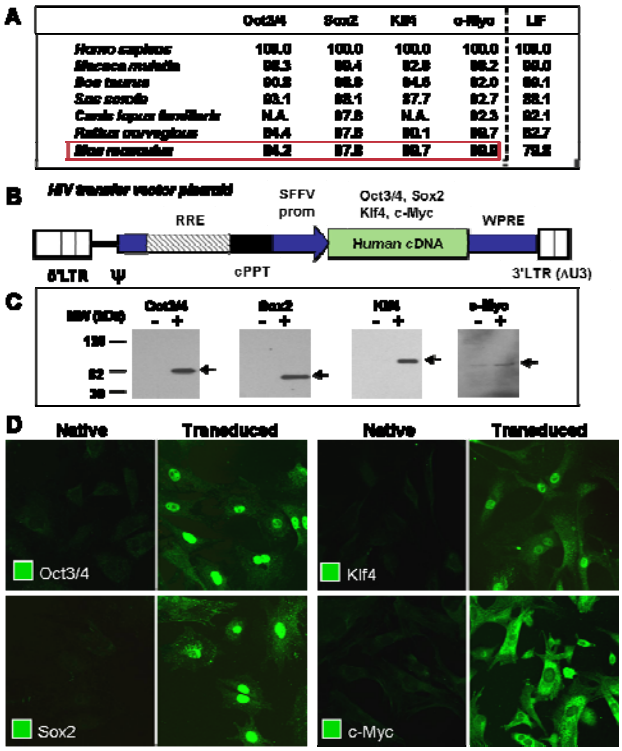

Figure 17. Efficient expression of stemness-associated factors in human and murine cell types. A) Percent amino acid homology among orthologous stemness-related factors. Homology for LIF served as benchmark. Homology was determined by LALIGN program (EMBNet). NA = protein sequence not available. B) Schematic representation of HIV-1 vector genome construct used to generate stemness factor-expressing vectors. ψ; packaging signal, LTR; long terminal repeat, RRE; Rev-responsive element, cPPT; central polypurine tract, SFFV; Spleen focus-forming virus promoter, WPRE; Woodchuck hepatitis virus post-transcriptional regulatory element. OCT3/4, SOX2, KLF4 and C-MYC cDNAs were driven by an internal SFFV promoter. The Klf4-encoding vector lacks the WPRE. B) 2 x 10^5 293T cells were infected with 50 µl of the factor-expressing vectors. Three days after infection, expression of full-length stemness factors was verified by western blotting with respective antibodies. C) 5 x 10^4 MEF cells were infected with 100 µl of unconcentrated vectors. Expression levels of transgene products were visualized by immunostaining with the specific antibodies 4 days after infection.

Oct-3/4, Sox2, Klf4, and c-Myc antibodies (**Figure 17C**). Robust transgene expression of the four human stemness-related factors was also detected in more than 90% of the MEFs (**Figure 17D**). Thus, the pEx-QV HIV-based lentiviral platform demonstrated cross-species tropism, and consistently delivered interspecies transduction of human pluripotent genes. Therefore, this vector packaging construct was selected to deliver stemness factors and ensure a high degree of infectivity within mouse somatic cells.

1.3. Virus-transduced reprogramming of mouse embryonic fibroblasts

To determine whether the human stemness-related factors can reprogram mouse somatic cells back to a pluripotent ground state, ectopic gene expression was achieved in MEFs with two different sets of genes, namely OCT4, SOX2, KLF4 and c-MYC (4F) and SOX2, OCT4 and KLF4 (3F) (**Figure 18**).

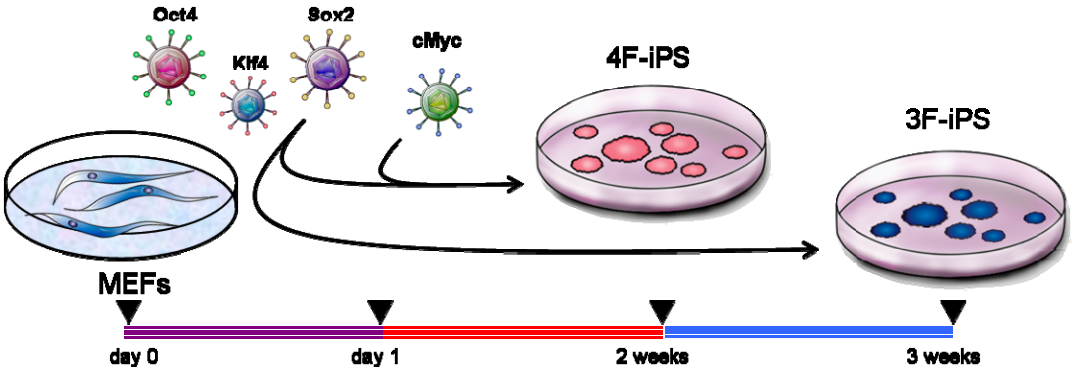

Figure 18. Time course of mouse embryonic fibroblast reprogramming with and without c-MYC. Mouse embryonic fibroblasts were transduced one day after plating with HIV-derived lentiviruses containing 4 (SOX2, OCT4, KLF4 and c-MYC) or 3 (SOX2, OCT4 and KLF4) human genes. Round and compact embryonic-stem-cell-like colonies were observed after 2 weeks in 4 factor-induced (4F-iPS) cultures and after 3 weeks in 3 factor-induced (3F-iPS) clones.

On cross-species transduction with 4 or 3 human stemness-related factors, vector-derived transgenes were stably integrated in engineered progeny and absent from the untransduced parental source as detected by genomic DNA PCR (**Figure 19A**). MEFs grew in monolayers demonstrating contact inhibition on culture confluence. Elongated flat cells typical of fibroblasts provided a homogenous population of starting somatic tissue (**Figure 19B**). MEFs were infected with lentivirus containing a GFP-expressing vector as control for any spontaneous cellular changes, 4 different lentivirus containing human cDNA for reprogramming genes SOX2, OCT4, KLF4 and c-MYC (4F) or 3 lentivirus, SOX2, OCT4 and KLF4 (3F).Two days post-infection, transduced cells were

passaged on to inactive feeders and monitored for the formation of embryonic stem cell-like colonies according to morphology consisting of compact clusters of condensed cytotypes (Meissner, 2007). In contrast to monomorphic single-cell layered fibroblasts in GFP-control groups, MEFs treated with the combination of four or three human factors produced numerous colonies that reached sufficient size to isolate individual clones after 14 days for 4F transduced cells and after 21 days for cells infected in absence of c-Myc (3F) (**Figure 18** and **19B**), in agreement with previously described protocols, revealing that reprogramming with cross-species factors is not delayed with respect to same-species transduction (Wernig, 2008).

Colonies were individually picked and clonally expanded for several passages to obtain sufficient amounts of cells to be further characterized. Morphological criteria, namely embryonic stem cell-like characteristics such as compact growth and round shaped defined edged cell aggregates, were applied for the isolation of individual colonies from the initially transduced cultures (Meissner, 2007). Other protocols have been described that based clonal selection on upregulation of pluripotency related genes such as Nanog (Okita, 2007; Wernig, 2007) or Oct4 (Wernig, 2007) visualized by GPF expression or neomycin resistance. However, comparative studies (Meissner, 2007) have demonstrated that embryonic stem cell-like morphology is a simple yet validated feature to identify *bona fide* reprogrammed clones, making further genetic modifications for selection purposes unnecessary and therefore rendering this technology more easily transposable to the human setting.

Growth characteristics of isolated cell lines were further characterized. Compared to native MEF, clonal expansion of isolated colonies produced rapidly dividing cell lines without contact inhibition and with maintained embryonic stem cell morphology through a minimum of 10 passages (**Figure 19B**, top). Tightly packed colonies, which represent clonal clusters of reprogrammed cells were

observed that robustly expressed markers of pluripotency, alkaline phosphatase (AP), and SSEA-1, all negligible in parental fibroblasts (**Figure 19B**, middle and bottom).

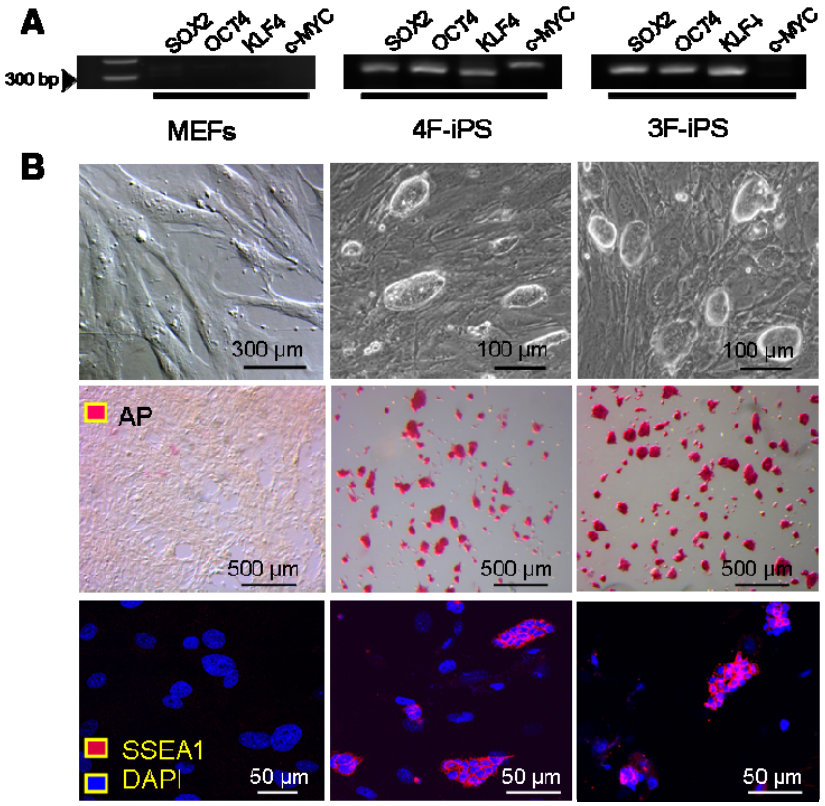

Figure 19. Reprogrammed cells demonstrate *in vitro* pluripotency in the presence and absence of c-MYC. A) Genomic integration of viral constructs was detected in transduced progeny, with c-MYC absent from the 3 factor-induced lines. Parental fibroblasts demonstrate no viral sequence integration and are shown as a negative control. B) Distinct morphology and stem cell markers, SSEA1 (red), and Alkaline Phosphatase (AP, pink) uniquely expressed within transduced progeny compared to native MEFs identified by nuclear staining with DAPI (blue).

.

Ultrastructural characterization by scanning electron microscopy (FESEM) documented structural metamorphosis, revealing isolated colonies that exhibited a condensed morphology consisting of clustered small round cells (Figure 4A, center and right) in contrast to the flat untransduced neighboring fibroblasts (**Figure 20A**, left). Transmission electron microscopy (TEM) imaged a distinct subcellular architecture reorganized from original fibroblasts characterized by a

densely populated cytoplasm with large mature mitochondria (**Figure 20B**, left). Reprogrammed progeny recapitulate salient features of undifferentiated embryonic stem cells (**Figure 20B**, center) with high nucleus/cytoplasmic ratio, predominance of nuclear euchromatin, and scant density of cytosolic organelles, including small immature mitochondria (**Figure 20B**, right).

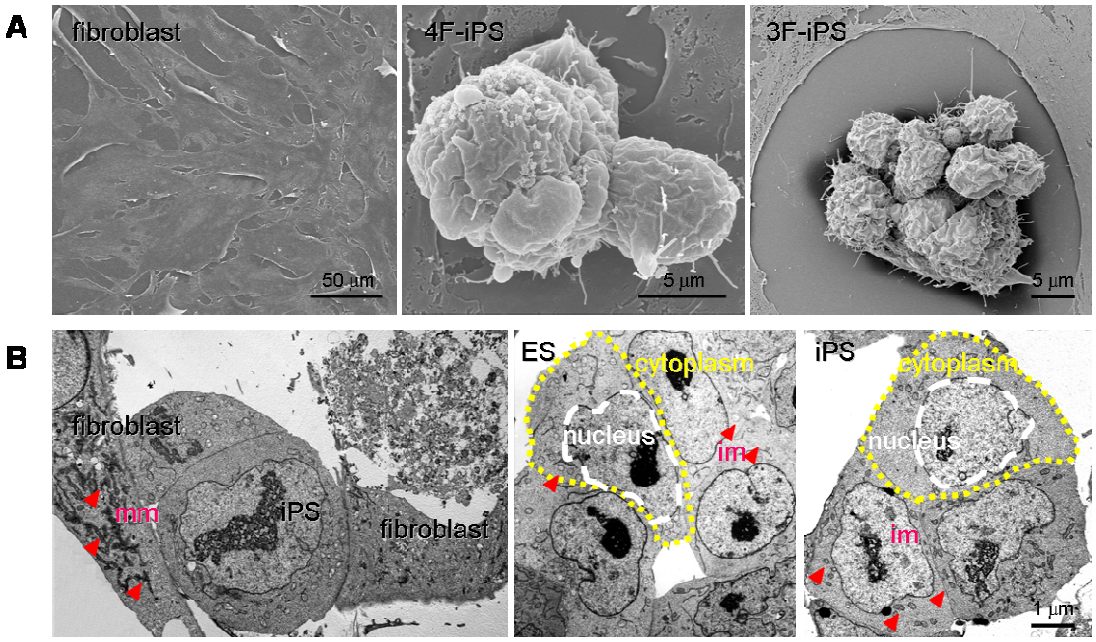

Figure 20. Microstructural changes revealed after reprogramming. A) Scanning electron microscopy reveals profound morphological changes from original fibroblasts to reprogrammed iPS. B) Cytoplasmic features detected by transmission electron microscopy, such as immature mitochondria (im) and high nucleus to cytoplasm ratio differentiate both iPS and embryonic stem (ES) cells from fibroblasts, with mature mitochondria (mm).

1.4. Pluripotent gene expression profile of engineered cells

In line with the morphological changes observed after the reprogramming process and the appearance of defining markers of pluripotency, quantitative PCT analysis of the expression profiles both in untransduced and transduced populations revealed a marked expression increase in stemness-related genes

such as Sox2, Oct4 and Fgf4 (**Figure 21**). Due to limitations of this technique, upregulation of Sox2 and Oct4 readings could be due to residual transgene expression that were detected simultaneously with the endogenous. However, the induction of another pluripotency marker, Fgf4, not comprised within the transduced factor set, was an independent criterion suggesting the direct relationship between engineering and pluripotent feature acquisition.

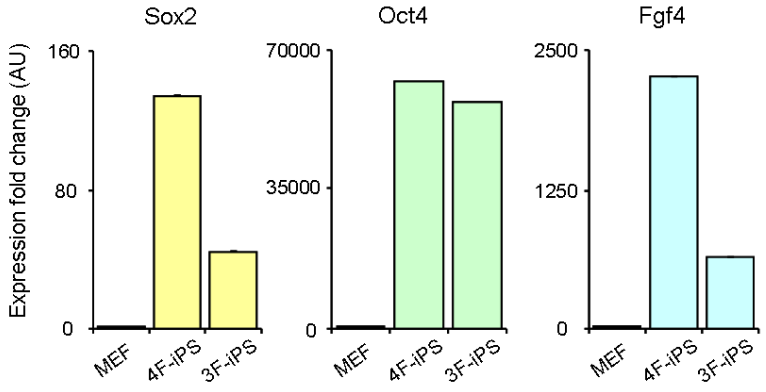

Figure 21. Reprogrammed expression profile for pluripotent markers in engineered cells. 4F and 3F transduced cells displayed distinct increased expression levels of pluripotency related markers Sox2, Oct4 and Fgf4 after the reprogramming process, compared to non-transduced parental MEFs.

Thus, the engineered platform induced efficient metamorphosis of fibroblasts into clonal populations recapitulating growth kinetics and a cellular expression profile consistent with an embryonic stem cell phenotype.

1.5. *In vivo* lineage differentiation of transduced fibroblasts

Pluripotent cells form spontaneous teratomas following transplantation into immunodeficient mice, an established assay to demonstrate multi-lineage developmental capacity (Damjanov and Solter, 1976; Lensch, 2007; Yamada, 2008). Here, immunodeficient mice were subcutaneously injected with native MEFs or reprogrammed counterparts selected based on morphological criteria to assess their pluripotency in an *in vivo* model. Only transduced cells gave rise to teratoma formation following injection of a dose of 500,000 cells. Tumors could

be detected both for 4F-iPS and 3F-iPS, in contrast to undetectable growth for native MEFs injected on the contralateral side of host animal. (**Figure 22A**). Teratomas derived from reprogrammed MEFs were encapsulated and demonstrated a heterogenous appearance consisting of vascular networks and non-vascularized tissues on gross inspection (**Figure 22B**). Tissue histology of 4F-induced pluripotent stem cell teratoma revealed cellular architecture consisting of endoderm lineages comprised of epithelium, ectoderm lineages denoted by keratinized tissues and mesoderm lineages indicated by muscle (**Figure 22C**, top). Three germ layers were also detected on 3F-iPS derived

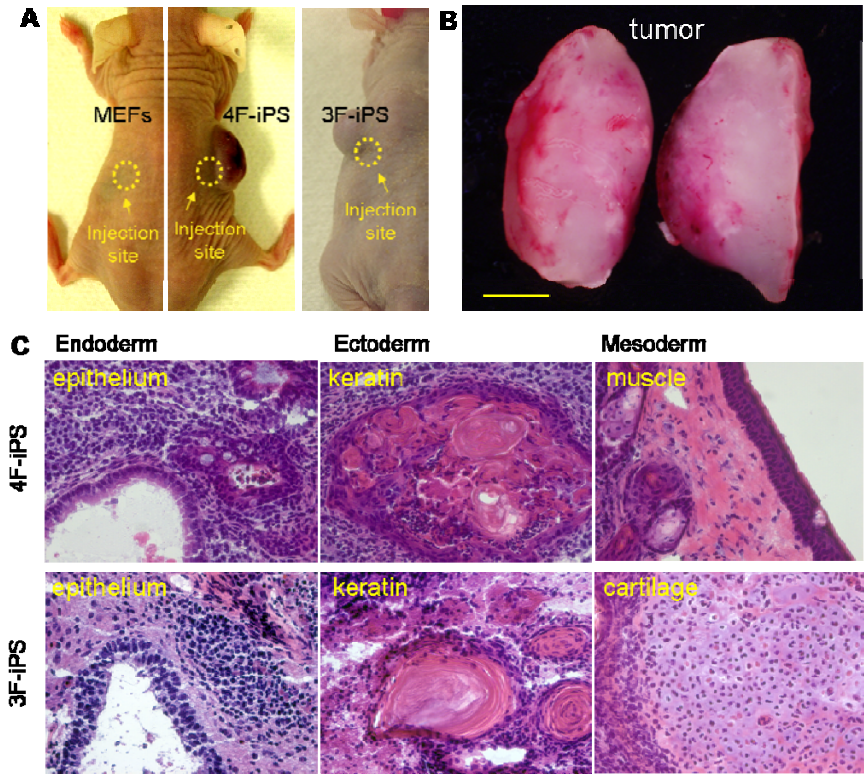

Figure 22. Multi-lineage *in vivo* differentiation within tumors. A) Spontaneous *in vivo* differentiation was monitored in immunodeficient mice following subcutaneous injection comparing native and transduced MEFs. B) Tumor growth was detected only from sites injected with transduced progeny after 1-2 weeks followed by rapid expansion of tumor bulk that was absence in native MEF injection sites. C) Tissue was harvested at 4-6 weeks post-injection. Cryosections and tissue staining demonstrated multiple lineages within the complex architecture of the tumor and included muscle, keratin, epithelium, and cartilage.

teratomas, including epithelium (endoderm), keratinized epidermal ectoderm (ectoderm), and cartilage (mesoderm; **Figure 22C**, bottom). Together, these data document the multiple tissues obtained from *in vivo* differentiation and establishes spontaneous formation of complex cytoarchitecture derived from mouse embryonic fibroblast cells reprogrammed by human stemness-related factors.

In summary, interspecies nuclear reprogramming guided by a human ortholog set demonstrates the robustness for ectopic expression of promiscuous stemness related factors for cellular de-differentiation. A robust model of nuclear reprogramming is consistent with prior studies that demonstrate the effectiveness of both xeno-cytoplasmic environments and ectopic combinations of stemness-related genes (Beyhan, 2007; Takahashi and Yamanaka, 2006; Yu, 2007). Obtained clonal populations selected based on morphology that resembled embryonic stem cells, fulfilled growth characteristics, cytoplasmic rearrangements, pluripotency gene expression profiles, and in vivo lineage differentiation potential expected for pluripotent stem cells.

2. Functional pluripotency of reprogrammed cells

According to the current standards, teratoma formation in immunodeficient mice is the most stringent criterion of pluripotency in human cells (Lensch, 2007). However, the mouse model offers the possibility of a more detailed characterization of stem cell features by placing competent cells in direct contact with early stage embryos. In this way, host embryos offer an unaltered differentiation environment that allows stochastic integration and propagation of engineered cells. Here, we study the behavior of 4 and 3F-iPS during embryonic development and their pluripotent characteristics.

2.1. Contribution of transduced progeny into *ex utero* blastocysts

A hallmark-characteristic of natural embryonic stem cells is the ability to incorporate into 8-cell embryos and form morula capable of developing into chimera blastocysts (Wood, 1993). Original studies using primitive stem cell populations demonstrated that only undifferentiated embryonic stem cells were able to engraft within ~50% of the host 8-cell embryos to form a mosaic blastocyst, but were universally excluded from the developing embryo if cells were partially differentiated or derived from non-stem cell types (Fujii and Martin, 1980; Stewart, 1980), even despite sustained cell surface expression of stem cell markers or stem-cell like morphology(Waters and Rossant, 1986). In order to determine the ability of MEFs and reprogrammed counterparts to incorporate into early stage morula, iPS cells were lentivirally labeled with GFP or lacZ, expanded *in vitro*, and prepared for diploid aggregation with unlabeled embryos (**Figure 23A** and **23B**). Whereas morula-derived blastomeres incorporated into an embryonic structure after 24 hours in microwells, fibroblasts aborted engraftment and failed to contribute to *ex utero* blastocyst development (**Figure 23C**, left).

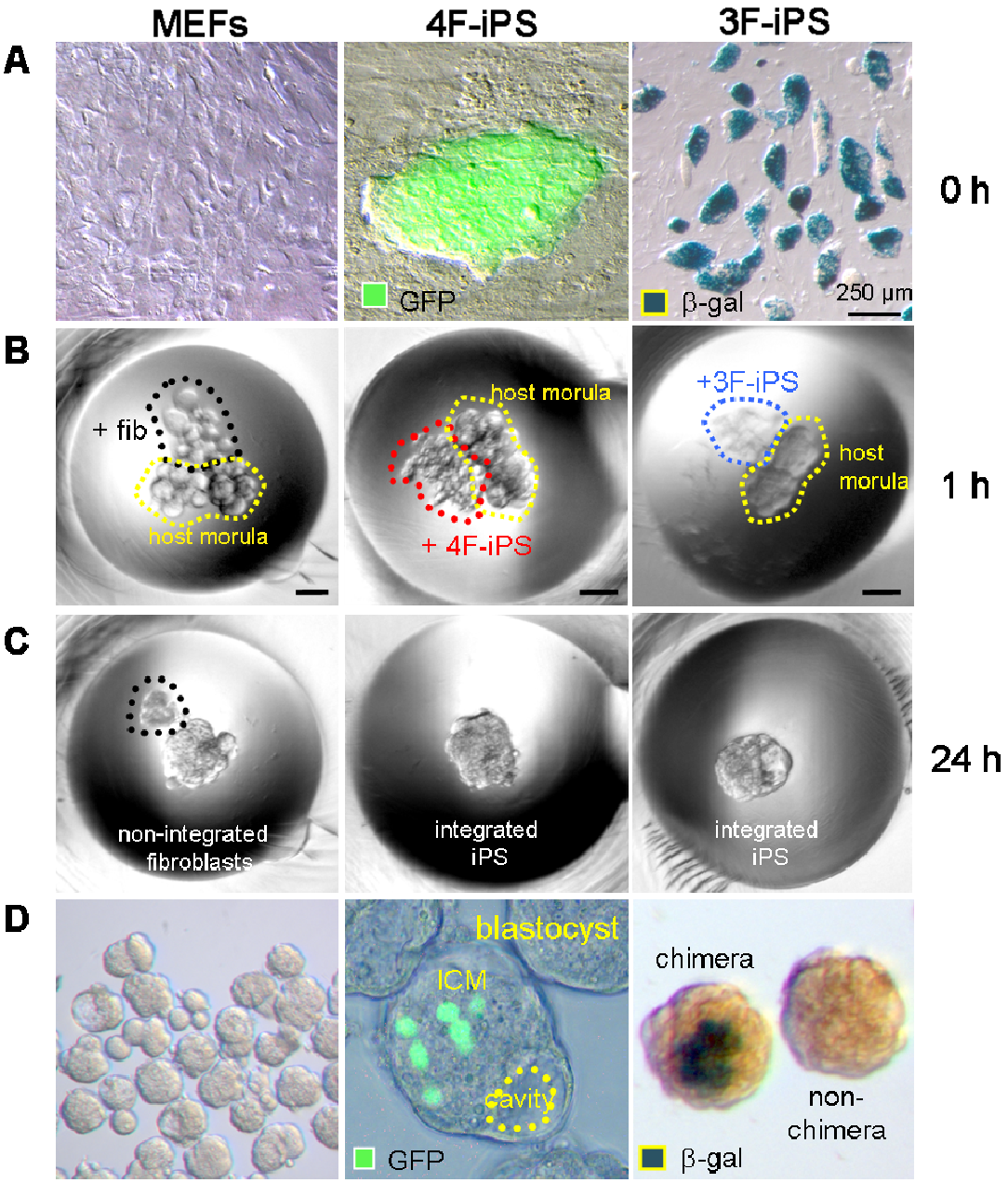

Figure 23. ***Ex utero*** **pluripotency of engineered progeny**. A-B) Transduced MEFs were labeled with GFP tag or lacZ for chimeric studies and allowed selection of progeny for *ex utero* integration into early stage embryogenesis. C) Diploid aggregation between labeled progeny and WT morula produced chimeric embryos at the compact morula stage of development, while parental fibroblasts were unable to integrate into the developing embryo. D) Chimeric embryos properly developed into blastocysts with early cavitation and formation of mosaic inner cell mass (ICM) with GFP or lacZ-labeled blastomeres.

GFP or lacZ-tagged transduced progeny retained the ability to engraft into 8-cell morula (**Figure 23C**, center and right) and contribute to chimeric embryos capable of spontaneously differentiating into preimplantation blastocysts with appropriate cavitating morphology (**Figure 23D**). Noncoerced assimilation into early-stage embryos thereby established bona fide iPS clones, providing a high-stringency quality control measure for functional pluripotency.

2.2. High-fidelity organogenesis from transduced progeny

Beyond *ex vivo* characterization, chimeric embryos establish *in situ* competency of transduced progeny during natural embryogenesis. Pluripotent stem cells contain the capacity to give rise to all lineages of the developing embryo upon blastocyst integration in a stochastic pattern depending on location of blastomere integration during early stage of pre-implantation development (Nagy, 1990). Mosaic embryos produced by diploid aggregation using GFP or lacZ-labeled progenitors were surgically transferred to the uterus of a pseudopregnant surrogate mother for *in utero* implantation and differentiation. Chimeric embryos were harvested at 9.5 d.p.c. and analyzed for engraftment and differentiation of non-native progeny. Embryos that demonstrated normal morphology and appropriate developmental stages of organogenesis were visualized for GFP (4F-iPS) or lacZ (3F-iPS) expression. For both c-MYC dependent and independent reprogrammed cells, transduced progenitors were identified throughout the embryo in multiple developing organs that included central nervous tissue (**Figure 2A4, 24B, 24A'** and **24B'**), pharyngeal arch (**Figure 24C** and **24C'**), heart (**Figure 24D** and **24D'**), emerging limb buds (**Figure 24E** and **24E'**), and somites (**Figure 24F** and **24F'**).

Thus, stochastic integration and widespread tissue contribution of reprogrammed cells demonstrated unrestricted differentiation potential and

competitive fitness equal to native blastomeres, achieving a rigorous criterion to define pluripotency with competent *in utero* orchestrated organogenesis.

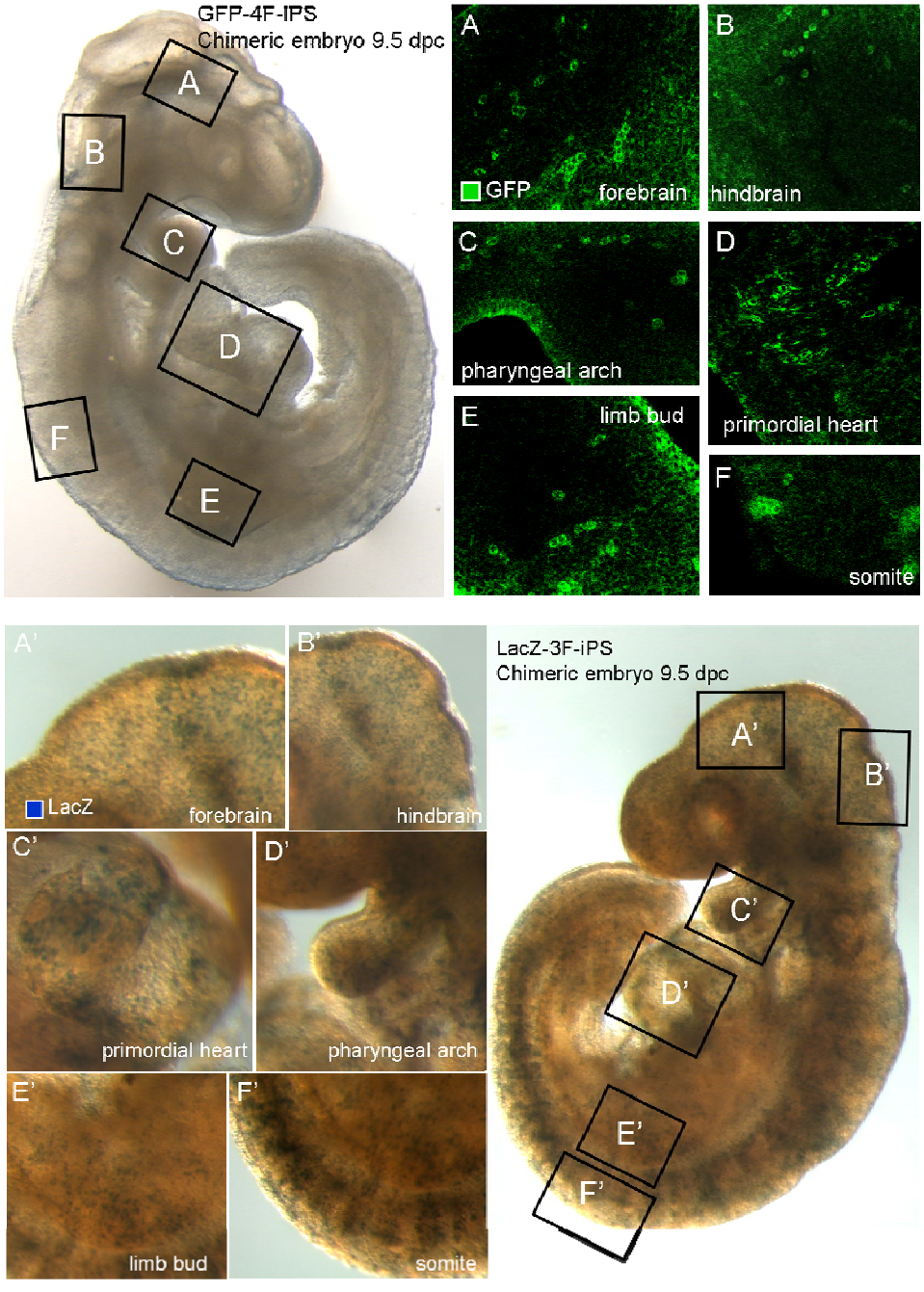

Figure 24. Organogenesis derived from transduced progeny. Chimeric embryos were transferred into a surrogate for *in utero* differentiation and were harvested at 9.5 d.p.c. for tissue analysis. Confocal microscopy (4F-iPS) or lacZ staining (3F-iPS) revealed transduced progeny throughout the embryo including neuronal tissues of forebrain (A, A') and hindbrain (B, B'), along with the multi-lineage pharyngeal arches that contains endoderm derivatives (C, C'). Mesoderm derived lineages were present in the heart (D, D'), limb bud (E, E'), and somites (F, F').

3. Comparative cardiac differentiation potential for 4F-iPS vs 3F-iPS (in the presence or absence of c-Myc)

Nuclear reprogramming reorganizes gene expression profiles in parental cells to reset cell fate, bioengineering pluripotent stem cells from ordinary somatic sources. This starting material can be subsequently re-differentiated using protocols optimized for embryonic stem cells allowing derivation of cell types that can be of interest for basic and translational science. However, little is known about the effects of the reprogramming process in the subsequent differentiation potential of the engineered cells. In this section, we perform a head-to-head comparison of the *in vitro* cardiogenicity of iPS reprogrammed in the presence or absence of c-MYC.

3.1. Early *in vitro* differentiation stages of 4F and 3F-iPS

Demonstration of functional pluripotency *in utero* indirectly revealed the cardiogenic capacity of both 4F and 3F-iPS (**Figure 24D** and **24D'**). Progeny derived from c-Myc dependent or independent reprogramming processes spontaneously contributed to the developing heart of 9.5 d.p.c. chimeric embryos after diploid aggregation. Following this results, *in vitro* growth and differentiation potential was studied comparatively for cells reprogrammed in the presence or absence of c-Myc. For this purpose, three independent isolated clones for each 4F-iPS and 3F-iPS were randomly selected and cultured using a hanging drop differentiation protocol. At day 0, all six undifferentiated iPS clones were indistinguishable as isolated clusters exhibited a condensed morphology in contrast to the flat untransduced neighboring fibroblasts (**Figure 25A**). This appearance was maintained for at least 5 passages from the original isolated colony. No gross morphological differences were observed among 4F-iPS and 3F-iPS grown under undifferentiation conditions. Allowing each clone to undergo spontaneous differentiation within hanging drop-embryoid bodies (EB) generated

similar growth kinetics leading to equivalent three-dimensional aggregates. In fact, each iPS clone was capable of forming spheroids with regular and defined edges that grew to within 300-400 µm in diameter after 5 days of culture (**Figure 25B**). Thus, homogeneous morphology was observed in undifferentiation conditions and early stages of differentiation in both 4F-iPS and 3F-iPS clones independent of c-MYC transduction.

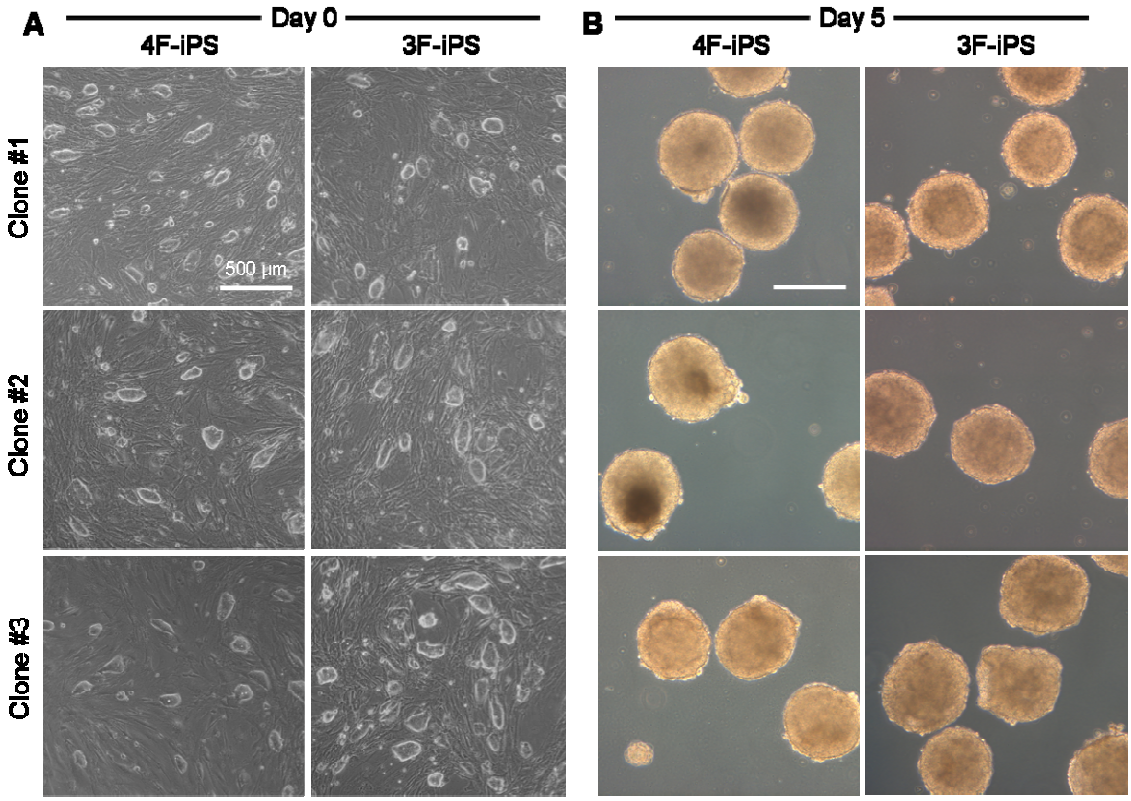

Figure 25. **4F-iPS and 3F-iPS show similar growth kinetics and embryoid body morphology**. A) Distinct clones of 4F-iPS (left) and 3F-iPS (right) were kept in the undifferentiated state on feeders, and showed indistinguishable morphology consisting of compact colonies. B) Hanging drops were made with multiple clones of 4F-iPS (left) and 3F-iPS (right). Embryoid bodies from each of the clones demonstrated equivalent size and shape within 5 days of differentiation. Bar=500 µm.

3.2. Absence of c-MYC accelerates cardiogenic gene expression during iPS differentiation

To further characterize the ability of 4F-iPS and 3F-iPS to differentiate into tissue-specific lineages, *in vitro* model systems were applied to discriminate innate cardiogenic potential. Pluripotent lines were differentiated in 3-dimensional cultures throughout a 12-day period. iPS progeny were sampled sequentially starting at day 0 monolayers, day 5 floating embryoid spheres and day 12 plated embryoid bodies. Gene expression analysis from three independent clones in each group, sampled throughout the continuum of differentiation demonstrated a persistent elevation of pluripotent genes such as Sox2, Oct3/4, and Fgf4 in 4F-iPS throughout the 12-day differentiation protocol (**Figure 26A**). Furthermore, spontaneous induction of gastrulation markers was inconsistently upregulated in 4F-iPS compared to the profile of peaking expression levels reliably demonstrated at day 5 in 3F-iPS clones with Lhx1, Goosecoid. Mesodermal Sox7 and endoderm-related Sox17 also peaked at day 5, allowing for further cardiac differentiation (**Figure 26B**) Sox17 has been shown to be an important factor in the non-autonomous specification of cardiac mesoderm in embryonic stem cells (Liu, 2007), therefore lack of expression at day 5 might have an effect in subsequent cardiac gene expression. Precardiac genes Cxcr4, Kdr (also know as Flk1), Mesp1 and Mesp2 increased expression around day 5 for all tested clones; yet, reproducible induction was augmented in 3F-iPS when compared to 4F-iPS clones (**Figure 26C**). Cardiac transcription factors were significantly up regulated at day 12 in 3F-iPS, although unreliable for 4F-iPS clones (**Figure 26D**). Thus, the transition from pluripotent gene expression into a gastrulation profile and further into *bona fide* cardiogenic transformation was apparently hampered in iPS clones generated using a c-MYC dependent approach.

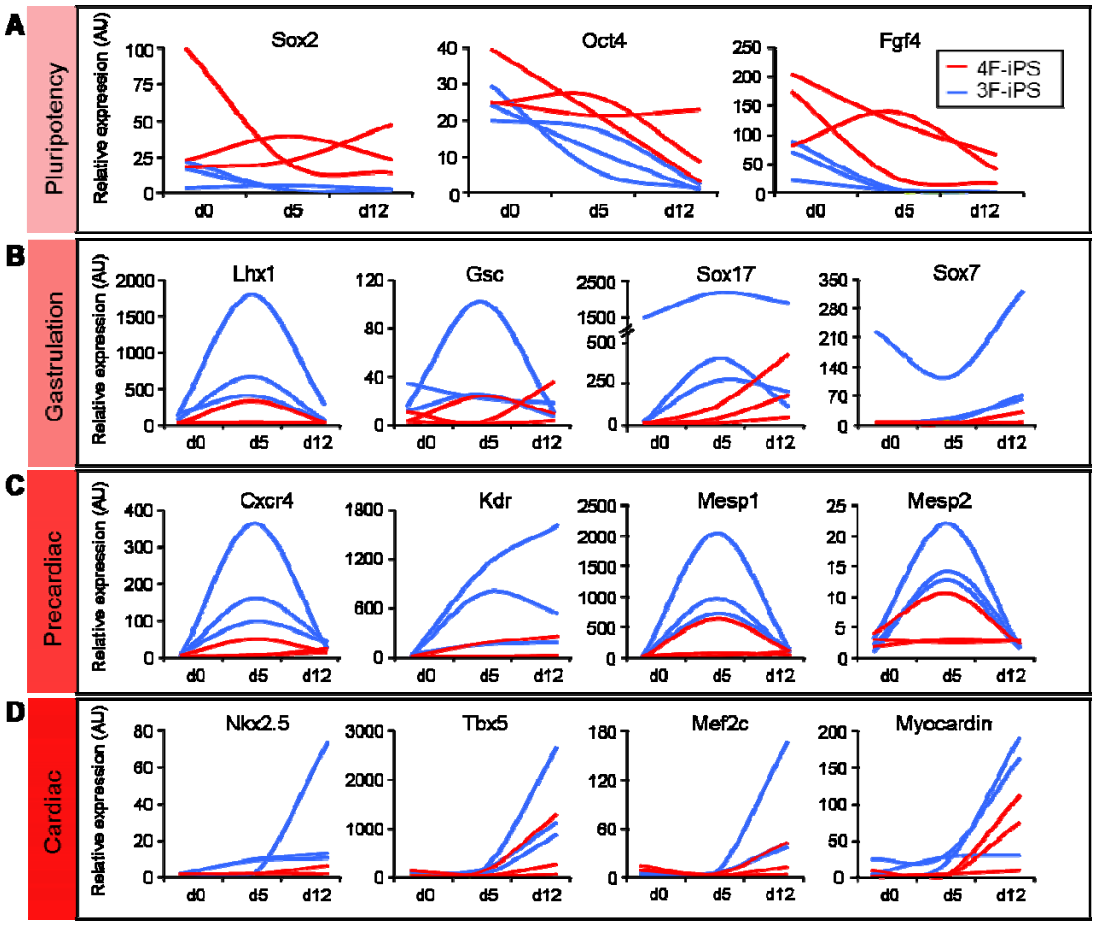

Figure 26. Divergent gene expression profiles for 4F-iPS and 3F-iPS during *in vitro* differentiation. Differentiation of iPS progenitors was promoted within hanging drops to form embryoid bodies followed by expansion of progeny on gelatinized plates in multi-layer tissues. Cells were sampled from undifferentiated cultures at day 0, floating embryoid bodies at day 5, and differentiating cultures at day 12 for gene expression analysis. A) Pluripotency genes were immediately downregulated in 3F-iPS with initiation of differentiation, whereas expression levels of pluripotent genes was protracted in 4F-iPS. B) Gastrulation markers consistently peaked at day 5 for 3F-iPS clones with inconsistent levels expressed in 4F-iPS. C) Precardiac genes increased at day 5 for all tested clones, However, relative expression was notably higher in 3F-iPS when compared to 4F-iPS clones. D) Upregulation of cardiac transcription factors was observed at day 12 in 3F-iPS with 4F-iPS clones maintaining lower baseline expression levels.

3.3. c-MYC independent nuclear reprogramming favors cardiogenesis in iPS progeny

Divergent gene expression profiles of 4F-iPS and 3F-iPS throughout the 12-day differentiation protocol were validated according to distinct morphology and different beating activities. Specifically, five day old-embryoid bodies from independent 4F-iPS and 3F-iPS clones were plated on gelatinized plates for spontaneous differentiation. After day 8, 4F-iPS clones were morphologically distinct from 3F-iPS clones with 4F-iPS progeny showing areas of detached cells (**Figure 27A**, left). 3F-iPS clones had a consistent growth profile with sustained

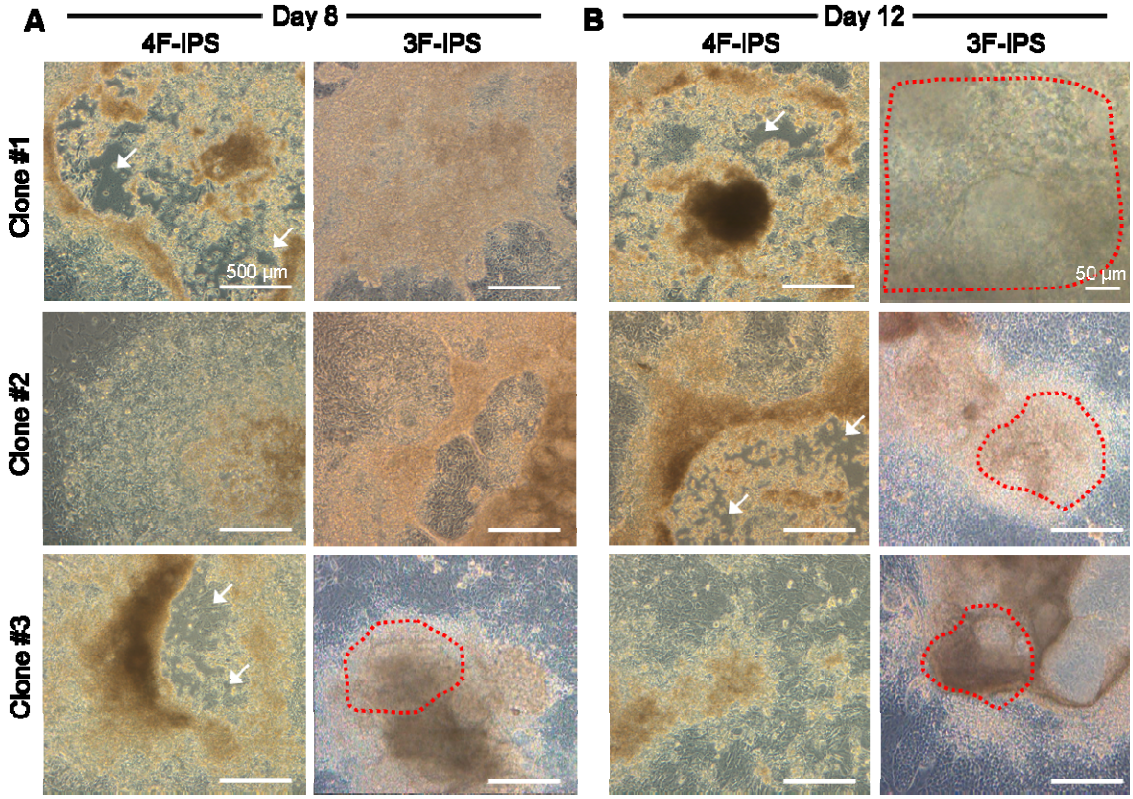

Figure 27. 3F-iPS differentiate into beating areas while 4F-iPS demonstrate inconsistent morphology and viability *in vitro*. iPS clones were differentiated into embryoid bodies and plated on day 5 onto gelatinized plates. A) Differences between 4F-iPS and 3F-iPS were noticeable in morphology after a total of 8 days as embryoid bodies. 4F-iPS clones showed areas of round and detached cells (arrows, left). 3F-iPS clones had predictable growth kinetics with sustained integrity of the cell layers that spread from the initial embryoid body towards the periphery of the plate. B) After 12 days, extensive cell loss was apparent in 4F-iPS cultures (arrows, left) while compact and continuous masses of 3F-iPS were observed in all studied clones, including areas of spontaneous beating activity (outlined in red dotted lines). Bar=500 μm.

integrity of the cell layer spreading from the initial embryoid body (**Figure 27B**, right). In contrast to c-MYC dependent iPS, 3F-iPS remained viable with areas of multi-layer cell growth that continuously expanded during the differentiation process (**Figure 27A**, right). By day 12, extensive cell death was apparent in 4F-iPS cultures (Figure 10B left) together with a slower growth rate while compact, confluent, and continuous masses of 3F-iPS were observed in all studied clones (**Figure 27B**, right). Furthermore, 3F-iPS areas of multi-cellular build-up demonstrated frequent sites of spontaneous beating activity, absent from 4F-iPS clones studied *in vitro*. During the differentiation time course, 4F-iPS and 3F-iPS were observed daily for beating activity. Within the follow-up period, 4F-iPS clones demonstrated no spontaneous contractility (**Figure 28**, n=8). However, robust beating activity was reproducibly documented in 3F-iPS clones with a sustained increasing tendency starting as early as day 7 (**Figure 28**, n=4) and reaching a 62% of EB containing at least one beating area by day 11.

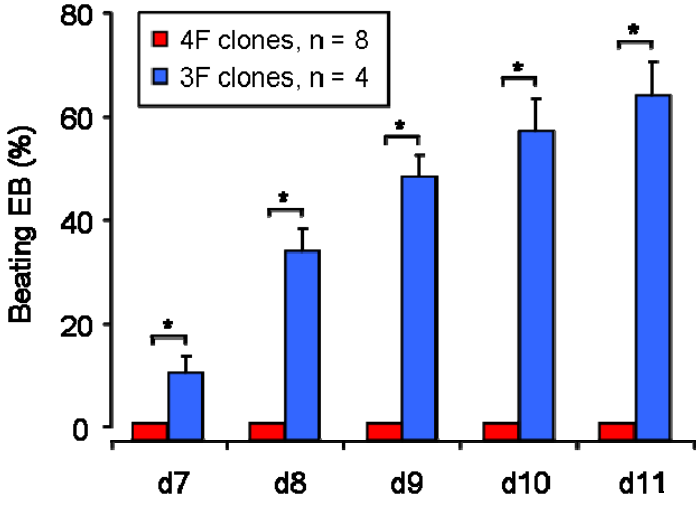

Figure 28. c-MYC independent nuclear reprogramming favors cardiogenic potential of iPS. Differentiating cultures of 4F-iPS and 3F-iPS were observed daily for appearance of beating activity. Between day 7 and 11 of differentiation, no spontaneous contractility was detected with 4F-iPS clones (n=8). In contrast, robust and sustained beating activity was documented in 3F-iPS (n=4).

Collectively, *in vivo* and *in vitro* profiling of 4F and 3F-iPS suggests that reprogramming independent of c-Myc results in pluripotent cells with a higher propensity to differentiate into cardiac tissue. This conclusion set the basis for a further characterization of the cardiac cells obtained from *in vitro* processing of 3F-iPS.

4. Characterization of functional cardiogenic potential of iPS reprogrammed independent of c-Myc

After determining that pluripotent cells reprogrammed in the absence of c-Myc displayed a higher propensity to differentiate into cardiac cells, we proceeded to further study their properties and the acquired features of the obtained cells, including their ability to contribute to the sustained cardiac function throughout development and into the adult heart.

4.1. Functional cardiogenesis derived from 3F-iPS

Beating activity and structural characteristics of 3F-iPS were studied

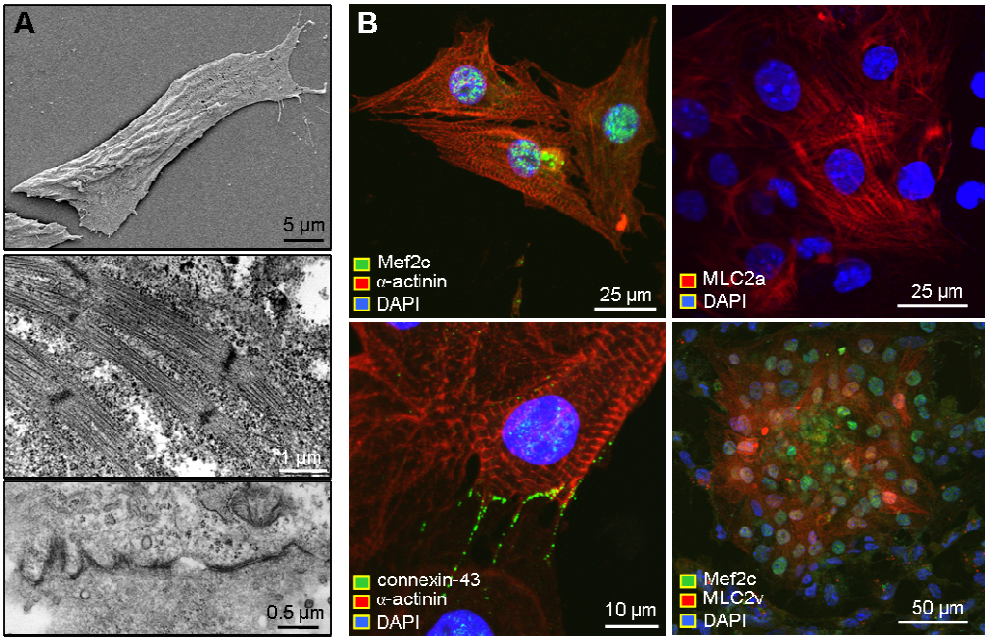

Figure 29. Structural cardiogenesis derived from 3F-iPS. A) Electron microscopy of 3F-iPS derived cardiomyocytes revealed morphological changes from compacted colonies to rod-shaped cardiomyocyte-like cells (top). High density contractile proteins were found in organizing sarcomeres (middle) as well as gap junction structures between adjacent cells (bottom). B) Immunostaining demonstrated presence of contractile protein alpha actinin in combination with cardiac transcription factor Mef2c (left-top), and gap junction-protein connexin 43 (left-bottom), atria (right-top) and ventricular (right-bottom) isoforms of myosin light chain protein were also found in isolated cardiomyocytes.

during spontaneous cardiac differentiation in three-dimensional cultures. Isolation of cardiomyocytes from beating EB was achieved using a selective density gradient. Structural changes consistent with cardiac differentiation were observed at day 12 as 3F-iPS progeny developed rod-shaped morphology (**Figure 29A**, top), a mature myofibrillar organization (**Figure 29A**, middle), and gap junctions that bridged adjacent progeny (**Figure 29A**, bottom) as shown by electron microscopy. Similarly, immunofluorescence of iPS-derived cells demonstrated nuclear presence of the cardiac transcription factor Mef2c or inter-cellular localization of gap junction-protein connexin 43 in cells co-stained for contractile protein alpha actinin (**Figure 29B**). Atrial and ventricular isoforms of the myosin light chain (MLC) protein were also identified in isolated cardiomyocytes derived from c-myc-less iPS (Figure 8B) revealing an ongoing maturation process in the cardiac sarcomeric structures towards a more specific phenotype.

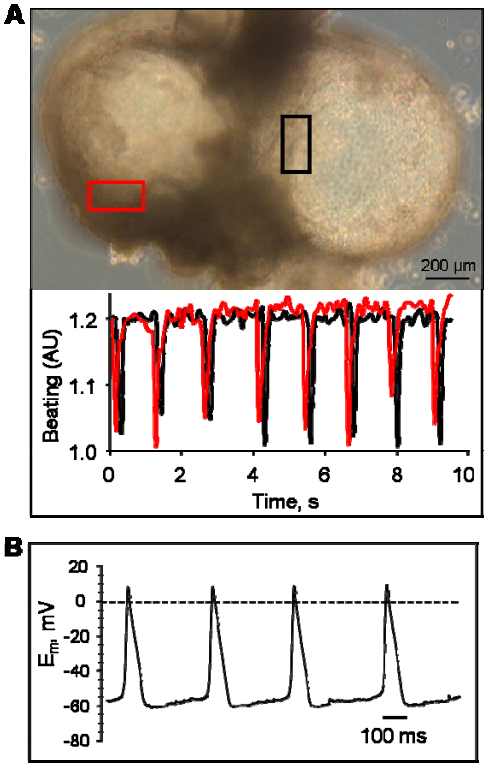

Figure 30. Functional cardiogenesis derived from 3F-iPS. A) Synchronized contractile activity (rectangles; top) was detected within floating EB (bottom). B) Action potentials were recorded in beating cells using patch clamp in the current clamp mode.

In a continuous suspension model, EB maintained the capacity to develop spontaneous contractility previously seen in cell complexes growing attached to gelatinized plates, revealing the presence of differentiating cardiac cells. EB that demonstrated multiple beating areas (**Figure 30A** top, rectangles) developed synchronized contractile rhythm underlying coordinated electric activity that propagated through the syncytium of nascent cardiac tissue (**Figure 30A**, bottom). Moreover, spontaneous action potential activity was recorded from isolated cells under the whole cell current-clamp mode of the patch clamp technique (**Figure 30B**), indicating the presence of components of the electrical

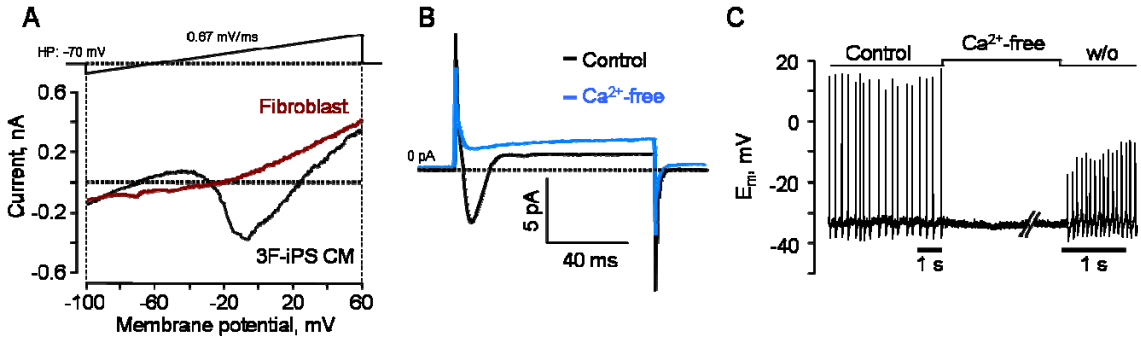

Figure 31. Calcium-dependent spontaneous action potentials in 3F-iPS-derived cardiomyocytes. A) An inward current was detected in iPS-derived cardiomyocytes (3F-iPS CM, black line) absent from parental fibroblasts (red line). B) Reversal of extracellular calcium suppressed inward current. C) Spontaneous action potentials were reversibly arrested in zero calcium milieu.

machinery of precardiac excitable tissue. Detailed electrophysiological evaluation of voltage-clamped isolated cells revealed prominent inward and outward current components in response to imposed depolarization by membrane potential ramp pulses from -100 to +60 mV which were not present in non-excitable parental fibroblasts (**Figure 31A**). The inward current component was eliminated in the absence of external Ca^{2+} as seen with single stimulation using a 50 mV pulse (**Figure 31B**). Furthermore, removal of Ca^{2+} from the bath solution reversibly abolished spontaneous action potential generation in 3F-iPS– derived cardiac cells (**Figure 31C**) indicating primarily calcium dependent electrical activity

suggesting a non-mature profile of cardiac membrane ionic channels. Loaded with the calcium selective Fluro-4AM probe, 3F-iPS derived cardiomyocytes demonstrated rhythmic fluorescent transients under live confocal microscopy consistent with intracellular calcium dynamics in diastole versus systole (**Figure 32A**). Recorded calcium oscillations were in synchrony with force-generating mechanical contractions (**Figure 32B**). Taken together, these data indicated reproducible derivation of 3F-iPS progeny that progressively acquired authentic cardiogenic machinery required for excitation-contraction coupling and generation of functional cardiomyocytes.

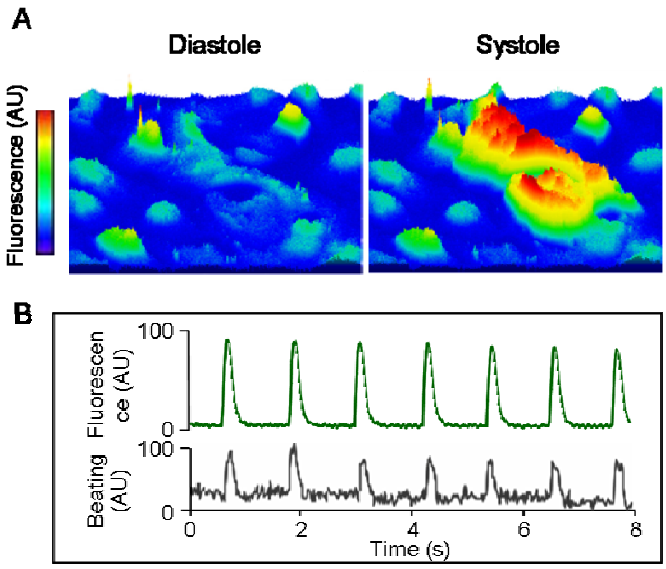

Figure 32. Calcium-dependent excitation-contraction coupling in 3F-iPS-derived cardiomyocytes. A) Fluo-4AM labeled iPS-derived cells demonstrated fluorescent dynamics consistent with calcium transients. B) Rhythmic calcium fluctuations coincided with cell contractions.

4.2. 3F-iPS chimerism contributes to de novo heart tissue formation in the embryo and sustains cardiac function in the adult heart

As described before, noncoerced diploid aggregation at the morula stage allows competent pluripotent stem cells to assimilate within a developing embryo and contribute to chimeric organogenesis (Nelson, 2009). Following this rational,

3F-iPS labeled with lacZ and luciferase expression cassettes were clonally expanded and allowed aggregation with 2 8-cell morula embryos. The process of diploid aggregation, which engages equivalent progenitors into a chimeric blastocyst, exploited the ability of 3F-iPS to integrate into host embryos and function as a blastomere, demonstrated by mosaic distribution of positive lacZ-expressing iPS progeny after 24 h of incubation (already shown in **Figure 23**). When chimeric blastocyst were surgically transferred into pseudopregnant females, iPS-derived tissue populated the embryo (n=7) during development and contributed to all stages of cardiogenesis from primitive heart fields to looped heart tubes corresponding to 8.0 to 9.5 d.p.c., respectively (**Figure 33A** through **33C**). By 9.5 d.p.c. when the heart tube has fully looped to form distinct inflow and outflow tracts, iPS progeny was detected throughout nascent heart parenchyma (**Figure 33C**, inset). Live born 3F-iPS chimera demonstrated iPS contribution and engraftment throughout adult tissues with dark coat color visible on the white background (**Figure 33D**, right, n=5). Transgenic luciferase expression emanating from labeled iPS progeny on *in vivo* imaging ranged from undetectable levels to a high degree of achieved chimerism in several imaged animals (**Figure 33E**).

Chimeric offspring (n=5), including those with the highest contribution of iPS progeny, demonstrated tumor-free assimilation of reprogrammed cells throughout the 3 months of follow-up. This was in agreement with previously reported data that suggest that the absence of the oncogene c-myc during iPS reprogramming renders these cells less tumorigenic than the 4F counterparts, the latter being responsible for the appearance of tumors in the first few months of life of engineered chimeric mice. This profile was independently verified by lack of tumor formation during 7.5 months of prospective follow-up on subcutaneous injection of 500 000 3F-iPS into the flank of immunocompent hosts (n=6).

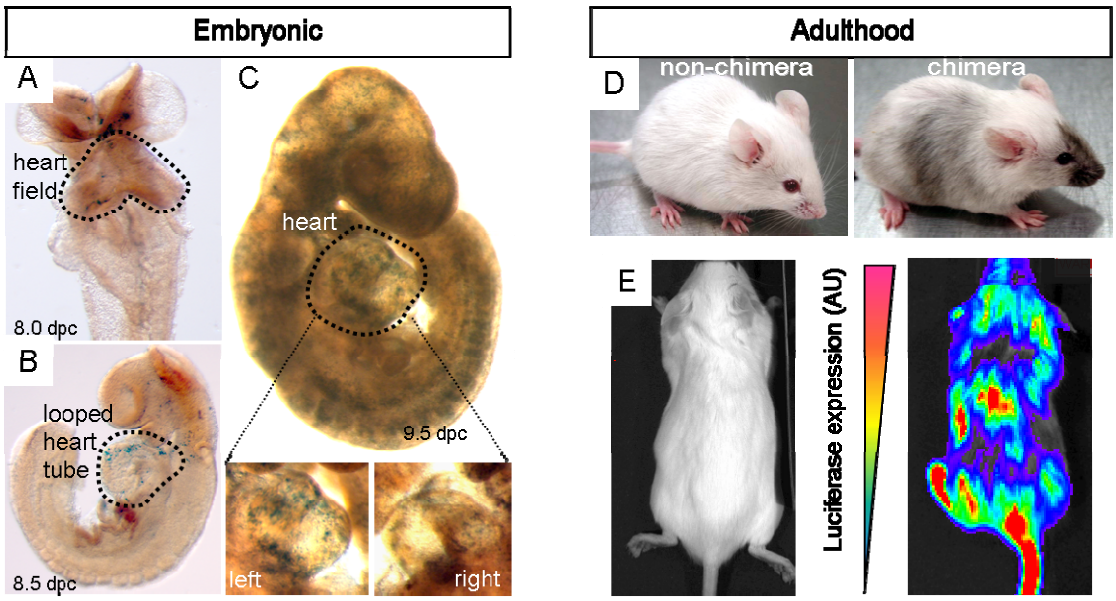

Figure 33. iPS bioengineered cells contribute to sustained chimersim throughout development and lifespan. A-C) Presence of iPS was sustained throughout embryonic development after diploid aggregation, as shown for 8.0 through 9.5 d.p.c. contributing to cardiac inflow and outflow tracts (C, inset). D) Other than mosaic coat color, adult chimeras were physically indistinguishable from non-chimeric littermates. E) Increasing levels of chimeric expressed luciferase distributed within tissues were detected according to molecular imaging with iPS-derived progeny.

In line with non-disruptive integration, adult 3F-iPS chimera exhibited vital signs, including average body weight, core temperature, heart and respiratory rates, that were indistinguishable from non-chimera counterparts (n=5; **Table 7**). Based on continuous electrocardiography, the chimeric cohort was devoid of ectopy, arrhythmias, or conduction blocks (**Figure 34A**) displaying a normal signal that included all PQRS complex peaks. Comprehensive echocardiography analysis further demonstrated consistent cardiac structure between 3F-iPS chimera and non-chimera cohorts with similar measured values for aortic, pulmonary, and right outflow tract diameters, along with equivalent left atrium and left ventricular volumes (**Table 7**). Left wall thickness and left ventricle to body weight ratio were also comparable to non-aggregated mice (**Table 7**).

	Non-chimera	Chimera	*p*
Cohort, n	5	5	
Vital signs			
Body weight, g	33 .8±1.0	36 .2±2.1	0.25
Body core temperature, □C	35 .2± 0.8	35 .8±0.6	0.46
Respiration rate, /min	117 ±3	112 ±2	0.34
Heart rate, beats/min	469 ±10	455 ±9	0.29
Cardiovascular structure			
Ascending aorta, mm	1 .68±1.09	1 .58±0.04	0.35
Main pulmonary artery, mm	1 .80±0.14	1 .81±0.14	0.75
Right ventricular outflow tract, mm	1 .32±0.18	1 .31±0.19	0.99
Left atrium, mm	1 .79±0.13	2 .04±0.19	0.35
LVDd/BW, mm/g	0 .106±0.01	0 .113±0.01	0.60
Left ventricular end -diastolic volume , _L	59 .2±3.3	61 .5±6.3	0.92
Left wall thickness (septum plus posterior wall), mm	1 .43±0.05	1 .56±0.08	0.25
Left ventricle/body weight, mg/g	2 .52±0.24	3 .22±0.30	0.12
Cardiac function			
Fractional shortening, %	46 .6±2.8	45 .4±3.1	0.75
Ejection fraction, %	61 .7±3.9	63 .6±1.8	0.92

LVDd, left ventricular diastolic diameter. BW, body weight.

Table 7. Cardiovascular comparison between non-chimera and 3F-iPS chimeric cohorts. Vital signs, cardiovascular structural parameters and cardiac function were compared between non-chimeric and chimeric mice, revealing indistinguishable features for both cohorts.

Synchronized 4-chamber function throughout systolic and diastolic cardiac cycles, indicating functional integration of 3F-iPS progeny into the adult organ, were also studied in acquired echocardiography images and were found to be also equivalent to non-chimera counterparts (n=5, **Figure 34B** and **Table 7**). Left ventricular functional performance of all 3F-iPS chimeras was essentially identical, according to measured fractional shortening (FS) and ejection fraction (EF), compared to age and sex-matched normal controls (**Table 7**).

Together, this evidence indicates a high proficiency for 3F-iPS progeny to acquire cardiac characteristics such as an organized sarcomeric architecture, intracellular communication structures and functional contractile machinery displaying operative excitation-contraction coupling. Under non-coerced aggregation conditions, undifferentiated myc-less reprogrammed cells integrated

into the developing embryo, populating the early heart flow and contributing to normal heart formation. Sustain chimerism did not disrupt myocardial structure or function throughout prenatal to postnatal development.

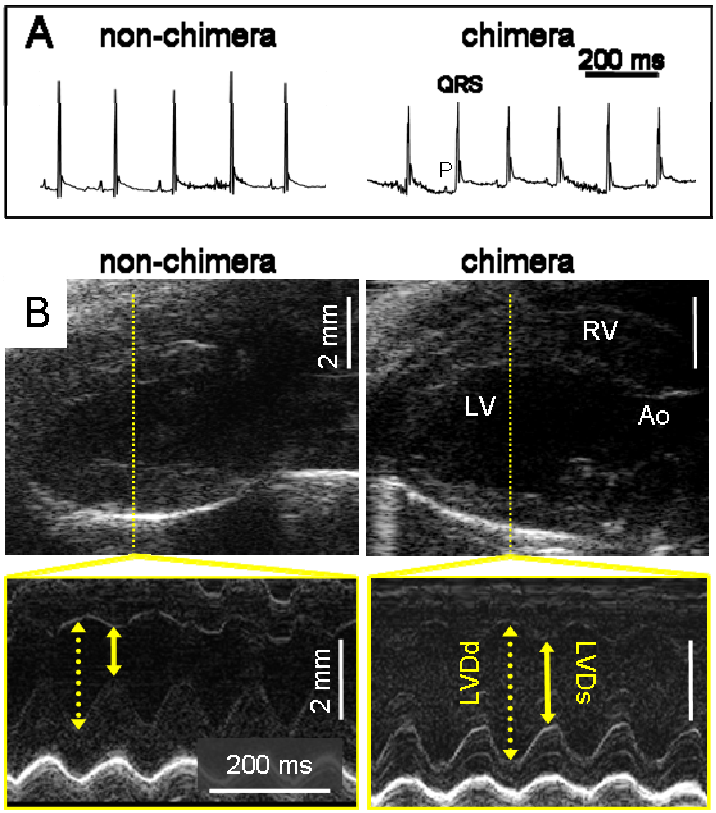

Figure 34. Cardiac chimerism contributes to sustained normal heart function. A) Cardiac electrocardiography was equivalent between non-chimera and chimera. B) Cardiac echocardiography demonstrated normal structure of heart, valves, and great-vessels with equivalent systolic and diastolic function between non-chimera and chimera. Ao: aorta, LV: left ventricle; LVDd: left ventricular diastolic diameter, LVDs: left ventricular systolic diameter, RV: right ventricle. Bar=2 mm.

5. Repair – Disease model

As a valuable tool for regenerative medicine, the ultimate use of induced pluripotent stem cells is their application as a therapy in degenerative diseases in order to reestablish lost tissue and organ homeostatic function. As proof of principle for the potential of this new technology in cardiovascular repair, we injected parental or reprogrammed cells into infarcted hearts, characterizing both the morphological and functional outcomes in a head to head comparison with parental fibroblasts.

5.1. Chimeric embryos authenticate iPS-derived patterning of normal cardiogenesis

In a first approach to cardiac differentiation, labeled iPS were studied during twelve days of *in* vitro differentiation, assessing their cardiac-related expression profile. As luciferase and β-galactosidase labeled 4F-iPS

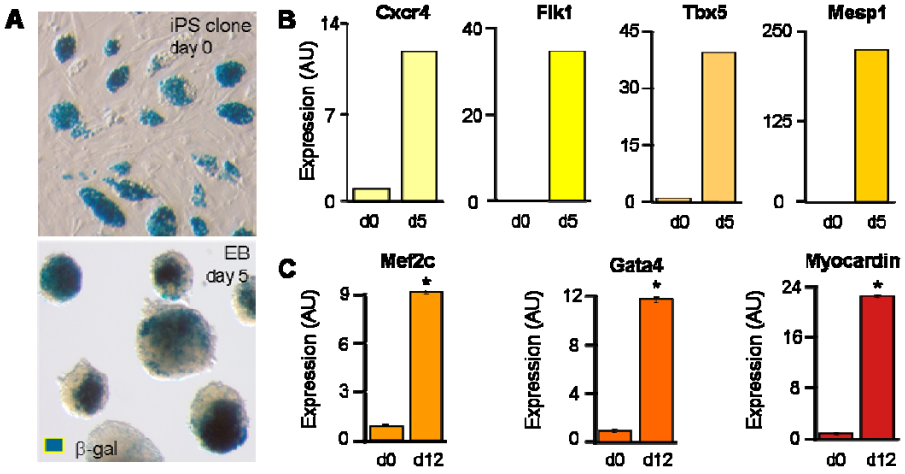

Figure 35. **iPS recapitulate *in vitro* cardiac differentiation**. A) LacZ-labeled iPS clones, detected by β-galactosidase (β-gal) staining, were maintained as undifferentiated colonies at day 0 before aggregation into embryoid bodies (EB). B) Gastrulation and cardiac mesoderm markers are upregulated at day 5 (d5) of differentiation. C) Gene expression profiles at day 0 (d0) compared with day 12 (d12) of differentiation demonstrated signinfcant induction of cardiac transcription factors Mef2c (*P*=0.049; n=3), Gata4 (*P*=0.049; n=3), and Myocardin (*P*=0.049; n=3).

differentiated within 5-day-old embryoid bodies persistent transgene expression was revealed by X-gal staining (**Figure 35A**). In this study system, upregulation of precardiac markers Cxcr4, Flk-1 (also known as Kdr), Mesp1 and Tbx5, indicated engagement beyond the original fibroblast lineage [29,30] five days into the differentiation course and suggested the ability of these cells to develop into cardiac precursors (**Figure 35B**). Within 12 days, significantly increased expression of canonical cardiac transcription factors Mef2c (P=0.049; n=3), Gata4 (P=0.049; n=3), and Myocardin (P=0.049; n=3) indicated the capacity for cardiac tissue maturation (**Figure 35C**).

Beyond redirection of somatic cell fate *in vitro*, chimeric embryos were utilized to examine the ability of iPS clones to ensure cardiac tissue formation during embryonic development *in utero*, comparing it to that of embryonic stem cells. Preimplantation blastocysts containing lacZ-labeled iPS progenitors (after diploid aggregation) were transferred into surrogate uterus and tracked at early stages of organogenesis. iPS labeled with a constitutively active reporter construct (**Figure 36A**, bottom right) mimicked the stochastic distribution of embryonic stem cells throughout the developing embryo at 9.5 d.p.c. (**Figure 36A**, top right). Labeled iPS progeny demonstrated robust contribution to the heart field, as delimited by embryonic stem cells labeled with a lacZ construct under the α-MHC promotor (**Figure 36A**, bottom left), including cardiac inflow and outflow tracts as well as left and right ventricles of the embryonic heart parenchyma, (**Figure 36B** and **36C**) revealed by X-gal staining in whole chimeric embryos or heart sections. Thereby, qualified iPS clones demonstrated *de novo* organogenesis and patterning of cardiogenic tissue within a developing embryo.

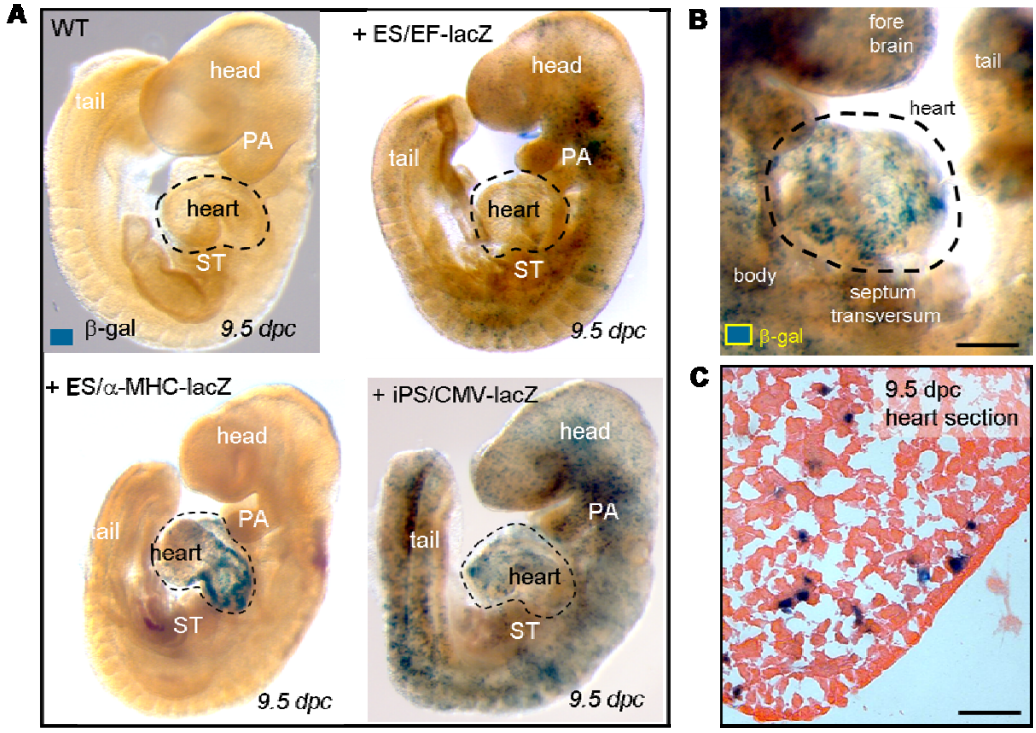

Figure 36. iPS recapitulate *in utero* cardiogenic propensity. A) Embryos provide a wild-type (WT) environment to determine tissue-specific differentiation (top left). Derived by diploid aggregations, embryonic stem cells (ES) stochastically contribute to tissue patterning with diffused integration tracked with constitutively labeled EF-lacZ cell line (top right) and cardiac-specific integration identified by α-MHC-lacZ reporter (bottom left). iPS, labeled with ubiquitously expressing reporter with CMV promoter, identify progeny throughout developing embryo (bottom right). B) Chimerism with lacZ-labeled iPS demonstrated robust contribution to developing hearts within 9.5 d.p.c. embryos. Bar=100 μm. C) Heart parenchyma of 9.5 d.p.c. chimeric embryo contained integrated iPS progeny expressing β -galactosidase. Bar=50 μm.

5.2. Risk of iPS-derived teratoma is determined by host immune competency

In contrast to fibroblasts at the same dose, unable to proliferate even after prolonged incubation, subcutaneous injection of 500 000 4F-iPS within an immunodeficient adult environment demonstrated aggressive growth, forming large teratomas (**Figure 37A**). Transplanted cells, initially labeled with luciferase and β-galactosidase retroviral reporter constructs and expanded through multiple passages (>5) *in vitro*, were tracked with *in vivo* imaging with the use of emitted

bioluminescence from iPS-derived progeny. After permanent occlusion of epicardial coronary vasculature, 200 000 labeled cells were microsurgically transferred into the ischemic myocardium. iPS from these low dose injections remained within injected hearts and produced gradual tumor outgrowth between 2 and 4 weeks (**Figure 37B**). Echocardiography confirmed a significant tumor burden, in some cases surpassing the size of the heart, which compromised

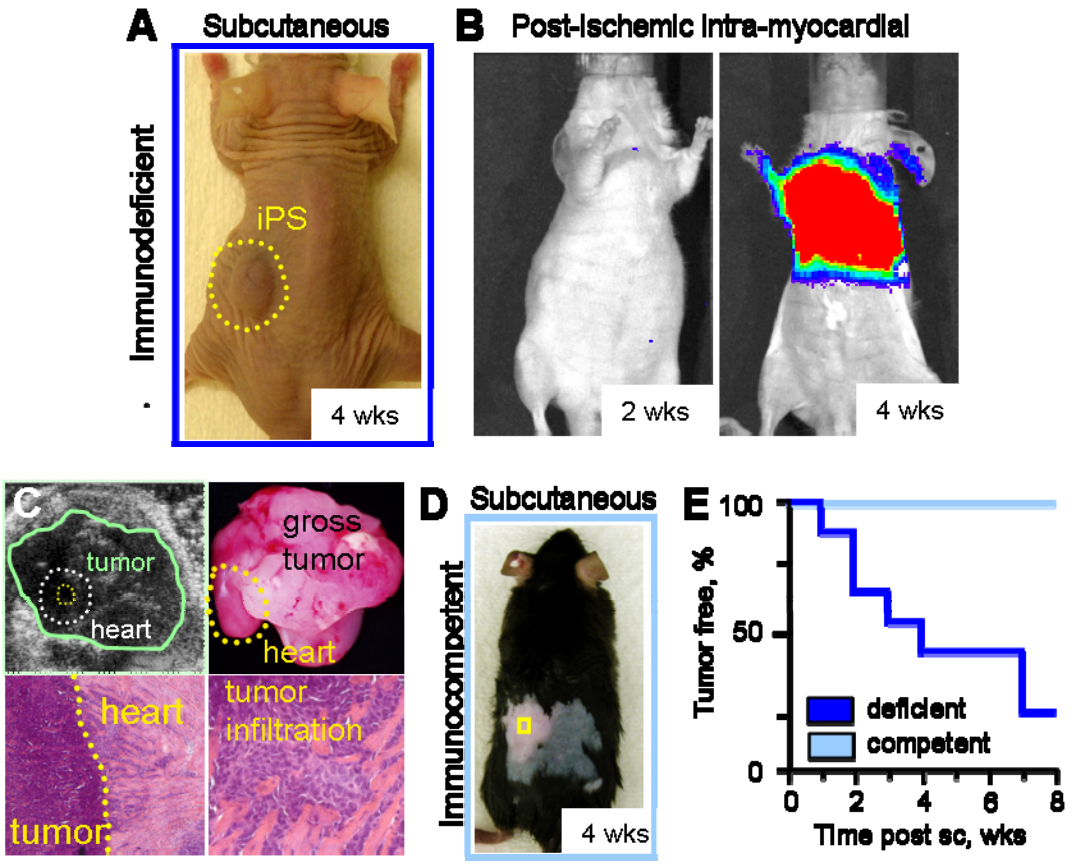

Figure 37. **iPS fate determined by host competency**. A) Subcutaneous injection of 500 000 iPS in immunodeficient host resulted in tumor growth (dotted circle). B) On acute myocardial infarction, 200 000 iPS transplanted intramyocardially were detected in the heart region by *in vivo* bioluminescence imaging dramatically expanding by 4 weeks. C) Tumor growth was detected by echocardiography (top left) and confirmed on necropsy in all immunodeficient hosts (top right). Histology demonstrated tumor expansion outside of the heart (bottom left) and infiltration within the wall of infarcted myocardium (bottom right). D) Immunocompetent hosts reproducibly averted tumor growth on subcutaneous injection (square) of 500 000 iPS throughout follow-up. E) Subcutaneous (sc) transplantation produced teratoma in immunodeficient (deficient) hosts in contrast to tumor-free outcome in all immunocompetent (competent) hosts.

hemodynamics 4 weeks after transplant (**Figure 37C**). Autopsy in immunodeficient recipients (n=6) verified consistent teratoma formation with extension beyond the myocardial wall and tumor infiltration within the post-injured myocardium (**Figure 37C**).

In contrast to tumorigenesis that compromised the safety within immunodeficient environments, subcutaneous transplantation of iPS at the same dose (500,000 cells) into immunocompetent hosts demonstrated a persistent absence of tumor growth (**Figure 37D**) in all animals (n=6), even at 8 weeks of follow-up, in contrast with 75% of immunodeficient mice subcutaneously injected that developed teratomas at 8 weeks (**Figure 37E**). Together, these data indicate that teratogenic outcome after injection of undifferentiated iPS depends on the immune competency of the injected host, both in the generic setting of a subcutaneous injection and in a more specific microenvironment as the created in the post-ischemic myocardium.

5.3. iPS engraft into infarcted immunocompetent adult hearts

Following the previous experiments, intramyocardial transplantation of 200 000 iPS per heart, a dose selected on the basis of tumor-free outcome with embryonic stem cell intervention (Behfar, 2007; Behfar, 2002), after surgical induction of myocardial infarction in immunocompetent mice, produced stable engraftment without detectable tumor formation (n=6; **Figure 38A**). According to bioluminescence emitted from labeled progeny, differentiated iPS within ischemic immunocompetent hearts were detectable by 2 weeks after transplantation without metastatic dissemination after 4 weeks of engraftment (n=6; **Figure 38A**) as shown by localized signal in the left side of the chest. In fact, immunostaining of hearts at 4 weeks post injection demonstrated rare undifferentiated iPS progeny positive for SSEA-1 expression within the postischemic myocardium (**Figure 38B**). Immunocompetent recipients thus ensured controlled iPS

engraftment with no tumor development in contrast to teratomas previously observed in immunodeficient transplanted mice (**Figure 37B**).

Electrocardiographic recording of post-treatment competent mice showed tissue integration that did not perturb electric homeostasis when compared to readings prior to cell injections (n=6; **Figure 38C**). In this way, the immunocompetent adult host provided a permissive environment for differentiation, offering the opportunity to test the therapeutic potential of iPS clones.

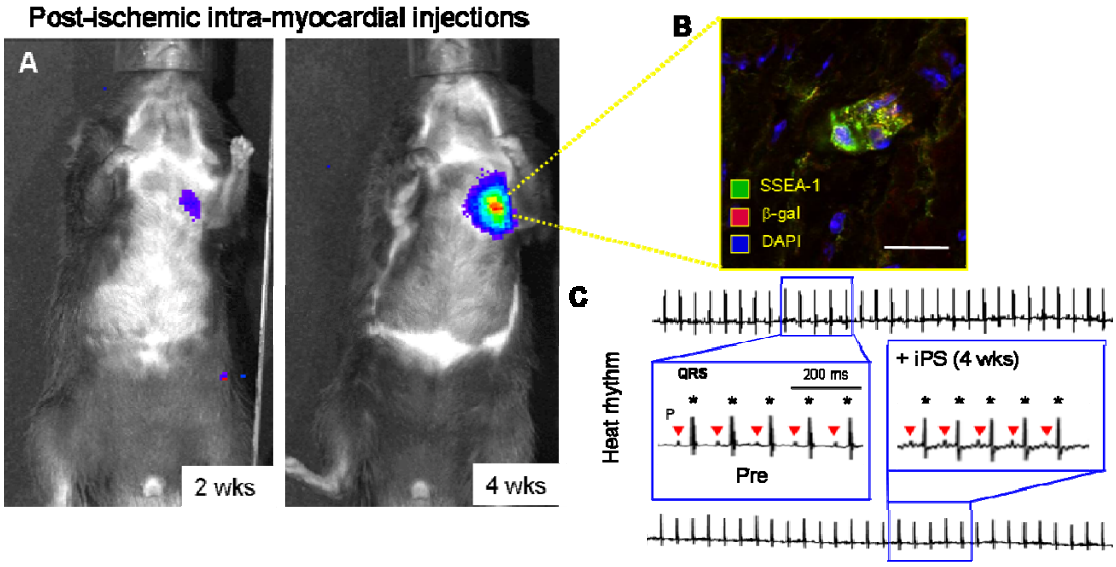

Figure 38. iPS integrate within host tissue without disrupting electric conductivity. A) iPS transplantation within infarcted myocardium of immunocompetent hosts produced stable engraftment detected by live-cell imaging throughout the 4-week follow-up. B) Postischemic myocardium transplanted with iPS at 4 weeks demonstrated rare pockets of SSEA-1–positive progeny. Bar=10 μm. C) Normal preinfarction (Pre) sinus rhythm was maintained after iPS transplantation throughout the 4-week follow-up, with P waves (triangles) preceding each QRS complex (stars) with no ventricular tachycardia or ectopy.

5.4. iPS therapy restores myocardial performance lost by ischemic injury

Within immunocompetent hosts, recovery of postischemic cardiac performance was compared in randomized cohorts transplanted with parental fibroblasts versus derived iPS. Monitored by echocardiography, irreversible occlusion of the epicardial coronary blood flow consistently impaired anterior wall motion, depressed global cardiac function, and halved EF from 82±3% before infarction (n=8) to 38±3% within 1 day after infarction (n=12; **Figure 39A**).

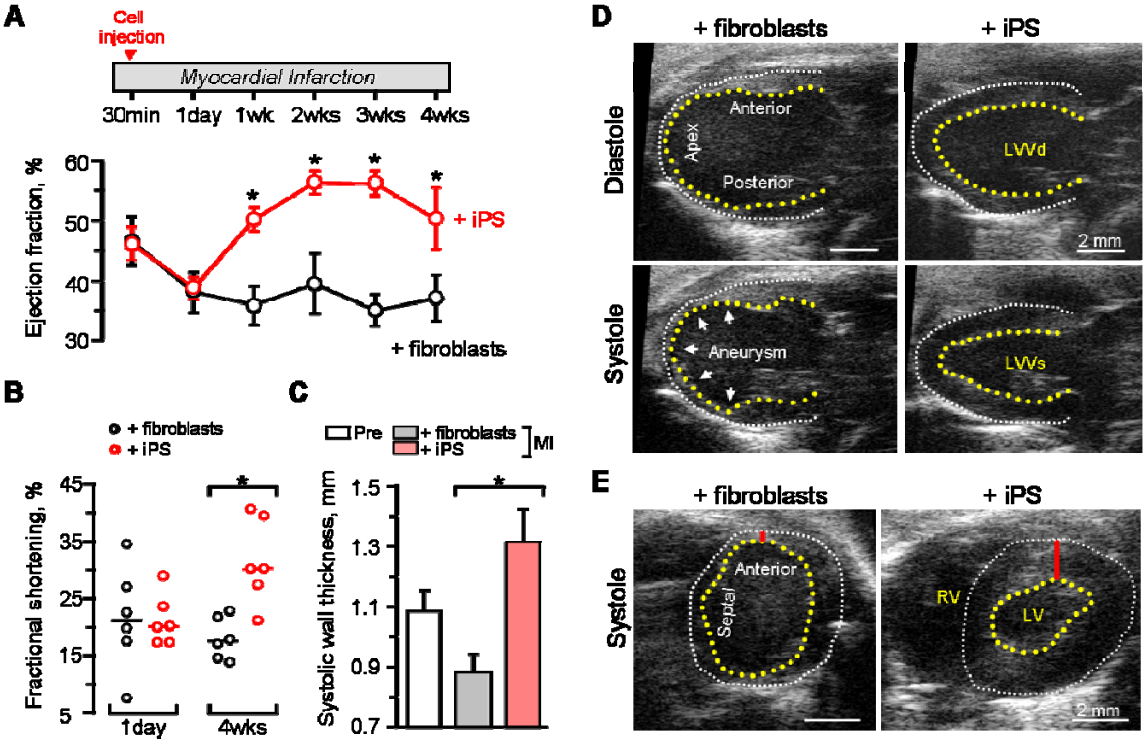

Figure 39. iPS restored function after acute myocardial infarction (MI). A) On randomization, cell-based intervention was performed at 30 minutes after coronary ligation. Divergent EFs were noted in iPS- (n=6) versus fibroblast-treated (n=6) hearts within 1 week after therapy, maintained throughout follow-up. *P=0.002 by 2-way repeated-measures ANOVA. B) Fractional shortening was similar at day 1 after infarction, but significant improvement was observed only in iPS-treated hearts. Line indicates median value. *P=0.01. C) Septal wall thickness was preserved in systole after iPS (n=6) compared with fibroblast (n=6) treatment. *P=0.006. D) Echocardiography with long-axis views revealed anterior wall thinning and apex aneurysmal formation (arrowheads) in fibroblast-treated hearts, as indicated by akinetic wall (left) in contrast to normalized systolic wall motion in iPS-treated hearts (right). E) Short-axis views confirmed thinning in the anterior wall (red bar) and overall decreased cardiac performance with fibroblast- compared with iPS-based interventions. Yellow and white dotted lines indicate endocardium and epicardium, respectively.

Whereas blinded transplantation with parental fibroblasts demonstrated persistent functional decline with EF dropping to 37±4% at 4 weeks (n=6), iPS intervention improved cardiac contractility to achieve an EF of 56±2% within the first 2 weeks of therapy and 50±5% by 4 weeks (n=6; *P*=0.002, iPS versus fibroblasts; **Figure 39A**). Functional benefit in response to iPS was verified by the improved fractional shortening, from 20±1% (median 18%; n=6) at 1 day after infarction to 31±3% (median 29%; n=6) after 4 weeks, in contrast to a lack of recovery in fibroblast-treated hearts (n=6; *P*=0.01; **Figure 39B**). Moreover, the regional septal wall thickness in systole was significantly rebuilt with iPS (1.31±0.11 mm; median 1.20 mm; n=5) but not with fibroblast (0.88±0.06 mm; median 0.90 mm; n=6) treatment (*P*=0.006; **Figure 39C**). Impaired cardiac contractility in the injured anterior wall resulted in akinetic regions with paradoxical motion in systole indicative of aneurysms in fibroblast-treated hearts, in contrast to coordinated concentric contractions in response to iPS treatment visualized by long-axis and short-axis imaging (**Figure 39D** and **39E**). Thus, compared with non-reparative parental fibroblasts, iPS intervention improved functional performance after acute myocardial infarction.

5.5. iPS therapy halts progression of pathological remodeling in infarcted hearts

Beyond functional deterioration, maladaptive remodeling with detrimental structural changes prognosticates poor outcome after ischemic injury. In this study, iPS-based intervention attenuated global left ventricular end-diastolic dimension (LVDd) increase. Preinfarction LVDd measured 3.2±0.1 mm (median 3.1 mm) but increased after infarction to 4.9±0.1 mm (median 4.9 mm) by 4 weeks of fibroblast treatment (n=6), a value significantly higher (*P*=0.007) than 4.2±0.2 mm (median 4.2 mm) with iPS treatment (n=6; **Figure 40A**). Furthermore, M-mode echocardiography demonstrated regional structural deficits with deleterious wall thinning and chamber dilation in fibroblast-treated hearts

(n=6), rescued by iPS intervention (n=6; **Figure 40B**), where thicker and more actively contracting walls were visualized (**Figure 40B**, bottom). Pathological structural remodeling leads to electrophysiological consequences with

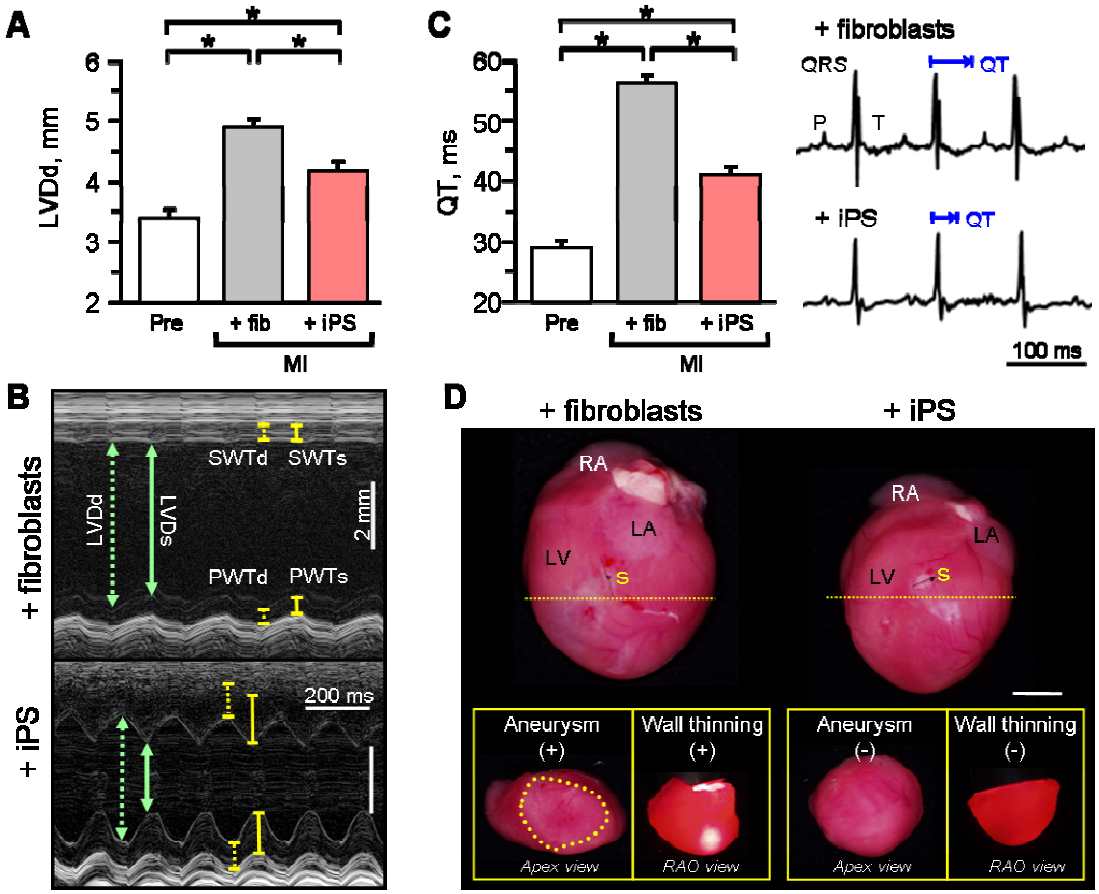

Figure 40. iPS halt maladaptive remodeling and preserve structure. A) Diastolic parameters revealed a significant decrease in global LVDd in hearts treated with iPS (n=6) compared with fibroblasts (n=6) at 4 weeks after therapy (*P=0.007). B) M-mode echocardiography demonstrated dilated ventricular lumen with reduced anterior and septal wall thickness (SWTd) during systole in fibroblast-treated hearts (top), which improved with iPS intervention (lower). C) Time required for ventricular repolarization and depolarization, measured by the QT interval, was significantly prolonged in fibroblast- (n=6) compared with iPS-treated (n=6) hearts. *P=0.004. D) Hearts were pathologically enlarged in the fibroblast-treated group with aneurysmal formation (+) and severe wall thinning (+) visible with translumination compared with structurally preserved iPS-treated hearts with normal apex geometry (-) and opaque thick walls (-) on right anterior-oblique (RAO) view on transverse sectioning of hearts immediately inferior to the site of surgical ligation (yellow dotted line). Bar=5 mm. Aneurysm is delineated by yellow dotted circle. RA indicates right atrium; LA, left atrium; LV, left ventricle; s, suture; SWTd, septal wall thickness in diastole; SWTs, septal wall thickness in systole; PWTd, posterior wall thickness in diastole; and PWTs, posterior wall thickness in systole.

prolongation of the QT interval, which increases risk of arrhythmia. Infarction increased QT interval from 28.9±1.4 ms (median 28.1 ms) to 55.9±1.3 ms (median 55.8 ms) in fibroblast-treated hearts (n=6), which was abrogated to 40.8±1.5 ms (median 40.3 ms, n=6) with iPS treatment (*P*=0.004; **Figure 40C)**. These real-time surrogates for tissue remodeling were confirmed on autopsy on inspection of gross specimens that demonstrated reduced heart size, lack of aneurysmal formation, and absence of severe wall thinning in iPS- compared with fibroblast-treated hearts (**Figure 40D**). Collectively, the favorable remodeling at global, regional, and electric levels demonstrates the overall benefit of iPS therapy in the setting of myocardial infarction.

5.6. Multilineage cardiac tissue regeneration after iPS therapy

Histological analysis of mouse hearts 4 weeks after myocardial infarction and cell therapy, demarcated demuscularization and extensive scarring within left ventricles distal to coronary ligation in hearts treated with fibroblasts (**Figure 41A**, left). In contrast, iPS treatment halted structural deterioration of infarcted tissue with antifibrotic benefit and remuscularization within the left ventricular free wall (**Figure 41A**, right) as revealed by absence of stained fibrotic areas and increased anterior wall thickness. Surgical dissection and postmortem histopathological analysis verified absence of tumor infiltration or dysregulated cell expansion after iPS transplantation in the myocardium itself, as well as in the liver, lung, and spleen, organs with high metastatic risk (n=10 staggered sections throughout respective organs; **Figure 41B**) suggesting that transplanted cells remained contained within the heart parenchyma after intracardiac injection. In postischemic myocardium, immunohistochemistry confirmed engraftment of iPS-derived progeny that expressed transgene markers luciferase (not illustrated) or β-galactosidase (**Figure 41C** through **41E**). Colocalization of transgene expression with cardiac α-actinin was consistent within the damaged territory, as documented by microscopy of serial transverse sections (n=10 at 10- to 20-μm

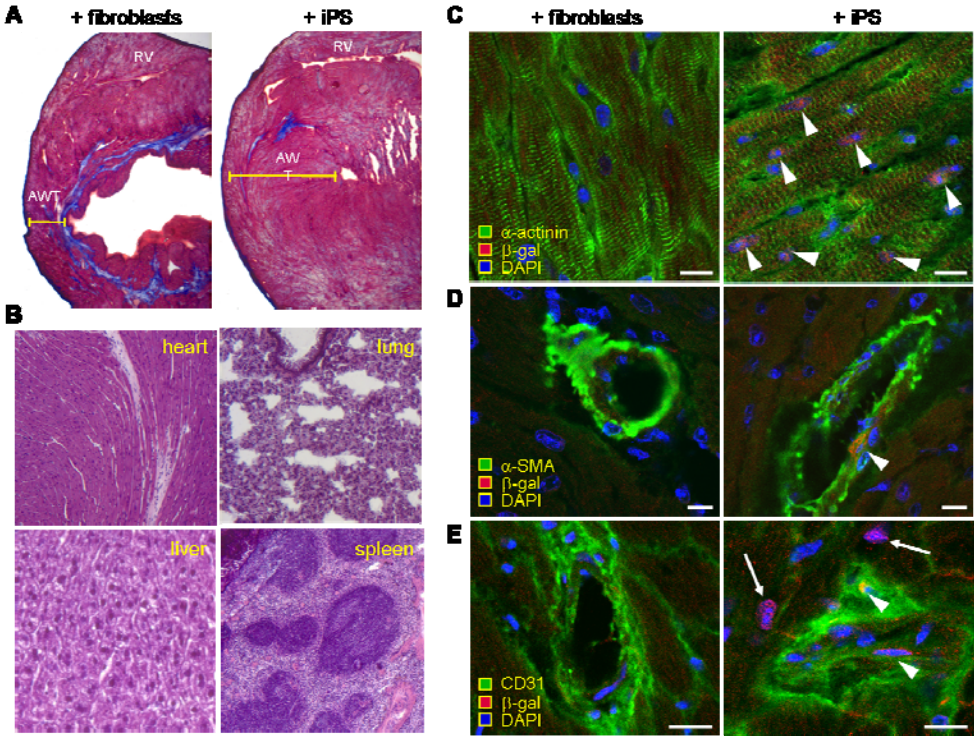

Figure 41. iPS treatment reduced scar and contributed to multilineage reconstruction. A) After 4 week of therapy, Masson's trichrome staining demonstrated reduced anterior wall thickness (AWT) and fibrosis (blue staining) in hearts treated with fibroblasts (left) compared with iPS (right). RV indicates right ventricle. B) Autopsy demonstrated tumor-free heart, liver, lung, or spleen in the iPS-treated cohort. C) After 4 weeks, integrated iPS progeny expressed markers of remuscularization according to α-actinin (right) and β-gal coexpression (arrowheads), not detected with fibroblast treatment (left). D, E) Smooth muscle actin (α-SMA) and CD31- positive endothelium colocalized with β-gal (arrowheads) in iPS progeny (right) compared with no expression with fibroblast treatment (left). DAPI visualized nuclei. Bar=5 μm.

intervals) immediately adjacent to the site of coronary ligation (**Figure 41C**). Smooth muscle α-actin (**Figure 41D**) and endothelial CD31 (**Figure 41E**) were also detectable colocalized with β-galactosidase, albeit at lower frequency, consistent with multilineage cardiovascular differentiation of iPS. Thus, in contrast to ineffective parental fibroblasts, targeted delivery of iPS generated *de novo* cardiovascular tissue in postischemic adult myocardium.

In summary, injected iPS responded to cardiac injury with controlled integration and chimeric tissue formation within allogeneic host. Cell integration translated into performance recovery as qualified iPS clones contributed to tissue reconstruction with synchronized cardiovasculogenesis, composed predominantly of cardiac lineage with accompanying smooth muscle and endothelium, highlighting the potential of this platform as a new therapy in the treatment of cardiac injury.

VII. DISCUSSION

1. Promiscuous human stemness related factors induce interspecies pluripotent reprogramming

Nuclear reprogramming of somatic cells into pluripotent progenitors was originally demonstrated through transfer of a nucleus into the cytoplasm of a competent host oocyte (Campbell, 1996; Wilmut, 2007). The resulting intraspecies nuclear-to-cytosol interaction catalyzed the epigenetic influence on phenotypic outcome, reversing differentiation to achieve genetic reprogramming of an adult source into an embryonic state (Armstrong, 2006; Byrne, 2007; Hochedlinger and Jaenisch, 2006). The robustness of this process was further supported by somatic cell nuclear transfer applications in which xenogenic combinations of nucleus and cytoplasmic components were equally successful and revealed phylogenic conservation of the permissive oocyte environment (Beyhan, 2007). A functionally conserved ecogenetic interface for de-differentiation, although implied by the preserved responsiveness of somatic nucleus to multiple environments, has yet to be proven.

Beyond whole nucleus-based transplantation, equivalent reprogramming of differentiated cytotypes has been achieved most recently by ectopic exposure to pluripotent components (Henderson, 2008; Jaenisch and Young, 2008). Delivery of stemness-related genes *Oct-3/4, Sox2, Klf4* and *c-Myc* reprogram adult somatic cells, promoting re-acquisition of embryonic traits (Okita, 2007; Takahashi and Yamanaka, 2006). The resulting induced pluripotent stem (iPS) cells recapitulate morphology and expression patterns of authentic embryonic stem cells (Maherali, 2007; Meissner, 2007; Takahashi, 2007). The alternative combination of Oct-3/4, Sox2, Nanog and Lin28 has also produced pluripotency induction from somatic tissues, suggesting mechanisms that can be reactivated by non-exclusive inductors (Yu, 2007). iPS cells have been derived through intraspecies reprogramming with gene sets from murine, monkey and human sequences (Liu, 2008; Park, 2008; Park, 2008; Stadtfeld, 2008; Wernig, 2007;

Yamanaka, 2008), without however evidence for interspecies pluripotent reprogramming.

Although orthologs are frequently assumed to be functionally conserved (Koonin, 2005), differences in stem cell-related genes between reproductively isolated species mandate an empiric examination of cross-species gene/environment communication. Comparative studies of mammalian embryonic stem cells have uncovered both conserved and divergent factors required to maintain pluripotency (Surani, 2007). Pathways requiring Oct3/4, Sox2, Nanog as well as Stat3 signaling are essential for self-renewal of both mouse and human embryonic stem cells, and demonstrate highly conserved genetic structures across mammalian species (Loh, 2006). In contrast, leukemia inhibitory factor (LIF) and basic fibroblast growth factor (FGF2) are exclusively required for self-renewal in mouse or human embryonic stem cells, respectively (Daheron, 2004; Xu, 2005). Thus, the question arises whether stemness-associated factors used to derive iPS cells are functionally conserved when expressed in distant mammalian species.

To examine the feasibility of interspecies induction of stemness traits requires platforms that enable consistent xenotransduction (Ikeda, 2002) of pluripotent transcription factors. To this end, human stemness related factors were expressed from an HIV-based lentiviral vector system with enhanced cross-species tropism, and evaluated in distant mammalian systems. Utilizing the developed vector system and the validated hybrid progenitor cell analysis approach, this study demonstrates evolutionarily a conserved function for pluripotent gene sets. Human stemness related factors induced morphological changes consistent with the embryonic stem cell phenotype, lineage-specific gene expression, teratoma tissue formation, and contribution to organogenesis in non-human milieu.

Together, these data indicate that genetic mechanisms responsible for reverting somatic tissue to pluripotent state represent a robust process of reprogramming that has been evolutionarily conserved to contribute to the overall fitness of developmental competency and regenerative capacity. Further assessing this concept, human somatic cells have been recently derived using four mouse genes (Woltjen, 2009) re-strengthening the concept of conserved pluripotent function among evolutionary distant species. At the same time, this type of approach highlights the convenience of a unique platform that would allow the use of the same reagents to reprogram both mouse cells to be used in animal model systems and human-derived cells for drug screen or tailored therapy.

2. Diploid aggregation as a high-throughput model of functional pluripotency.

Establishing functionality within an atypic environment necessitates readouts to capture innate pluripotent initiation, gastrulation, lineage specification, and ultimately organogenesis (Mali, 2008; Stadtfeld, 2008). Beyond cell autonomous differentiation, embryonic development provides further stringency to discriminate the function of pluripotent progenitors based on the ability to integrate within the context of a host morula and produce an independent source of blastomeres equally competent to orchestrate complex organogenesis (Singla, 2006; Strang, 2005). The development of functional dynamics between engineered progeny and native cytotypes *in vivo* are comprehensively examined during normal embryogenesis (Singla, 2006).

Until two years ago, only two types of cells outside the developing embryo up to the inner cell mass (ICM) stage (Moustafa and Brinster, 1972; Moustafa

and Brinster, 1972) had been shown to reproducibly engraft within early embryos, participating in their development and contributing to several tissues; these were teratocarcinoma cells (TC) and embryonic stem cells (ESC). However, from these original reagents, only ESC contributed to normal development in a controlled manner, with TC giving rise to abnormal mid gestation embryos and persistent tumors in obtained chimeras (Rossant and McBurney, 1982). Further studies aimed at reducing TC tumorigenicity demonstrated that undifferentiated state is needed for cells to engraft in the early embryo (Waters and Rossant, 1986) since downregulation of malignancy following retinoic acid treatment (aimed at promote differentiation in TC cells) completely averted the ability of these cells to generate chimeras. This is further supported for the lack of successful studies reporting contribution to chimeric animals from any type of differentiated or partially differentiated cells.

TC cells and ESC have in common high expression levels of the transcription factor Oct4, necessary to maintain the malignant stem cell component of teratocarcinomas (Chambers and Smith, 2004) and playing a fundamental role in regulating self-renewal and lineage commitment (Gidekel, 2003; Niwa, 2000). Oct4 is also one of the core components of the two different reprogramming sets (Takahashi and Yamanaka, 2006; Yu, 2007) that have been so far described and used for the generation of iPS (**Figure 11**), highlighting its importance in the induction and maintenance of pluripotency. Given this and all the other features shared by iPS and ESC, it seems fair to consider reprogrammed cells as a third cell type able to fulfill the stringent pluripotency criterion of embryonic integration.

The ‘gold standard’ test for pluripotency has been described as the ability of the cells to functionally replace all cell types in the developing organism (Smith, 2009) represented at the practical level by chimera derivation, germ line transmission or tetraploid complementation assays. High-stringency testing for

bona fide pluripotency has been restricted to low-throughput procedures, such as germline transmission and tetraploid aggregation (Okita, 2007; Wernig, 2007). In this work, non-coerced diploid aggregation offers a rapid yet reliable surrogate marker for functional pluripotency with definitive readout feasible within 24 hours. Together with this, simple equipment requirements and easiness of performance allowing these experiments to be done independent of specialized personnel or facilities (as opposed to blastocyst injections or tetraploid aggregations) render this approach affordable and useful in the context of pluripotency and differentiation capacity assessment. However, inherent limitations, such as partial contribution and inefficient germ line transmission due to uncontrolled random integration, restrict its applicability.

3. Effect of nuclear reprogramming on subsequent differentiation

Large efforts in the iPS field are focusing in understanding the reprogramming process in order to optimize it, rendering this platform amenable to the clinical setting. However, the potential use of these cells for regenerative applications warrants detailed study of the effects of pluripotency re-set in the developmental and differentiation potential of the reprogrammed cells. Along the reprogramming process, two types of memory may affect the final outcome, namely secondary effects caused by the persistent expression of the reprogramming factors and carry over-features retained from the original cell type. In this regard, it has been shown that upon nuclear reprogramming of immortalized human neural stem cells (hNSC), the resulting iPS displayed both insufficient induction of some human embryonic stem cell-upregulated genes and deficient silencing of other hNSC-related genes (Marchetto, 2009). This leads to the initial conclusion that the bioengineering process does not completely erase

the transcriptional signature of the parental cells, giving rise to iPS that carry over some memory from their previous state (Marchetto, 2009). This fact could easily interfere with subsequent differentiation, especially into cell types distinct from the basal one, remaining an interesting area of study.

Non-specific of tissue of origin, but related to the bioengineering process itself, we have demonstrated that presence of the c-Myc transgene after re-setting of the pluripotent ground state impairs cardiac differentiation, otherwise proficient in c-Myc-less conditions. The same idea was recently described regarding *in vitro* endodermal differentiation in the presence or absence of the reprogramming factors beyond the pluripotency induction process. In this study, parental iPS containing a polycistronic vector that codified for the four reprogramming factors showed a diminished capacity to respond to soluble growth factor-differentiation cues, while their transgene-free progeny responded to the same protocol upregulating key endodermal transcription factors (Sommer, 2009). The same outcome was observed with a limited panel of markers for ectoderm and mesoderm tissue, in both cases revealing that differentiation was enhanced by excision of the reprogramming factors.

Both our work describing the deleterious effect of c-Myc on cardiac differentiation and that from Sommer, base their reprogramming strategies on lentiviral vectors. Lentiviruses, a complex subtype of retroviruses, have been shown to sustain stable transgene expression during proliferation of undifferentiated ESC (Pfeifer, 2002). Moreover, lentiviral transgenes are expressed during differentiation of ESC *in vitro* (embryoid bodies) and *in vivo* (teratomas) (Pfeifer, 2002). This is in agreement with our results (**Figure 35**) in which lentivirally labeled cells expressed lacZ transgene in 5 day old-embryoid bodies. In such a case, residual expression of the reprogramming transgenes may be responsible for beyond-normal perpetuation of pluripotency circuitry that should be overcome as cells progress towards a differentiated state, disrupting

expected developmental processes and therefore impairing differentiation. This would justify overall decreased differentiation caused by sustained presence of pluripotency-related transgenes introduced in the cells using lentiviral systems.

In particular, c-Myc expression has long been associated with the inhibition of terminal differentiation (Lin, 2009), with its overexpression impairing cartilage (Piedra, 2002), erythroid (Acosta, 2008) or neural (Leon, 2009) differentiation among others. Also c-Myc has been shown to have an important role in the maintenance of ESC identity, acting downstream of the LIF/STAT3 pathway that maintains pluripotency and self-renewal in mice (Cartwright, 2005). This is consistent with the negative effect that exogenous sustained c-Myc expression coming from the reprogramming lentiviral transgene-set might have on the differentiation proficiency of the bioengineered cells, as we have shown by comparing cardiogenic capacity of iPS reprogrammed with or without c-Myc.

In related studies, deficient differentiation has been reported to be reduced when assessed through *in vivo* assays consisting of blastocyst injections (Sommer, 2009). In this setting, both cells containing the reprogramming factors and cells from which they had been removed (therefore no remaining effect is expected), were able to contribute to several tissue types, although developmental aberrancies were observed with the parental clones past mid-gestation. This observation highlights the powerful effect of the embryonic environment in the induction and control of differentiation patterns, since factor-containing cells contributed to embryonic development for several days despite their inability to differentiate *in vitro* in response to validated protocols (Sommer, 2009). We obtained similar results with 4F-iPS, unable to give rise to *bona fide* cardiomyocytes *in vitro* following standard differentiation, but reproducibly capable of populating the embryonic heart (**Figure 36**) in all its different developing compartments upon diploid aggregation. However, we did not follow 4F-iPS contribution after 9.5 d.p.c.

The concept of the embryo as the ideal developmental environment was already considered in the early 70's, when teratocarcinoma cells were shown to be able to integrate with morula stage embryos, synchronizing their development state to that of the embryos and giving rise to chimeric mice (Brinster, 1974). In spite of the powerful control exerted by the embryonic environment, salient dysregulated features such as those causing tumor development in TC-chimeras (Rossant and McBurney, 1982) and developmental defects observed in factor-present iPS chimeras (Sommer, 2009) overcome the nurturing embryonic environment revealing intrinsic deficiencies. These inadequacies might arise during embryonic development or might stay silent for longer periods of time, such as the reported tumor formation due to c-Myc reactivation in animals containing four factor-reprogrammed cells (Okita, 2007), even though these cells produce normal embryo contribution and germ line transmission.

Together, these observations lead to the hypothesis that beyond pluripotency induction, preservation of differentiation capacity of the engineered pluripotent stem cells also needs to be carefully characterized, including both *in vitro* and *in vivo* studies, with embryonic contribution functioning as a double marker of pluripotency and differentiation potential. Memory retained from the original cell source should be considered as a possible limitation for broad differentiation profiles. Newer traceless reprogramming strategies might solve the after-effects due to residual transgene expression, however, epigenetic carry-over will still need to be monitored.

4. iPS cardiogenesis in the context of embryonic stem cell differentiation

Cardiac differentiation from mouse and human embryonic stem cells is a broadly studied subject. One significant advantage for this field is the readily identifiable outcome consisting of spontaneously contracting areas (Boheler, 2002) whose size and pace can be easily monitored and characterized. Based on this, differentiation stages of mouse ESC derived cardiomyocytes have been divided in early (pacemaker-like or primary myocardial-like cells), intermediate, and terminal (atrial, ventricular, nodal, His and Purkinje-like cells) (Hescheler, 1997).

Descriptive analysis addressing ESC-derived cardiomyocyte derivation (Hescheler, 1997), stated that all cardiac phenotypes simultaneously coexisting in the EB, the percentage of the different cell types changes from early, pacemaker-like cardiomyocytes predominate in early EB around culture day 11, while a higher percentage of atrial-ventricular like cells is found in older EB around days 17 to 21 (**Figure 42**). According to this classification, the cardiomyocytes presented in this work should fall into the early-intermediate state, since the applied differentiation protocols lasted for 11 to 12 days.

Based on ultrastructural studies, ESC-derived sarcomeres are described as acquiring defined A bands, I bands, and Z discs at the terminally differentiated stage (Westfall, 1997). Our cells, however, do not show very clear A and I bands, despite presence of moderately organized Z discs (**Figure 29A**, middle), therefore, they are behind the terminally differentiated stage. Intercellular gap junctions were apparent in our samples (**Figure 29A**, bottom), as they had been previously described (Westfall, 1997).

At the gene expression level (**Figure 26**), we have found similarities in all the studied genes, although we did not include the entire panel for our studies. As previously reported, Oct4 expression is present from the undifferentiated state and goes down during differentiation. Gastrulation marker Goosecoid is present in the initial stages, going down after day 7 in ESC and around day 5 in our studies (**Figure 26B**). Expression levels of muscle gene Nkx2.5 are detectable shortly after beginning of differentiation for ESC and 3F-iPS, indicating a certain intrinsic propensity for cardiac differentiation in both types of cells (**Figure 26D**).

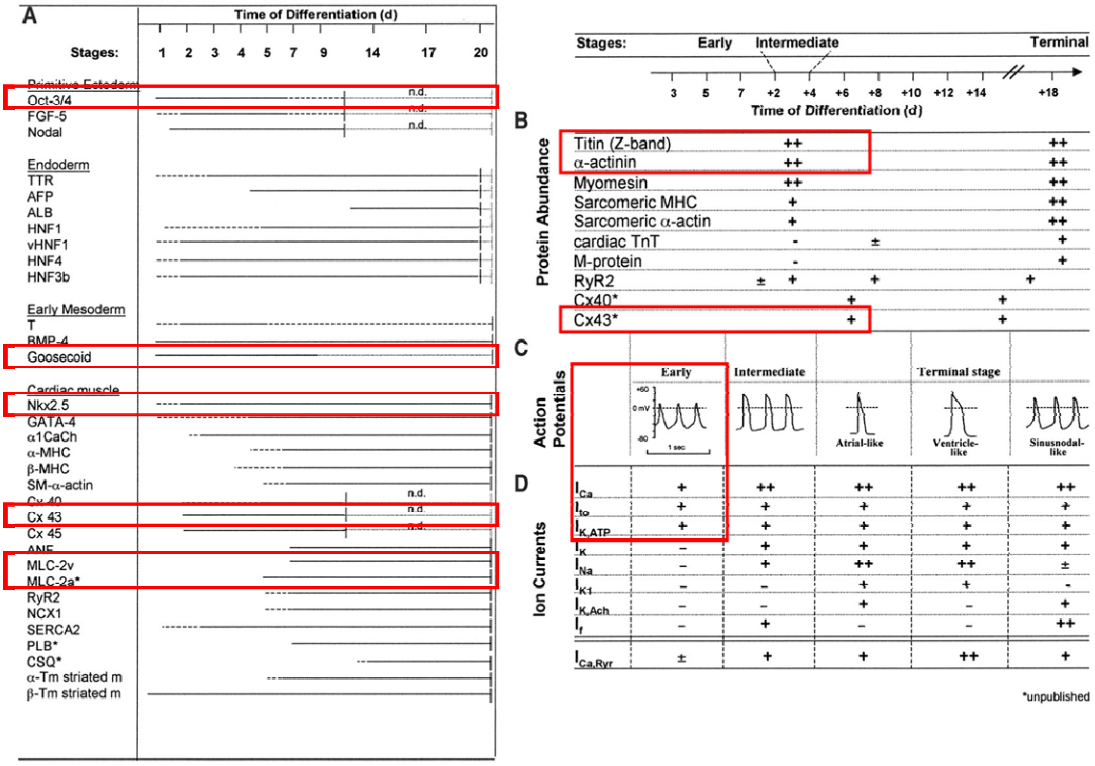

Figure 42. ***In vitro*** **differentiation markers for mouse embryonic stem cells**. Adapted from Boheler, 2002 (Boheler, 2002).

Structural proteins such as connexin 43, myosin light chain (atrial and ventricular) or alpha-actinin are present at day 12 as shown in our immunofluorescence

(**Figure 29B**), again situating our cells in the early to intermediate stage of differentiation.

Electrophysiology of early ESC-derived cardiomyocytes is characterized by action potentials typical of primary myocardium, with primitive pacemaker action potentials generated by only two main types of ion channels, i.e. voltage-dependent L-type Ca^{2+} (I_{ca}) and transient K^{+} channels ($I_{K,to}$) (Hescheler, 1997). Coinciding with this, our iPS-derived cardiomyocytes showed an inward component dependent on presence of Ca^{2+} in the medium, and no signs of more mature sodium channels (**Figure 31**), usually appearing at a later stage of differentiation (Hescheler, 1997). Also distinctive of this early phase is the presence of spontaneous beating activity, easily detected in our samples (**Figure 30B**), and disappearing as cells differentiate towards a more defined atrial or ventricular type.

Overall, our isolated cardiomyocytes display phenotypic characteristics concordant with ESC-derived cardiomyocytes at an early stage, which also corresponds to the applied differentiation protocols. Further differentiation would be needed to define if iPS derived cardiac cells acquire, *in vitro,* the whole arrange of markers and properties proper of mature cardiomyocytes.

5. Mechanisms of heart repair

5.1. Intrinsic repair capacity

Endogenous stem cells and self-repair mechanisms have been increasingly recognized as a natural process for tissue homeostasis (Lowry and Plath, 2008). Fundamental to cardiac tissue rejuvenation is cardiomyocyte renewal through recruitment of endogenous progenitor pools within the body (Aoi, 2008; Ebert, 2009). Notably, stem cell contribution to postnatal heart formation has been validated by the self/non-self chimerism characteristic of patients following allogeneic transplantation (Deb, 2003; Kajstura, 2008; Quaini, 2002). Furthermore, innate stem cell loads increase in failing hearts and contribute to a regenerative response, involving ongoing derivation of cardiomyocytes from circulating or resident progenitors (Schenke-Layland, 2008; Xu, 2009). However, in the context of large-scale destruction following ischemic injury, the regenerative response required for tissue homeostasis is limited in its ability to salvage a deteriorating myocardium (Narazaki, 2008).

The magnitude of the natural process of cardiac tissue self-renewal is likely dependent on multiple factors such as patient age, disease status, co-morbidities, patient-specific medications, as well as genetic predispositions, epigenetics or ecogenetic influences. Utilizing quantification of radio-isotopes, introduced at high levels into the atmosphere during above ground nuclear bomb testing between the years 1955 and 1963 leading to subsequent DNA incorporation within living material, the birth date of individual cardiomyocytes was recently calculated (Mauritz, 2008). Based on these data, it has been estimated that cardiomyocytes can renew at <1% annually to achieve on average a renewal approaching up to 50% of the total heart mass over a lifespan (Mauritz, 2008). Although the magnitude is generally thought to be insufficient to compensate for severe tissue loss in acute disease states, the natural chimerism

that is produced as a result of rejuvenation may gradually contribute to the prevention of heart disease and provide a significant protective mechanism of self-renewal to the heart, as originally suggested in transplant patients (Aoi, 2008; Ebert, 2009). The precise mechanism of autologous self-renewal remains only partially addressed, but mounting evidence confirms the presence of *in situ* cardiogenic differentiation (Zhang, 2009). Direct evidence of allogeneic circulating stem cell contribution to the heart has been demonstrated in multiple patient-derived samples (Aoi, 2008; Dimos, 2008; Ebert, 2009; Hanna, 2007). Importantly, this data from chromosomal mismatch does not preclude an active participation of resident stem cells in cardiac tissue renewal as calculated by the spectrum of de-identified cardiomyocyte birth dates. Therefore, based on the established paradigm of heart rejuvenation it is appropriate to surmise that augmentation of natural chimerism, either by reactivation of endogenous or transplantation of exogenous progenitor cells, offers a legitimate target to ameliorate the burden of chronic, degenerative heart disease presented herein as a disease paradigm.

5.2. Cell therapy approach

In view of the insufficient innate reparative capacity of the heart, complementary strategies have been studied to improve cardiac response to cell damage by delivery of supplementary cells or derived factors.

Stem cell-based repair integrates multifactorial mechanisms with cardiac regeneration predicated on the ability of diseased myocardium to be replenished with healthy multilineage tissue (Anversa, 2007; Chien, 2008; Gnecchi, 2008; Hodgson, 2004; Kolossov, 2006; Singla, 2006; Wu, 2008). Rejuvenation can be achieved from endogenous stem cell pools that respond to injury, albeit at levels typically insufficient to compensate for severe cardiac damage (Anversa, 2007). Exogenous stem cell types have been employed to augment therapeutic healing

through paracrine-mediated mechanisms (Gnecchi, 2008) and/or cell-autonomous contribution to tissue reconstruction (Chien, 2008; Kolossov, 2006; Wu, 2008).

Transplantation of exogenous stem cells in the damaged heart triggers a broad array of consequences leading to overall improvement of cardiac function that some times can not be directly linked to physical presence of transplanted cells, mainly due to failure in detection of engraftment or differentiated progeny (Balsam, 2004; Murry, 2004) or to the number of newly generated cardiomyocytes being too low to explain significant improvement (Gnecchi, 2008). In such situation, benefits of stem cells are attributed to secretion of soluble factors that, acting in a paracrine fashion, protect the heart (Gnecchi, 2005; Gnecchi, 2006; Kinnaird, 2004). Mechanisms involved include release of cytoprotective molecules that contribute to myocardial protection by means of increased cardiomyocyte survival (Gnecchi, 2006; Takahashi, 2006; Uemura, 2006; Xu, 2007) and contractility (Gnecchi, 2008), neovascularization leading to increased microvessel density (Kamihata, 2001; Takahashi, 2006) and limitation of cardiac remodeling and local inflammation (Nagaya, 2005; Ohnishi, 2007).

Embryonic stem cells transplanted into the post ischemic heart have reproduced the complete cardiac cellular repertoire including differentiation into cardiomyocytes, smooth muscle vascular cells and vascular epithelium (Hodgson, 2004; Kolossov, 2006; Singla, 2006), therefore contributing to improved outcome through a cell autonomous mechanism. The synchronized insertion of newly developed cardiac tissue participates in the anatomical and functional improvement by replenishing the damaged tissue limiting the scar size (Hodgson, 2004) and increasing the physical force of cardiac contraction (Kolossov, 2006).

5.3. Repair of acute myocardial infarction by induced pluripotent stem cells

Our work introduces iPS therapy into the diseased myocardium as an alternative to produce cardiogenic tissue independently of an embryonic source. The iPS platform for cell-based regeneration relies on the acquired ground state of pluripotency to enable somatic tissue–derived cardiopoiesis.

Live-cell imaging documented sustained engraftment of iPS-derived progeny within the heart up to 4 weeks post-transplantation. Intramyocardial transplantation of parental fibroblasts within acutely infarcted tissue was unproductive, despite previous indications that a multitude of cell types may improve cardiac function (Passier, 2008). In contrast, iPS responded to cardiac injury with restricted integration and controlled differentiation within the host environment. Post-ischemic cardiac performance was compared in randomized cohorts transplanted with parental fibroblasts versus bioengineered iPS. As quantified by echocardiography, occlusion of anterior epicardial coronary blood flow permanently impaired regional wall motion and cardiac function. Treatment with parental fibroblasts was unable to improve performance of post-ischemic hearts. Yet, iPS intervention in the acute stages of myocardial infarction improved cardiac contractility by 4 weeks post-transplantation. Functional benefit in response to iPS therapy was verified by the improvement in fractional shortening and regional septal wall thickness during contraction that demonstrated coordinated concentric contractions visualized by long-axis and short-axis 2-D imaging. Beyond functional deterioration, maladaptive remodeling with detrimental structural changes prognosticates poor outcome following ischemic injury to the heart. In contrast to non-reparative fibroblasts, iPS-based intervention attenuated global left ventricular diastolic diameter predictive of decompensated heart disease. A consequence of pathologic structural remodeling is evident by prolongation of the QT interval, which increases risk of

life-threatening arrhythmias. Successful iPS treatment prevented structural remodeling to avoid deleterious effects on electrical conductivity.

These real-time surrogates for tissue remodeling were confirmed by gross inspection of specimens. Autopsy allowed histological analysis to determine the extent of scar tissue formation within the post-ischemic region of the anterior circulation distal to the coronary ligation. In contrast to parental fibroblasts, iPS treatment halted structural deterioration with decreased fibrotic scarring and induction of remuscularization with *de novo* heart muscle tissue along with evidence for angiogenesis according to vascular endothelial markers. iPS contribution to the three main lineages of the cardiac tissue mimics previously described embryonic stem cell differentiation in the diseased heart setting (Hodgson, 2004; Kolossov, 2006; Singla, 2006). Although multiple mechanisms are likely to contribute to the benefit associated with iPS-based therapy, our work documented the cell autonomous effect derived from the intracardiac injection of undifferentiated reprogrammed cells.

Surgical dissection verified absence of tumor infiltration or dysregulated cell expansion following iPS transplantation in the myocardium itself, as well as in organs with high metastatic risk such as the liver, lung and spleen. Collectively, iPS-derived regeneration of the ischemic heart was demonstrated at multiple levels of stringency that include cellular, tissue, structural and functional levels, providing a foundation for development of this novel platform towards clinical applicability .

The heterogeneity inherent to the epigenetics and gene expression profiles within pluripotent cells, however, raises concern for pleiotropic outcomes (Nelson, 2008; Segers and Lee, 2008; Zhang, 2009). Both embryonic stem cells and iPS harbor the potential risk of producing teratoma. The propensity for uncontrolled growth of embryonic stem cells is nevertheless modulated by the

immunity of nonnative environment, as here demonstrated for iPS within adult immunocompetent hosts.

Exemplified by the inability to integrate into the electric syncytium of failing myocardium, transplantation of non–stem cell progeny has been plagued by the rigidity associated with advanced cell fate (Passier, 2008; Roell, 2007). Accordingly, the risk/benefit of iPS-based interventions will critically depend on the state of lineage differentiation and the interface with host milieu. In conclusion, this study expands the therapeutic potential of iPS treatment from noncardiac to cardiac disease. Reprogrammed through ectopic expression of 4 human stemness-related factors, iPS demonstrated acquired cardiogenicity and ensured functional and structural repair of infarcted myocardium.

Even though promising results were obtained in this study with four factor-derived iPS, there is still room for further improvement regarding the reprogramming strategies used in the bioengineering part of this process. Absence of residual transgene expression in the event of a traceless approach might release the full cardiac potential of these cells reducing, at the same time, the residual teratogenicity imposed by oncogene reactivation.

6. Therapeutic value of iPS in cardiac repair

With ongoing understanding of principles of myocardial regeneration (Srinivas, 2009), clinical translation of iPS technology faces similar challenges that have in part been addressed by natural stem cell applications, including embryonic stem cells approved early in 2009 by the Food and Drug Administration in the United States for trials involving patients with incurable spinal cord injuries. The first universal obstacle for clinical translation of pluripotent stem cell technology is unregulated tumor formation (Li, 2008). Even

a limited contamination of undifferentiated cells can, in theory, result in the formation of dysregulated tumors. Therefore, a critical milestone is to secure differentiation of iPS into the required cell type, purifying them away from residual undifferentiated precursors prior to transplantation (Li, 2008; Yamanaka, 2009). This becomes a unique challenge for iPS technology when the immune system is no longer involved in the elimination process of dysregulated foreign tissue, active with embryonic stem cell applications. This issue has been recently address in the cardiovascular setting by the discovery of a new technology allowing a simple sorting based on mitochondrial state that leads to highly purified cardiomyocyte populations REF. However, similar applications for other tissue types together with the optimal differentiation stage for cardiac regeneration are still unresolved.

The second issue that is unique to iPS is the accuracy of complete reprogramming of ordinary cells into pluripotent progeny. Inadequate conversion according to nuclear reprogramming strategies could result in impaired differentiation of iPS cells into target tissues required for specific applications (Yamanaka, 2009). Third, the issue of persistent transgene expression in iPS progeny requires careful consideration. Generally, iPS cells have been produced by transduction of ordinary cells with retroviruses or lentiviruses carrying ectopic transgenes in order to efficiently transfer stable expression into the host nucleus. This creates the risk of not only continuous expression of transgenes that are known to promote dysregulated tumor growth and impaired differentiation, but also involves permanent genomic modifications that raise the concern for insertional mutagenesis of endogenous loci.

Cardiac tissue specificity from stem cells has been investigated for more than a decade and as of yet no single gene or cluster of genes has been identified to secure cardiac differentiation. However, recent studies have significantly enriched the cardiac propensity with either exogenous growth factors (Behfar, 2008), cell sorting of cardiac progenitors (Kattman, 2006; Moretti, 2006;

Nelson, 2008; Yang, 2008), or genetically engineering pre-cardiac pathways all to encourage cardiogenesis from primitive stem cell pools (Takeuchi and Bruneau, 2009). Collectively, these technologies offer the rational basis to design strategies to ensure cardiogenic specification and avoidance of undifferentiated subpopulations prior to transplantation. The crucial balance between lineage specification and progenitor cell proliferation will be essential to develop a robust manufacturing process that can be scaled and applied to clinical grade production of a cardiac stem cell-based product. At this point, the stage of differentiation that most adequately serves the purpose of regenerative therapy will have to be determined. An equilibrium will be needed in which the ideal cell population shows sustained engraftment, is able to integrate into the host tissue without disrupting it and is depleted from undifferentiated progenitors that may give rise to teratomas.

In order to translate iPS technology into clinical reality for heart disease, additional milestones will need to be considered. First, the target patient population will need to be identified based on disease-severity and lack of alternative options to justify inclusion into a first-in-man study. Many patients are too severely deconditioned or have significant co-morbidities to allow consideration for heart transplant, thus limiting treatment strategies to palliative medicines and procedures. This category of patients needs to be considered a priority in terms of experimental cell-based interventions. An advantage with autologous iPS technology is that no toxic immunosuppression is required, yet provides a unique strategy to overcome poor natural stem cell pools in elderly patients that limit more traditional regenerative approaches. Thus, iPS-based products should be considered in patients with no other options to decrease not only symptoms but also the need for hospitalization along with expensive yet invasive palliative management strategies such as destination left ventricular assist devices. Next, a good-manufacturing-practice production process and facility will need to be developed and implemented to ensure clinical-grade production of patient-derived iPS cells, as well as tissue-specific differentiation

for targeted applications. Finally, regulatory agencies will require evidence of proper engraftment, survival, and safety of transplanted iPS-derived progeny (Nelson, 2008). This will require proof-of-principle studies using clinical grade cell products in disease model systems encompassing comparative effectiveness for optimized outcomes (Nelson, 2008).

VIII. CONCLUSIONS

1. Murine embryonic fibroblasts can be reprogrammed to a pluripotent state by transduction with modified HIV-derived lentiviruses containing human factors SOX2, OCT4 and KLF4 in the presence or absence of c-MYC.

2. Bioengineered cells fulfill increasingly stringent pluripotency criteria including morphological rearrangement, *in vitro* expression of pluripotency markers, *in vivo* teratoma, and integration within early blastocyst leading to *in utero* contribution to embryonic organogenesis.

3. Including the oncogene c-Myc during the reprogramming process has a negative effect on the cardiogenicity of the bioengineered pluripotent stem cells.

4. Induced pluripotent stem cells are cardiogenic, spontaneously giving rise to cells with morphological and functional characteristics of developing cardiomyocytes.

5. Reprogrammed cells are capable of sustained engraftment in the post-infarcted heart without developing teratomas when injected into an immunocompetent host.

6. Integration of induced pluripotent stem cells in the infarcted area leads to *de novo* tissue formation, reduced damage and improved cardiac function.

To date, the primary experience in regenerative medicine is so far based on the use of natural sources. This thesis provides direct evidence for the utility of bioengineered platforms that would solve limitations regarding tissue access, stem populations depletion or disease effects on the natural cell source. In that

way, we are expanding the existing resources to be applicable to regenerative therapies with the added value of an autologous pluripotent approach.

Collectively, this thesis demonstrates the feasibility of reprogramming mouse somatic cells with human stemness factors and tests the cardiac regenerative potential of this platform. By providing proof of principle of the cardiogenic capacity of induced pluripotent stem cells, this works establishes the foundation for a curative approach to ischemic heart disease through bioengineered autologous biologics.

IX. References

Aasen T, Raya A, Barrero MJ, Garreta E, Consiglio A, Gonzalez F, Vassena R, Bilic J, Pekarik V, Tiscornia G, Edel M, Boue S, Izpisua Belmonte JC. Efficient and rapid generation of induced pluripotent stem cells from human keratinocytes. *Nat Biotechnol*. 2008;26:1276-84.

Acosta JC, Ferrandiz N, Bretones G, Torrano V, Blanco R, Richard C, O'Connell B, Sedivy J, Delgado MD, Leon J. Myc inhibits p27-induced erythroid differentiation of leukemia cells by repressing erythroid master genes without reversing p27-mediated cell cycle arrest. *Mol Cell Biol*. 2008;28:7286-95.

Anversa P, Leri A, Rota M, Hosoda T, Bearzi C, Urbanek K, Kajstura J, Bolli R. Concise review: Stem cells, myocardial regeneration, and methodological artifacts. *Stem Cells*. 2007;25:589-601.

Anversa P, Nadal-Ginard B. Myocyte renewal and ventricular remodelling. *Nature*. 2002;415:240-3.

Aoi T, Yae K, Nakagawa M, Ichisaka T, Okita K, Takahashi K, Chiba T, Yamanaka S. Generation of pluripotent stem cells from adult mouse liver and stomach cells. *Science*. 2008;321:699-702.

Armstrong L, Lako M, Dean W, Stojkovic M. Epigenetic modification is central to genome reprogramming in somatic cell nuclear transfer. *Stem Cells*. 2006;24:805-14.

Atala A. Advances in tissue and organ replacement. *Curr Stem Cell Res Ther*. 2008;3:21-31.

Bagutti C, Wobus AM, Fassler R, Watt FM. Differentiation of embryonal stem cells into keratinocytes: Comparison of wild-type and beta 1 integrin-deficient cells. *Dev Biol*. 1996;179:184-96.

Bain G, Kitchens D, Yao M, Huettner JE, Gottlieb DI. Embryonic stem cells express neuronal properties in vitro. *Dev Biol*. 1995;168:342-57.

Balsam LB, Wagers AJ, Christensen JL, Kofidis T, Weissman IL, Robbins RC. Haematopoietic stem cells adopt mature haematopoietic fates in ischaemic myocardium. *Nature*. 2004;428:668-73.

Banito A, Rashid ST, Acosta JC, Li S, Pereira CF, Geti I, Pinho S, Silva JC, Azuara V, Walsh M, Vallier L, Gil J. Senescence impairs successful reprogramming to pluripotent stem cells. *Genes Dev*. 2009;23:2134-9.

Behfar A, Faustino RS, Arrell DK, Dzeja PP, Perez-Terzic C, Terzic A. Guided stem cell cardiopoiesis: Discovery and translation. *J Mol Cell Cardiol*. 2008;45:523-9.

Behfar A, Perez-Terzic C, Faustino RS, Arrell DK, Hodgson DM, Yamada S, Puceat M, Niederlander N, Alekseev AE, Zingman LV, Terzic A. Cardiopoietic programming of embryonic stem cells for tumor-free heart repair. *J Exp Med*. 2007;204:405-20.

Behfar A, Terzic A. Mesenchymal stem cells: Engineering regeneration. *Clinical and Translational Science*. 2008;1:34-35.

Behfar A, Zingman LV, Hodgson DM, Rauzier JM, Kane GC, Terzic A, Puceat M. Stem cell differentiation requires a paracrine pathway in the heart. *Faseb J*. 2002;16:1558-66.

Beyhan Z, Iager AE, Cibelli JB. Interspecies nuclear transfer: Implications for embryonic stem cell biology. *Cell Stem Cell*. 2007;1:502-12.

Boheler KR, Czyz J, Tweedie D, Yang HT, Anisimov SV, Wobus AM. Differentiation of pluripotent embryonic stem cells into cardiomyocytes. *Circ Res*. 2002;91:189-201.

Boland MJ, Hazen JL, Nazor KL, Rodriguez AR, Gifford W, Martin G, Kupriyanov S, Baldwin KK. Adult mice generated from induced pluripotent stem cells. *Nature*. 2009;461:91-4.

Brinster RL. The effect of cells transferred into the mouse blastocyst on subsequent development. *J Exp Med*. 1974;140:1049-56.

Bru T, Clarke C, McGrew MJ, Sang HM, Wilmut I, Blow JJ. Rapid induction of pluripotency genes after exposure of human somatic cells to mouse es cell extracts. *Exp Cell Res*. 2008;314:2634-42.

Buchholz DE, Hikita ST, Rowland TJ, Friedrich AM, Hinman CR, Johnson LV, Clegg DO. Derivation of functional retinal pigmented epithelium from induced pluripotent stem cells. *Stem Cells*. 2009;27:2427-34.

Byrne JA, Pedersen DA, Clepper LL, Nelson M, Sanger WG, Gokhale S, Wolf DP, Mitalipov SM. Producing primate embryonic stem cells by somatic cell nuclear transfer. *Nature*. 2007;450:497-502.

Campbell KH, McWhir J, Ritchie WA, Wilmut I. Sheep cloned by nuclear transfer from a cultured cell line. *Nature*. 1996;380:64-6.

Cartwright P, McLean C, Sheppard A, Rivett D, Jones K, Dalton S. Lif/stat3 controls es cell self-renewal and pluripotency by a myc-dependent mechanism 10.1242/dev.01670. *Development*. 2005;132:885-896.

Chamberlain G, Fox J, Ashton B, Middleton J. Concise review: Mesenchymal stem cells: Their phenotype, differentiation capacity, immunological features, and potential for homing. *Stem Cells*. 2007;25:2739-49.

Chambers I, Smith A. Self-renewal of teratocarcinoma and embryonic stem cells. *Oncogene*. 2004;23:7150-60.

Chambers SM, Fasano CA, Papapetrou EP, Tomishima M, Sadelain M, Studer L. Highly efficient neural conversion of human es and ips cells by dual inhibition of smad signaling. *Nat Biotechnol*. 2009;27:275-80.

Chang CW, Lai YS, Pawlik KM, Liu K, Sun CW, Li C, Schoeb TR, Townes TM. Polycistronic lentiviral vector for "hit and run" reprogramming of adult skin fibroblasts to induced pluripotent stem cells. *Stem Cells*. 2009;27:1042-9.

Chatterji U, Bobardt MD, Stanfield R, Ptak RG, Pallansch LA, Ward PA, Jones MJ, Stoddart CA, Scalfaro P, Dumont J-M, Besseghir K, Rosenwirth B, Gallay PA. Naturally occurring capsid substitutions render hiv-1 cyclophilin a independent in human cells and trim-cyclophilin-resistant in owl monkey cells 10.1074/jbc.M506314200. *Journal of Biological Chemistry*. 2005;280:40293-40300.

Chien KR. Regenerative medicine and human models of human disease. *Nature*. 2008;453:302-5.

Chien KR, Domian IJ, Parker KK. Cardiogenesis and the complex biology of regenerative cardiovascular medicine. *Science*. 2008;322:1494-7.

Choi KD, Yu J, Smuga-Otto K, Salvagiotto G, Rehrauer W, Vodyanik M, Thomson J, Slukvin I. Hematopoietic and endothelial differentiation of human induced pluripotent stem cells. *Stem Cells*. 2009;27:559-67.

Coraux C, Nawrocki-Raby B, Hinnrasky J, Kileztky C, Gaillard D, Dani C, Puchelle E. Embryonic stem cells generate airway epithelial tissue. *Am J Respir Cell Mol Biol*. 2005;32:87-92.

Daheron L, Opitz SL, Zaehres H, Lensch MW, Andrews PW, Itskovitz-Eldor J, Daley GQ. Lif/stat3 signaling fails to maintain self-renewal of human embryonic stem cells. *Stem Cells*. 2004;22:770-8.

Daley GQ, Scadden DT. Prospects for stem cell-based therapy. *Cell*. 2008;132:544-8.

Damjanov I, Solter D. Animal model of human disease: Teratoma and teratocarcinoma. *Am J Pathol*. 1976;83:241-4.

De Coppi P, Bartsch G, Jr., Siddiqui MM, Xu T, Santos CC, Perin L, Mostoslavsky G, Serre AC, Snyder EY, Yoo JJ, Furth ME, Soker S, Atala A. Isolation of amniotic stem cell lines with potential for therapy. *Nat Biotechnol*. 2007;25:100-6.

De Sousa PA, Galea G, Turner M. The road to providing human embryo stem cells for therapeutic use: The uk experience. *Reproduction*. 2006;132:681-9.

Deb A, Wang S, Skelding KA, Miller D, Simper D, Caplice NM. Bone marrow-derived cardiomyocytes are present in adult human heart: A study of gender-mismatched bone marrow transplantation patients. *Circulation*. 2003;107:1247-9.

Demaison C, Parsley K, Brouns G, Scherr M, Battmer K, Kinnon C, Grez M, Thrasher AJ. High-level transduction and gene expression in hematopoietic repopulating cells using a human immunodeficiency [correction of imunodeficiency] virus type 1-based lentiviral vector containing an internal spleen focus forming virus promoter. *Hum Gene Ther*. 2002;13:803-13.

Dimos JT, Rodolfa KT, Niakan KK, Weisenthal LM, Mitsumoto H, Chung W, Croft GF, Saphier G, Leibel R, Goland R, Wichterle H, Henderson CE, Eggan K. Induced pluripotent stem cells generated from patients with als can be differentiated into motor neurons. *Science*. 2008;321:1218-21.

Eakin GS, Hadjantonakis AK. Production of chimeras by aggregation of embryonic stem cells with diploid or tetraploid mouse embryos. *Nat Protoc*. 2006;1:1145-53.

Ebert AD, Yu J, Rose FF, Jr., Mattis VB, Lorson CL, Thomson JA, Svendsen CN. Induced pluripotent stem cells from a spinal muscular atrophy patient. *Nature*. 2009;457:277-80.

Eminli S, Foudi A, Stadtfeld M, Maherali N, Ahfeldt T, Mostoslavsky G, Hock H, Hochedlinger K. Differentiation stage determines potential of hematopoietic cells for reprogramming into induced pluripotent stem cells. *Nat Genet*. 2009;41:968-76.

Fairchild PJ, Nolan KF, Waldmann H. Genetic modification of dendritic cells through the directed differentiation of embryonic stem cells. *Methods Mol Biol*. 2007;380:59-72.

Fraidenraich D, Benezra R. Embryonic stem cells prevent developmental cardiac defects in mice. *Nat Clin Pract Cardiovasc Med*. 2006;3 Suppl 1:S14-7.

French AJ, Adams CA, Anderson LS, Kitchen JR, Hughes MR, Wood SH. Development of human cloned blastocysts following somatic cell nuclear transfer with adult fibroblasts. *Stem Cells*. 2008;26:485-93.

Fujii JT, Martin GR. Incorporation of teratocarcinoma stem cells into blastocysts by aggregation with cleavage-stage embryos. *Dev Biol*. 1980;74:239-44.

Gheorghiade M BR. Heart failure as consequence of ischemic heart disease. In: DL M, ed. *Iheart failure: A companion to braunwald's heart disease*. St Louis, Mo: Elsevier; 2003:351-362.

Gidekel S, Pizov G, Bergman Y, Pikarsky E. Oct-3/4 is a dose-dependent oncogenic fate determinant. *Cancer Cell*. 2003;4:361-70.

Gnecchi M, He H, Liang OD, Melo LG, Morello F, Mu H, Noiseux N, Zhang L, Pratt RE, Ingwall JS, Dzau VJ. Paracrine action accounts for marked protection of ischemic heart by akt-modified mesenchymal stem cells. *Nat Med*. 2005;11:367-8.

Gnecchi M, He H, Noiseux N, Liang OD, Zhang L, Morello F, Mu H, Melo LG, Pratt RE, Ingwall JS, Dzau VJ. Evidence supporting paracrine hypothesis for akt-modified mesenchymal stem cell-mediated cardiac protection and functional improvement. *Faseb J*. 2006;20:661-9.

Gnecchi M, Zhang Z, Ni A, Dzau VJ. Paracrine mechanisms in adult stem cell signaling and therapy. *Circ Res*. 2008;103:1204-19.

Goldman S. Stem and progenitor cell-based therapy of the human central nervous system. *Nat Biotechnol*. 2005;23:862-71.

Guo W, Lasky JL, Chang CJ, Mosessian S, Lewis X, Xiao Y, Yeh JE, Chen JY, Iruela-Arispe ML, Varella-Garcia M, Wu H. Multi-genetic events collaboratively contribute to pten-null leukaemia stem-cell formation. *Nature*. 2008;453:529-33.

Hanna J, Markoulaki S, Schorderet P, Carey BW, Beard C, Wernig M, Creyghton MP, Steine EJ, Cassady JP, Foreman R, Lengner CJ, Dausman JA, Jaenisch R. Direct reprogramming of terminally differentiated mature b lymphocytes to pluripotency. *Cell*. 2008;133:250-64.

Hanna J, Saha K, Pando B, van Zon J, Lengner CJ, Creyghton MP, van Oudenaarden A, Jaenisch R. Direct cell reprogramming is a stochastic process amenable to acceleration. *Nature*. 2009;462:595-601.

Hanna J, Wernig M, Markoulaki S, Sun CW, Meissner A, Cassady JP, Beard C, Brambrink T, Wu LC, Townes TM, Jaenisch R. Treatment of sickle cell anemia mouse model with ips cells generated from autologous skin. *Science*. 2007;318:1920-3.

Hasegawa K, Nakamura T, Harvey M, Ikeda Y, Oberg A, Figini M, Canevari S, Hartmann LC, Peng K-W. The use of a tropism-modified measles virus in folate receptorâ€“targeted virotherapy of ovarian cancer 10.1158/1078-0432.Ccr-06-0992. *Clinical Cancer Research*. 2006;12:6170-6178.

Henderson JT. Lazarus's gate: Challenges and potential of epigenetic reprogramming of somatic cells. *Clin Pharmacol Ther*. 2008;83:889-93.

Hescheler J, Fleischmann BK, Lentini S, Maltsev VA, Rohwedel J, Wobus AM, Addicks K. Embryonic stem cells: A model to study structural and functional properties in cardiomyogenesis. *Cardiovasc Res*. 1997;36:149-62.

Hochedlinger K, Jaenisch R. Nuclear reprogramming and pluripotency. *Nature*. 2006;441:1061-7.

Hockemeyer D, Soldner F, Cook EG, Gao Q, Mitalipova M, Jaenisch R. A drug-inducible system for direct reprogramming of human somatic cells to pluripotency. *Cell Stem Cell*. 2008;3:346-53.

Hodgson DM, Behfar A, Zingman LV, Kane GC, Perez-Terzic C, Alekseev AE, Puceat M, Terzic A. Stable benefit of embryonic stem cell therapy in myocardial infarction. *Am J Physiol Heart Circ Physiol*. 2004;287:H471-9.

Hofmann W, Schubert D, LaBonte J, Munson L, Gibson S, Scammell J, Ferrigno P, Sodroski J. Species-specific, postentry barriers to primate immunodeficiency virus infection. *J Virol*. 1999;73:10020-10028.

Hong H, Takahashi K, Ichisaka T, Aoi T, Kanagawa O, Nakagawa M, Okita K, Yamanaka S. Suppression of induced pluripotent stem cell generation by the p53-p21 pathway. *Nature*. 2009;460:1132-5.

Hotta A, Ellis J. Retroviral vector silencing during ips cell induction: An epigenetic beacon that signals distinct pluripotent states. *J Cell Biochem*. 2008;105:940-8.

Huangfu D, Maehr R, Guo W, Eijkelenboom A, Snitow M, Chen AE, Melton DA. Induction of pluripotent stem cells by defined factors is greatly improved by small-molecule compounds. *Nat Biotechnol*. 2008;26:795-7.

Ikeda Y, Collins MK, Radcliffe PA, Mitrophanous KA, Takeuchi Y. Gene transduction efficiency in cells of different species by hiv and eiav vectors. *Gene Ther*. 2002;9:932-8.

Ikeda Y, Ylinen LM, Kahar-Bador M, Towers GJ. Influence of gag on human immunodeficiency virus type 1 species-specific tropism. *J Virol*. 2004;78:11816-22.

Jaenisch R, Young R. Stem cells, the molecular circuitry of pluripotency and nuclear reprogramming. *Cell*. 2008;132:567-82.

Kahan BW, Jacobson LM, Hullett DA, Ochoada JM, Oberley TD, Lang KM, Odorico JS. Pancreatic precursors and differentiated islet cell types from murine embryonic stem cells: An in vitro model to study islet differentiation. *Diabetes*. 2003;52:2016-24.

Kaji K, Norrby K, Paca A, Mileikovsky M, Mohseni P, Woltjen K. Virus-free induction of pluripotency and subsequent excision of reprogramming factors. *Nature*. 2009;458:771-5.

Kajstura J, Hosoda T, Bearzi C, Rota M, Maestroni S, Urbanek K, Leri A, Anversa P. The human heart: A self-renewing organ. *Clin Transl Sci*. 2008;1:80-86.

Kamihata H, Matsubara H, Nishiue T, Fujiyama S, Tsutsumi Y, Ozono R, Masaki H, Mori Y, Iba O, Tateishi E, Kosaki A, Shintani S, Murohara T, Imaizumi T, Iwasaka T. Implantation of bone marrow mononuclear cells into ischemic myocardium enhances collateral perfusion and regional function via side supply of angioblasts, angiogenic ligands, and cytokines. *Circulation*. 2001;104:1046-52.

Karger AB, Park S, Reyes S, Bienengraeber M, Dyer RB, Terzic A, Alekseev AE. Role for sur2a ed domain in allosteric coupling within the katp channel complex 10.1085/jgp.200709852. *J Gen Physiol*. 2008;131:185-196.

Karumbayaram S, Novitch BG, Patterson M, Umbach JA, Richter L, Lindgren A, Conway AE, Clark AT, Goldman SA, Plath K, Wiedau-Pazos M, Kornblum HI, Lowry WE. Directed differentiation of human-induced pluripotent stem cells generates active motor neurons. *Stem Cells*. 2009;27:806-11.

Kattman SJ, Huber TL, Keller GM. Multipotent flk-1+ cardiovascular progenitor cells give rise to the cardiomyocyte, endothelial, and vascular smooth muscle lineages. *Dev Cell*. 2006;11:723-32.

Kawamura T, Suzuki J, Wang YV, Menendez S, Morera LB, Raya A, Wahl GM, Belmonte JC. Linking the p53 tumour suppressor pathway to somatic cell reprogramming. *Nature*. 2009;460:1140-4.

Kim D, Kim CH, Moon JI, Chung YG, Chang MY, Han BS, Ko S, Yang E, Cha KY, Lanza R, Kim KS. Generation of human induced pluripotent stem cells by direct delivery of reprogramming proteins. *Cell Stem Cell*. 2009;4:472-6.

Kim JB, Zaehres H, Arauzo-Bravo MJ, Scholer HR. Generation of induced pluripotent stem cells from neural stem cells. 2009;4:1464-1470.

Kim JB, Zaehres H, Wu G, Gentile L, Ko K, Sebastiano V, Arauzo-Bravo MJ, Ruau D, Han DW, Zenke M, Scholer HR. Pluripotent stem cells induced from adult neural stem cells by reprogramming with two factors. *Nature*. 2008;454:646-50.

Kinnaird T, Stabile E, Burnett MS, Lee CW, Barr S, Fuchs S, Epstein SE. Marrow-derived stromal cells express genes encoding a broad spectrum of arteriogenic cytokines and promote in vitro and in vivo arteriogenesis through paracrine mechanisms. *Circ Res*. 2004;94:678-85.

Klimanskaya I, Rosenthal N, Lanza R. Derive and conquer: Sourcing and differentiating stem cells for therapeutic applications. 2008;7:131-142.

Kolossov E, Bostani T, Roell W, Breitbach M, Pillekamp F, Nygren JM, Sasse P, Rubenchik O, Fries JW, Wenzel D, Geisen C, Xia Y, Lu Z, Duan Y, Kettenhofen R, Jovinge S, Bloch W, Bohlen H, Welz A, Hescheler J, Jacobsen SE, Fleischmann BK. Engraftment of engineered es cell-derived cardiomyocytes but not bm cells restores contractile function to the infarcted myocardium. *J Exp Med*. 2006;203:2315-27.

Koonin EV. Orthologs, paralogs, and evolutionary genomics. *Annu Rev Genet*. 2005;39:309-38.

Kootstra NA, Munk C, Tonnu N, Landau NR, Verma IM. Abrogation of postentry restriction of hiv-1-based lentiviral vector transduction in simian cells. *Proc Natl Acad Sci U S A*. 2003;100:1298-303.

Korbling M, Estrov Z. Adult stem cells for tissue repair - a new therapeutic concept? *N Engl J Med*. 2003;349:570-82.

Kramer J, Hegert C, Hargus G, Rohwedel J. Chondrocytes derived from mouse embryonic stem cells. *Cytotechnology*. 2003;41:177-87.

Kroon E, Martinson LA, Kadoya K, Bang AG, Kelly OG, Eliazer S, Young H, Richardson M, Smart NG, Cunningham J, Agulnick AD, D'Amour KA, Carpenter MK, Baetge EE. Pancreatic endoderm derived from human embryonic stem cells generates glucose-responsive insulin-secreting cells in vivo. *Nat Biotechnol*. 2008;26:443-52.

Kyba M, Daley GQ. Hematopoiesis from embryonic stem cells: Lessons from and for ontogeny. *Exp Hematol*. 2003;31:994-1006.

Laflamme MA, Murry CE. Regenerating the heart. *Nat Biotechnol*. 2005;23:845-56.

Le Blanc K, Ringden O. Immunomodulation by mesenchymal stem cells and clinical experience. *J Intern Med*. 2007;262:509-25.

Leal J, Luengo-Fernandez R, Gray A, Petersen S, Rayner M. Economic burden of cardiovascular diseases in the enlarged european union. *Eur Heart J*. 2006;27:1610-9.

Lee G, Papapetrou EP, Kim H, Chambers SM, Tomishima MJ, Fasano CA, Ganat YM, Menon J, Shimizu F, Viale A, Tabar V, Sadelain M, Studer L. Modelling pathogenesis and treatment of familial dysautonomia using patient-specific ipscs. *Nature*. 2009;461:402-6.

Lensch MW, Schlaeger TM, Zon LI, Daley GQ. Teratoma formation assays with human embryonic stem cells: A rationale for one type of human-animal chimera. *Cell Stem Cell*. 2007;1:253-8.

Leon J, Ferrandiz N, Acosta JC, Delgado MD. Inhibition of cell differentiation: A critical mechanism for myc-mediated carcinogenesis? *Cell Cycle*. 2009;8:1148-57.

Li H, Collado M, Villasante A, Strati K, Ortega S, Canamero M, Blasco MA, Serrano M. The ink4/arf locus is a barrier for ips cell reprogramming. *Nature*. 2009;460:1136-9.

Li JY, Christophersen NS, Hall V, Soulet D, Brundin P. Critical issues of clinical human embryonic stem cell therapy for brain repair. *Trends Neurosci*. 2008;31:146-53.

Lin CH, Lin C, Tanaka H, Fero ML, Eisenman RN. Gene regulation and epigenetic remodeling in murine embryonic stem cells by c-myc. *PLoS One*. 2009;4:e7839.

Lin T, Ambasudhan R, Yuan X, Li W, Hilcove S, Abujarour R, Lin X, Hahm HS, Hao E, Hayek A, Ding S. A chemical platform for improved induction of human ipscs. *Nat Methods*. 2009;6:805-8.

Liu H, Zhu F, Yong J, Zhang P, Hou P, Li H, Jiang W, Cai J, Liu M, Cui K, Qu X, Xiang T, Lu D, Chi X, Gao G, Ji W, Ding M, Deng H. Generation of induced pluripotent stem cells from adult rhesus monkey fibroblasts. *Cell Stem Cell*. 2008;3:587-90.

Liu Y, Asakura M, Inoue H, Nakamura T, Sano M, Niu Z, Chen M, Schwartz RJ, Schneider MD. Sox17 is essential for the specification of cardiac mesoderm in embryonic stem cells
10.1073/pnas.0609100104. *Proceedings of the National Academy of Sciences*. 2007;104:3859-3864.

Lloyd-Jones D, Adams R, Carnethon M, De Simone G, Ferguson TB, Flegal K, Ford E, Furie K, Go A, Greenlund K, Haase N, Hailpern S, Ho M, Howard V, Kissela B, Kittner S, Lackland D, Lisabeth L, Marelli A, McDermott M, Meigs J, Mozaffarian D, Nichol G, O'Donnell C, Roger V, Rosamond W, Sacco R, Sorlie P, Stafford R, Steinberger J, Thom T, Wasserthiel-Smoller S, Wong N, Wylie-Rosett J, Hong Y, for the American Heart Association Statistics Committee and Stroke Statistics Subcommittee. Heart disease and stroke statistics--2009 update: A report from the american heart association statistics committee and stroke statistics subcommittee
10.1161/circulationaha.108.191261. *Circulation*. 2009;119:e21-181.

Loh YH, Agarwal S, Park IH, Urbach A, Huo H, Heffner GC, Kim K, Miller JD, Ng K, Daley GQ. Generation of induced pluripotent stem cells from human blood. *Blood*. 2009;113:5476-9.

Loh YH, Wu Q, Chew JL, Vega VB, Zhang W, Chen X, Bourque G, George J, Leong B, Liu J, Wong KY, Sung KW, Lee CW, Zhao XD, Chiu KP, Lipovich L, Kuznetsov VA, Robson P, Stanton LW, Wei CL, Ruan Y, Lim B, Ng HH. The oct4 and nanog transcription network regulates pluripotency in mouse embryonic stem cells. *Nat Genet*. 2006;38:431-40.

Lowry WE, Plath K. The many ways to make an ips cell. *Nat Biotechnol*. 2008;26:1246-8.

Lyssiotis CA, Foreman RK, Staerk J, Garcia M, Mathur D, Markoulaki S, Hanna J, Lairson LL, Charette BD, Bouchez LC, Bollong M, Kunick C, Brinker A, Cho CY, Schultz PG, Jaenisch R. Reprogramming of murine fibroblasts to induced pluripotent stem cells with chemical complementation of klf4
10.1073/pnas.0903860106. *Proceedings of the National Academy of Sciences*. 2009;106:8912-8917.

Maehr R, Chen S, Snitow M, Ludwig T, Yagasaki L, Goland R, Leibel RL, Melton DA. Generation of pluripotent stem cells from patients with type 1 diabetes. *Proc Natl Acad Sci U S A*. 2009;106:15768-73.

Maherali N, Ahfeldt T, Rigamonti A, Utikal J, Cowan C, Hochedlinger K. A high-efficiency system for the generation and study of human induced pluripotent stem cells. *Cell Stem Cell*. 2008;3:340-5.

Maherali N, Sridharan R, Xie W, Utikal J, Eminli S, Arnold K, Stadtfeld M, Yachechko R, Tchieu J, Jaenisch R, Plath K, Hochedlinger K. Directly reprogrammed fibroblasts show global epigenetic remodeling and widespread tissue contribution. *Cell Stem Cell*. 2007;1:55-70.

Mali P, Ye Z, Hommond HH, Yu X, Lin J, Chen G, Zou J, Cheng L. Improved efficiency and pace of generating induced pluripotent stem cells from human adult and fetal fibroblasts. *Stem Cells*. 2008;26:1998-2005.

Marchetto MC, Yeo GW, Kainohana O, Marsala M, Gage FH, Muotri AR. Transcriptional signature and memory retention of human-induced pluripotent stem cells. *PLoS One*. 2009;4:e7076.

Marion RM, Strati K, Li H, Murga M, Blanco R, Ortega S, Fernandez-Capetillo O, Serrano M, Blasco MA. A p53-mediated DNA damage response limits reprogramming to ensure ips cell genomic integrity. *Nature*. 2009;460:1149-53.

Martin MJ, Muotri A, Gage F, Varki A. Human embryonic stem cells express an immunogenic nonhuman sialic acid. *Nat Med*. 2005;11:228-32.

Mauritz C, Schwanke K, Reppel M, Neef S, Katsirntaki K, Maier LS, Nguemo F, Menke S, Haustein M, Hescheler J, Hasenfuss G, Martin U. Generation of functional murine cardiac myocytes from induced pluripotent stem cells. *Circulation*. 2008;118:507-17.

Meissner A, Wernig M, Jaenisch R. Direct reprogramming of genetically unmodified fibroblasts into pluripotent stem cells. *Nat Biotechnol*. 2007;25:1177-81.

Meyer JS, Shearer RL, Capowski EE, Wright LS, Wallace KA, McMillan EL, Zhang SC, Gamm DM. Modeling early retinal development with human embryonic and induced pluripotent stem cells. *Proc Natl Acad Sci U S A*. 2009;106:16698-703.

Mikkelsen TS, Hanna J, Zhang X, Ku M, Wernig M, Schorderet P, Bernstein BE, Jaenisch R, Lander ES, Meissner A. Dissecting direct reprogramming through integrative genomic analysis. *Nature*. 2008;454:49-55.

Miura K, Okada Y, Aoi T, Okada A, Takahashi K, Okita K, Nakagawa M, Koyanagi M, Tanabe K, Ohnuki M, Ogawa D, Ikeda E, Okano H, Yamanaka S. Variation in the safety of induced pluripotent stem cell lines. *Nat Biotechnol*. 2009;27:743-5.

Moretti A, Caron L, Nakano A, Lam JT, Bernshausen A, Chen Y, Qyang Y, Bu L, Sasaki M, Martin-Puig S, Sun Y, Evans SM, Laugwitz KL, Chien KR. Multipotent embryonic isl1+ progenitor cells lead to cardiac, smooth muscle, and endothelial cell diversification. *Cell*. 2006;127:1151-65.

Morrison SJ, Spradling AC. Stem cells and niches: Mechanisms that promote stem cell maintenance throughout life. *Cell*. 2008;132:598-611.

Moustafa LA, Brinster RL. The fate of transplanted cells in mouse blastocysts in vitro. *J Exp Zool*. 1972;181:181-91.

Moustafa LA, Brinster RL. Induced chimaerism by transplanting embryonic cells into mouse blastocysts. *J Exp Zool*. 1972;181:193-201.

MSC. Mortalidad por enfermedades crónicas. *Instituto de Información Sanitaria Ministerio de Sanidad*. 2006.

Murry CE, Keller G. Differentiation of embryonic stem cells to clinically relevant populations: Lessons from embryonic development. *Cell*. 2008;132:661-80.

Murry CE, Soonpaa MH, Reinecke H, Nakajima H, Nakajima HO, Rubart M, Pasumarthi KB, Virag JI, Bartelmez SH, Poppa V, Bradford G, Dowell JD, Williams DA, Field LJ. Haematopoietic stem cells do not transdifferentiate into cardiac myocytes in myocardial infarcts. *Nature*. 2004;428:664-8.

Nagaya N, Kangawa K, Itoh T, Iwase T, Murakami S, Miyahara Y, Fujii T, Uematsu M, Ohgushi H, Yamagishi M, Tokudome T, Mori H, Miyatake K, Kitamura S. Transplantation of mesenchymal stem cells improves cardiac function in a rat model of dilated cardiomyopathy. *Circulation*. 2005;112:1128-35.

Nagy A, Gocza E, Diaz EM, Prideaux VR, Ivanyi E, Markkula M, Rossant J. Embryonic stem cells alone are able to support fetal development in the mouse. *Development*. 1990;110:815-21.

Nakagawa M, Koyanagi M, Tanabe K, Takahashi K, Ichisaka T, Aoi T, Okita K, Mochiduki Y, Takizawa N, Yamanaka S. Generation of induced pluripotent stem cells without myc from mouse and human fibroblasts. *Nat Biotechnol*. 2008;26:101-6.

Narazaki G, Uosaki H, Teranishi M, Okita K, Kim B, Matsuoka S, Yamanaka S, Yamashita JK. Directed and systematic differentiation of cardiovascular cells from mouse induced pluripotent stem cells. *Circulation*. 2008;118:498-506.

Nelson T, Behfar A, Terzic A. Stem cells: Biologics for regeneration. *Clin Pharmacol Ther*. 2008;84:620-3.

Nelson TJ, Behfar A, Yamada S, Martinez-Fernandez A, Terzic A. Stem cell platforms for regenerative medicine. *Clin Transl Sci*. 2009;2:222-227.

Nelson TJ, Duncan SA, Misra RP. Conserved enhancer in the serum response factor promoter controls expression during early coronary vasculogenesis. *Circ Res*. 2004;94:1059-66.

Nelson TJ, Faustino RS, Chiriac A, Crespo-Diaz R, Behfar A, Terzic A. Cxcr4+/flk-1+ biomarkers select a cardiopoietic lineage from embryonic stem cells. *Stem Cells*. 2008;26:1464-73.

Nelson TJ, Ge ZD, Van Orman J, Barron M, Rudy-Reil D, Hacker TA, Misra R, Duncan SA, Auchampach JA, Lough JW. Improved cardiac function in infarcted mice after treatment with pluripotent embryonic stem cells. *Anat Rec A Discov Mol Cell Evol Biol*. 2006;288:1216-24.

Nelson TJ, Martinez-Fernandez A, Terzic A. Kcnj11 knockout morula re-engineered by stem cell diploid aggregation. *Philos Trans R Soc Lond B Biol Sci*. 2009;364:269-76.

Nelson TJ M-FA, Yamada S, Ikeda T, Terzic A. Induced pluripotent stem cells: Advances to applications. *Stem Cells Cloning: Adv and App*. 2010;0:00-00.

Nelson TJ, Terzic A. Induced pluripotent stem cells: Reprogrammed without a trace. *Regen Med*. 2009;4:333-5.

Niwa A, Umeda K, Chang H, Saito M, Okita K, Takahashi K, Nakagawa M, Yamanaka S, Nakahata T, Heike T. Orderly hematopoietic development of induced pluripotent stem cells via flk-1(+) hemoangiogenic progenitors. *J Cell Physiol*. 2009;221:367-77.

Niwa H, Miyazaki J, Smith AG. Quantitative expression of oct-3/4 defines differentiation, dedifferentiation or self-renewal of es cells. *Nat Genet*. 2000;24:372-6.

Noser JA, Towers GJ, Sakuma R, Dumont JM, Collins MK, Ikeda Y. Cyclosporine increases human immunodeficiency virus type 1 vector transduction of primary mouse cells. *J Virol*. 2006;80:7769-74.

Ohnishi S, Yanagawa B, Tanaka K, Miyahara Y, Obata H, Kataoka M, Kodama M, Ishibashi-Ueda H, Kangawa K, Kitamura S, Nagaya N. Transplantation of mesenchymal stem cells attenuates myocardial injury and dysfunction in a rat model of acute myocarditis. *J Mol Cell Cardiol*. 2007;42:88-97.

Okita K, Ichisaka T, Yamanaka S. Generation of germline-competent induced pluripotent stem cells. *Nature*. 2007;448:313-7.

Okita K, Nakagawa M, Hyenjong H, Ichisaka T, Yamanaka S. Generation of mouse induced pluripotent stem cells without viral vectors. *Science*. 2008;322:949-53.

Olivier EN, Rybicki AC, Bouhassira EE. Differentiation of human embryonic stem cells into bipotent mesenchymal stem cells. *Stem Cells*. 2006;24:1914-22.

Orkin SH, Zon LI. Hematopoiesis: An evolving paradigm for stem cell biology. *Cell*. 2008;132:631-44.

Osakada F, Jin ZB, Hirami Y, Ikeda H, Danjyo T, Watanabe K, Sasai Y, Takahashi M. In vitro differentiation of retinal cells from human pluripotent stem cells by small-molecule induction. *J Cell Sci*. 2009;122:3169-79.

Park IH, Arora N, Huo H, Maherali N, Ahfeldt T, Shimamura A, Lensch MW, Cowan C, Hochedlinger K, Daley GQ. Disease-specific induced pluripotent stem cells. *Cell*. 2008;134:877-86.

Park IH, Lerou PH, Zhao R, Huo H, Daley GQ. Generation of human-induced pluripotent stem cells. *Nat Protoc*. 2008;3:1180-6.

Park I-H, Zhao R, West JA, Yabuuchi A, Huo H, Ince TA, Lerou PH, Lensch MW, Daley GQ. Reprogramming of human somatic cells to pluripotency with defined factors. 2008;451:141-146.

Passier R, van Laake LW, Mummery CL. Stem-cell-based therapy and lessons from the heart. *Nature*. 2008;453:322-9.

Perez-Terzic C, Behfar A, Mery A, van Deursen JM, Terzic A, Puceat M. Structural adaptation of the nuclear pore complex in stem cell-derived cardiomyocytes. *Circ Res*. 2003;92:444-52.

Pfeifer A, Ikawa M, Dayn Y, Verma IM. Transgenesis by lentiviral vectors: Lack of gene silencing in mammalian embryonic stem cells and preimplantation embryos. *Proc Natl Acad Sci U S A*. 2002;99:2140-5.

Phinney DG, Prockop DJ. Concise review: Mesenchymal stem/multipotent stromal cells: The state of transdifferentiation and modes of tissue repair--current views. *Stem Cells*. 2007;25:2896-902.

Piedra ME, Delgado MD, Ros MA, Leon J. C-myc overexpression increases cell size and impairs cartilage differentiation during chick limb development. *Cell Growth Differ*. 2002;13:185-93.

Quaini F, Urbanek K, Beltrami AP, Finato N, Beltrami CA, Nadal-Ginard B, Kajstura J, Leri A, Anversa P. Chimerism of the transplanted heart. *N Engl J Med*. 2002;346:5-15.

Raya A, Rodriguez-Piza I, Guenechea G, Vassena R, Navarro S, Barrero MJ, Consiglio A, Castella M, Rio P, Sleep E, Gonzalez F, Tiscornia G, Garreta E, Aasen T, Veiga A, Verma IM, Surralles J, Bueren J, Izpisua Belmonte JC. Disease-corrected haematopoietic progenitors from fanconi anaemia induced pluripotent stem cells. *Nature*. 2009;460:53-9.

Risau W, Sariola H, Zerwes HG, Sasse J, Ekblom P, Kemler R, Doetschman T. Vasculogenesis and angiogenesis in embryonic-stem-cell-derived embryoid bodies. *Development*. 1988;102:471-8.

Rodriguez-Piza I, Richaud-Patin Y, Vassena R, Gonzalez F, Barrero MJ, Veiga A, Raya A, Izpisua Belmonte JC. Reprogramming of human fibroblasts to induced pluripotent stem cells under xeno-free conditions. *Stem Cells*. 2009.

Roell W, Lewalter T, Sasse P, Tallini YN, Choi BR, Breitbach M, Doran R, Becher UM, Hwang SM, Bostani T, von Maltzahn J, Hofmann A, Reining S, Eiberger B, Gabris B, Pfeifer A, Welz A, Willecke K, Salama G, Schrickel JW, Kotlikoff MI, Fleischmann BK. Engraftment of connexin 43-expressing cells prevents post-infarct arrhythmia. *Nature*. 2007;450:819-24.

Rohwedel J, Maltsev V, Bober E, Arnold HH, Hescheler J, Wobus AM. Muscle cell differentiation of embryonic stem cells reflects myogenesis in vivo: Developmentally regulated expression of myogenic determination genes and functional expression of ionic currents. *Dev Biol*. 1994;164:87-101.

Rossant J, McBurney MW. The developmental potential of a euploid male teratocarcinoma cell line after blastocyst injection. *J Embryol Exp Morphol*. 1982;70:99-112.

Safinia N, Minger SL. Generation of hepatocytes from human embryonic stem cells. *Methods Mol Biol*. 2009;481:169-80.

Saha K, Jaenisch R. Technical challenges in using human induced pluripotent stem cells to model disease. *Cell Stem Cell*. 2009;5:584-95.

Schenke-Layland K, Rhodes KE, Angelis E, Butylkova Y, Heydarkhan-Hagvall S, Gekas C, Zhang R, Goldhaber JI, Mikkola HK, Plath K, MacLellan WR. Reprogrammed mouse fibroblasts differentiate into cells of the cardiovascular and hematopoietic lineages. *Stem Cells*. 2008;26:1537-46.

Schocken DD, Benjamin EJ, Fonarow GC, Krumholz HM, Levy D, Mensah GA, Narula J, Shor ES, Young JB, Hong Y. Prevention of heart failure: A scientific statement from the american heart association councils on epidemiology and prevention, clinical cardiology, cardiovascular nursing, and high blood pressure research; quality of care and outcomes research interdisciplinary working group; and functional genomics and translational biology interdisciplinary working group. *Circulation*. 2008;117:2544-65.

SEC. Informe 2009. *Sociedad Española Cardiología*. 2009.

Segers VF, Lee RT. Stem-cell therapy for cardiac disease. *Nature*. 2008;451:937-42.

Senju S, Haruta M, Matsunaga Y, Fukushima S, Ikeda T, Takahashi K, Okita K, Yamanaka S, Nishimura Y. Characterization of dendritic cells and macrophages generated by directed differentiation from mouse induced pluripotent stem cells. *Stem Cells*. 2009;27:1021-31.

Shizuru JA, Negrin RS, Weissman IL. Hematopoietic stem and progenitor cells: Clinical and preclinical regeneration of the hematolymphoid system. *Annu Rev Med*. 2005;56:509-38.

Silva J, Barrandon O, Nichols J, Kawaguchi J, Theunissen TW, Smith A. Promotion of reprogramming to ground state pluripotency by signal inhibition. *PLoS Biol*. 2008;6:e253.

Silva J, Smith A. Capturing pluripotency. *Cell*. 2008;132:532-6.

Singla DK, Hacker TA, Ma L, Douglas PS, Sullivan R, Lyons GE, Kamp TJ. Transplantation of embryonic stem cells into the infarcted mouse heart: Formation of multiple cell types. *J Mol Cell Cardiol*. 2006;40:195-200.

Smith KP, Luong MX, Stein GS. Pluripotency: Toward a gold standard for human es and ips cells. *J Cell Physiol*. 2009;220:21-9.

Soldner F, Hockemeyer D, Beard C, Gao Q, Bell GW, Cook EG, Hargus G, Blak A, Cooper O, Mitalipova M, Isacson O, Jaenisch R. Parkinson's disease patient-derived induced pluripotent stem cells free of viral reprogramming factors. *Cell*. 2009;136:964-77.

Sommer CA, Gianotti Sommer A, Longmire TA, Christodoulou C, Thomas DD, Gostissa M, Alt FW, Murphy GJ, Kotton DN, Mostoslavsky G. Excision of reprogramming transgenes improves the differentiation potential of ips cells generated with a single excisable vector. *Stem Cells*. 2009.

Song Z, Cai J, Liu Y, Zhao D, Yong J, Duo S, Song X, Guo Y, Zhao Y, Qin H, Yin X, Wu C, Che J, Lu S, Ding M, Deng H. Efficient generation of hepatocyte-like cells from human induced pluripotent stem cells. *Cell Res*. 2009;19:1233-42.

Srinivas G, Anversa P, Frishman WH. Cytokines and myocardial regeneration: A novel treatment option for acute myocardial infarction. *Cardiol Rev*. 2009;17:1-9.

Stadtfeld M, Brennand K, Hochedlinger K. Reprogramming of pancreatic beta cells into induced pluripotent stem cells. *Curr Biol*. 2008;18:890-4.

Stadtfeld M, Maherali N, Breault DT, Hochedlinger K. Defining molecular cornerstones during fibroblast to ips cell reprogramming in mouse. *Cell Stem Cell*. 2008;2:230-40.

Stadtfeld M, Nagaya M, Utikal J, Weir G, Hochedlinger K. Induced pluripotent stem cells generated without viral integration. *Science*. 2008;322:945-9.

Stewart C. Aggregation between teratocarcinoma cells and preimplantation mouse embryos. *J Embryol Exp Morphol*. 1980;58:289-302.

Strang BL, Takeuchi Y, Relander T, Richter J, Bailey R, Sanders DA, Collins MK, Ikeda Y. Human immunodeficiency virus type 1 vectors with alphavirus envelope glycoproteins produced from stable packaging cells. *J Virol*. 2005;79:1765-71.

Stremlau M, Owens CM, Perron MJ, Kiessling M, Autissier P, Sodroski J. The cytoplasmic body component trim5alpha restricts hiv-1 infection in old world monkeys. *Nature*. 2004;427:848-53.

Sullivan GJ, Hay DC, Park IH, Fletcher J, Hannoun Z, Payne CM, Dalgetty D, Black JR, Ross JA, Samuel K, Wang G, Daley GQ, Lee JH, Church GM, Forbes SJ, Iredale JP, Wilmut I. Generation of functional human hepatic endoderm from human induced pluripotent stem cells. *Hepatology*. 2009.

Sun N, Panetta NJ, Gupta DM, Wilson KD, Lee A, Jia F, Hu S, Cherry AM, Robbins RC, Longaker MT, Wu JC. Feeder-free derivation of induced pluripotent stem cells from adult human adipose stem cells. *Proc Natl Acad Sci U S A*. 2009;106:15720-5.

Surani MA, Hayashi K, Hajkova P. Genetic and epigenetic regulators of pluripotency. *Cell*. 2007;128:747-62.

Surani MA, McLaren A. Stem cells: A new route to rejuvenation. 2006;443:284-285.

Sutton MG, Sharpe N. Left ventricular remodeling after myocardial infarction: Pathophysiology and therapy. *Circulation*. 2000;101:2981-8.

Tachibana M, Sparman M, Sritanaudomchai H, Ma H, Clepper L, Woodward J, Li Y, Ramsey C, Kolotushkina O, Mitalipov S. Mitochondrial gene replacement in primate offspring and embryonic stem cells. *Nature*. 2009;461:367-72.

Takahashi K, Tanabe K, Ohnuki M, Narita M, Ichisaka T, Tomoda K, Yamanaka S. Induction of pluripotent stem cells from adult human fibroblasts by defined factors. *Cell*. 2007;131:861-72.

Takahashi K, Yamanaka S. Induction of pluripotent stem cells from mouse embryonic and adult fibroblast cultures by defined factors. *Cell*. 2006;126:663-76.

Takahashi M, Li TS, Suzuki R, Kobayashi T, Ito H, Ikeda Y, Matsuzaki M, Hamano K. Cytokines produced by bone marrow cells can contribute to functional improvement of the infarcted heart by protecting cardiomyocytes from ischemic injury. *Am J Physiol Heart Circ Physiol*. 2006;291:H886-93.

Takeuchi JK, Bruneau BG. Directed transdifferentiation of mouse mesoderm to heart tissue by defined factors. *Nature*. 2009;459:708-11.

Tashiro K, Inamura M, Kawabata K, Sakurai F, Yamanishi K, Hayakawa T, Mizuguchi H. Efficient adipocyte and osteoblast differentiation from mouse induced pluripotent stem cells by adenoviral transduction. *Stem Cells*. 2009;27:1802-11.

Tateishi K, He J, Taranova O, Liang G, D'Alessio AC, Zhang Y. Generation of insulin-secreting islet-like clusters from human skin fibroblasts. *J Biol Chem*. 2008;283:31601-7.

Taura D, Noguchi M, Sone M, Hosoda K, Mori E, Okada Y, Takahashi K, Homma K, Oyamada N, Inuzuka M, Sonoyama T, Ebihara K, Tamura N, Itoh H, Suemori H, Nakatsuji N, Okano H, Yamanaka S, Nakao K. Adipogenic differentiation of human induced pluripotent stem cells: Comparison with that of human embryonic stem cells. *FEBS Lett*. 2009;583:1029-33.

Thali M, Bukovsky A, Kondo E, Rosenwlrth B, Walsh CT, Sodroski J, Gottlinger HG. Functional association of cyclophilin a with hiv-1 virions. 1994;372:363-365.

Thomson JA, Itskovitz-Eldor J, Shapiro SS, Waknitz MA, Swiergiel JJ, Marshall VS, Jones JM. Embryonic stem cell lines derived from human blastocysts. *Science*. 1998;282:1145-7.

Uemura R, Xu M, Ahmad N, Ashraf M. Bone marrow stem cells prevent left ventricular remodeling of ischemic heart through paracrine signaling. *Circ Res*. 2006;98:1414-21.

USDH. U.S. Department of health and human services, the centers for disease control and prevention, national center for health statistics. *Vital Health Statistics I*. 1994;32:407.

Utikal J, Polo JM, Stadtfeld M, Maherali N, Kulalert W, Walsh RM, Khalil A, Rheinwald JG, Hochedlinger K. Immortalization eliminates a roadblock during cellular reprogramming into ips cells. *Nature*. 2009;460:1145-8.

van de Ven C, Collins D, Bradley MB, Morris E, Cairo MS. The potential of umbilical cord blood multipotent stem cells for nonhematopoietic tissue and cell regeneration. *Exp Hematol*. 2007;35:1753-65.

Wagers AJ, Weissman IL. Plasticity of adult stem cells. *Cell*. 2004;116:639-48.

Waldman SA, Terzic A. Individualized medicine and the imperative of global health. *Clin Pharmacol Ther*. 2007;82:479-83.

Waldman SA, Terzic A. Clinical and translational sciences: At the intersection of molecular and individualized medicine. *Clinical and Translational Science*. 2008;1:6-8.

Waldman SA, Terzic MR, Terzic A. Molecular medicine hones therapeutic arts to science. 2007;82:343-347.

Waters BK, Rossant J. The effect of retinoic acid pretreatment on the ability of murine embryonal carcinoma and inner cell mass cells to participate in chimaera development. *J Embryol Exp Morphol*. 1986;98:99-110.

Wernig M, Meissner A, Cassady JP, Jaenisch R. C-myc is dispensable for direct reprogramming of mouse fibroblasts. *Cell Stem Cell*. 2008;2:10-2.

Wernig M, Meissner A, Foreman R, Brambrink T, Ku M, Hochedlinger K, Bernstein BE, Jaenisch R. In vitro reprogramming of fibroblasts into a pluripotent es-cell-like state. *Nature*. 2007;448:318-24.

Wernig M, Zhao JP, Pruszak J, Hedlund E, Fu D, Soldner F, Broccoli V, Constantine-Paton M, Isacson O, Jaenisch R. Neurons derived from reprogrammed fibroblasts functionally integrate into the fetal brain and improve symptoms of rats with parkinson's disease. *Proc Natl Acad Sci U S A*. 2008;105:5856-61.

Westfall MV, Pasyk KA, Yule DI, Samuelson LC, Metzger JM. Ultrastructure and cell-cell coupling of cardiac myocytes differentiating in embryonic stem cell cultures. *Cell Motil Cytoskeleton*. 1997;36:43-54.

WHO WHO. Cardiovascular diseases. *Fact sheet #317*. 2007.

Wilmut I, Schnieke AE, McWhir J, Kind AJ, Campbell KH. Viable offspring derived from fetal and adult mammalian cells. *Cloning Stem Cells*. 2007;9:3-7.

Woltjen K, Michael IP, Mohseni P, Desai R, Mileikovsky M, Hamalainen R, Cowling R, Wang W, Liu P, Gertsenstein M, Kaji K, Sung HK, Nagy A. Piggybac transposition reprograms fibroblasts to induced pluripotent stem cells. *Nature*. 2009;458:766-70.

Wood SA, Allen ND, Rossant J, Auerbach A, Nagy A. Non-injection methods for the production of embryonic stem cell-embryo chimaeras. *Nature*. 1993;365:87-9.

Wu SM, Chien KR, Mummery C. Origins and fates of cardiovascular progenitor cells. *Cell*. 2008;132:537-43.

Xu C, Rosler E, Jiang J, Lebkowski JS, Gold JD, O'Sullivan C, Delavan-Boorsma K, Mok M, Bronstein A, Carpenter MK. Basic fibroblast growth factor supports undifferentiated human embryonic stem cell growth without conditioned medium. *Stem Cells*. 2005;23:315-23.

Xu D, Alipio Z, Fink LM, Adcock DM, Yang J, Ward DC, Ma Y. Phenotypic correction of murine hemophilia a using an ips cell-based therapy. *Proc Natl Acad Sci U S A*. 2009;106:808-13.

Xu M, Uemura R, Dai Y, Wang Y, Pasha Z, Ashraf M. In vitro and in vivo effects of bone marrow stem cells on cardiac structure and function. *J Mol Cell Cardiol*. 2007;42:441-8.

Yamada S, Nelson TJ, Behfar A, Crespo-Diaz RJ, Fraidenraich D, Terzic A. Stem cell transplant into preimplantation embryo yields myocardial infarction-resistant adult phenotype. *Stem Cells*. 2009;27:1697-705.

Yamada S, Nelson TJ, Crespo-Diaz RJ, Perez-Terzic C, Liu XK, Miki T, Seino S, Behfar A, Terzic A. Embryonic stem cell therapy of heart failure in genetic cardiomyopathy. *Stem Cells*. 2008;26:2644-53.

Yamanaka S. Strategies and new developments in the generation of patient-specific pluripotent stem cells. *Cell Stem Cell*. 2007;1:39-49.

Yamanaka S. Pluripotency and nuclear reprogramming. *Philos Trans R Soc Lond B Biol Sci*. 2008;363:2079-87.

Yamanaka S. A fresh look at ips cells. *Cell*. 2009;137:13-7.

Yang L, Soonpaa MH, Adler ED, Roepke TK, Kattman SJ, Kennedy M, Henckaerts E, Bonham K, Abbott GW, Linden RM, Field LJ, Keller GM. Human cardiovascular progenitor cells develop from a kdr+ embryonic-stem-cell-derived population. *Nature*. 2008;453:524-8.

Yang X, Smith SL, Tian XC, Lewin HA, Renard JP, Wakayama T. Nuclear reprogramming of cloned embryos and its implications for therapeutic cloning. *Nat Genet*. 2007;39:295-302.

Ye Z, Zhan H, Mali P, Dowey S, Williams DM, Jang YY, Dang CV, Spivak JL, Moliterno AR, Cheng L. Human induced pluripotent stem cells from blood cells of healthy donors and patients with acquired blood disorders. *Blood*. 2009.

Yoshida Y, Takahashi K, Okita K, Ichisaka T, Yamanaka S. Hypoxia enhances the generation of induced pluripotent stem cells. *Cell Stem Cell*. 2009;5:237-41.

Yu J, Hu K, Smuga-Otto K, Tian S, Stewart R, Slukvin, II, Thomson JA. Human induced pluripotent stem cells free of vector and transgene sequences. *Science*. 2009;324:797-801.

Yu J, Vodyanik MA, Smuga-Otto K, Antosiewicz-Bourget J, Frane JL, Tian S, Nie J, Jonsdottir GA, Ruotti V, Stewart R, Slukvin, II, Thomson JA. Induced pluripotent stem cell lines derived from human somatic cells. *Science*. 2007;318:1917-20.

Zhang D, Jiang W, Liu M, Sui X, Yin X, Chen S, Shi Y, Deng H. Highly efficient differentiation of human es cells and ips cells into mature pancreatic insulin-producing cells. *Cell Res*. 2009;19:429-38.

Zhang J, Wilson GF, Soerens AG, Koonce CH, Yu J, Palecek SP, Thomson JA, Kamp TJ. Functional cardiomyocytes derived from human induced pluripotent stem cells. *Circ Res*. 2009;104:e30-41.

Zhang JX, Diehl GE, Littman DR. Relief of preintegration inhibition and characterization of additional blocks for hiv replication in primary mouse t cells. *PLoS One*. 2008;3:e2035.

Zhao C, Deng W, Gage FH. Mechanisms and functional implications of adult neurogenesis. *Cell*. 2008;132:645-60.

Zhao X, Liu J, Ahmad I. Differentiation of embryonic stem cells into retinal neurons. *Biochem Biophys Res Commun*. 2002;297:177-84.

Zhao XY, Li W, Lv Z, Liu L, Tong M, Hai T, Hao J, Guo CL, Ma QW, Wang L, Zeng F, Zhou Q. Ips cells produce viable mice through tetraploid complementation. *Nature*. 2009;461:86-90.

Zhou H, Wu S, Joo JY, Zhu S, Han DW, Lin T, Trauger S, Bien G, Yao S, Zhu Y, Siuzdak G, Scholer HR, Duan L, Ding S. Generation of induced pluripotent stem cells using recombinant proteins. *Cell Stem Cell*. 2009;4:381-4.

Zufferey R, Nagy D, Mandel RJ, Naldini L, Trono D. Multiply attenuated lentiviral vector achieves efficient gene delivery in vivo. *Nat Biotechnol*. 1997;15:871-5.

CONCLUSIONES

1. Los fibroblastos embrionarios de ratón se pueden reprogramar a un estado de pluripotencia mediante la transducción con lentivirus derivados de VIH modificados que contienen los factores humanos SOX2, OCT4 y KLF4 en presencia o ausencia de c-MYC.

2. Las células reprogramadas cumplen criterios de pluripotencia incluyendo cambios morfológicos, expresión *in vitro* de marcadores genéticos, formación de teratomas e integración en blastocisto con la consiguiente contribución a la organogénesis durante el desarrollo embrionario.

3. La inclusion del oncogén c-Myc durante el proceso de reprogramación afecta negativamente el potencial cardiogénico de las células con pluripotencia inducida resultantes.

4. Las células pluripotentes inducidas son cardiogénicas, diferenciándose espontáneamente en células con morfología y características funcionales propias de cardiomiocitos en desarrollo.

5. Las células reprogramadas son capaces de permanecer en el tejido cardiaco sin originar teratomas al ser inyectadas en el corazón de un receptor inmunocompetente después de un infarto

6. La integración de las células pluripotentes inducidas en el area infartada provoca formación de tejido *de novo*, reducción del daño causado por la isquemia y mejora de la función cardiaca.

Hasta el momento, la experiencia en Medicina Regenerativa se ha basado en el uso de los recursos naturales disponibles. Esta tesis aporta información sobre la utilidad de las plataformas obtenidas de la reprogramación

nuclear, que supondrían la superación de las limitaciones de acceso a tejido, depleción del contenido en células madre o los efectos de patologías concomitantes sobre las células naturales. De esta manera, se expanden los recursos disponibles para terapias regenerativas, con el valor añadido de la pluripotencia en células autólogas.

En conjunto, esta tesis demuestra la posibilidad de reprogramar células somáticas de ratón con factores humanos de pluripotencia y comprueba el potencial de regeneración cardiaca de esta plataforma. Al demostrar la capacidad cardiogénica de las células reprogramadas, este trabajo establece una nueva estrategia para el tratamiento curativo de la isquemia cardiaca mediante el uso de células autólogas manipuladas.